

Curriculum Vitae

Aksinija Aleksandrovna Kogan

University of Maryland School of Medicine
Graduate Program in Life Sciences
655 W. Baltimore St. BRB 8-020
Baltimore, MD 21201
email: akogan@som.umaryland.edu

EDUCATION:

Degree and Date Conferred: Doctor of Philosophy, December 2021

- | | |
|-------------|--|
| 2015 –2021 | Ph.D. in Molecular Medicine
Cancer Biology Track
University of Maryland School of Medicine
Baltimore, MD
Dissertation: “Activating STING-dependent immune signaling in AML” |
| 2011 – 2012 | M.S. in Biology
Fairleigh Dickinson University
Teaneck, NJ |
| 2007 – 2011 | B.S. in Biology (<i>magna cum laude</i>)
University Honors Program
Fairleigh Dickinson University
Teaneck, NJ
Senior Thesis: “Photoprotective Mechanism of Nicotinamide via the Beneficial Regulation of Extracellular Matrix and Heat Shock Proteins” |

PROFESSIONAL SOCIETY MEMBERSHIP:

- | | |
|----------------|--|
| 2017 – present | American Society of Hematology (ASH) |
| 2009 – present | Beta Beta Beta National Biological Honors Society,
Fairleigh Dickinson University |
| 2007 – present | Phi Omega Epsilon Honors Society,
Fairleigh Dickinson University |

HONORS AND AWARDS:

- 2007 – 2011 Honors List, Fairleigh Dickinson University, awarded for outstanding scholastic performance
- 2007 – 2011 Colonel S. Fairleigh Dickinson Scholarship, awarded for outstanding scholastic performance

RESEARCH EXPERIENCE:

- 2016 – 2021 Graduate Research Assistant
University of Maryland Baltimore, Department of Radiation Oncology Baltimore, MD
Mentor: Feyruz V. Rassool, Ph.D.
- Demonstrate that DNMTi and PARPi combination treatment operates via STING signaling in a *TP53* dependent manner.
 - Test how STING signaling influences double-stranded DNA break repair in AML samples with and without TP53 mutations.
 - Characterize the role of STING signaling in anti-leukemia immune responses using immune-competent mouse models.
- 2008 – 2011 Undergraduate Laboratory Research Assistant
Fairleigh Dickinson University, Department of Biological Sciences
Teaneck, NJ
Mentor: Neena Philips, Ph.D.
- Investigated effects of nicotinamide and its derivatives on non-irradiated and UV radiated cells
 - Tested role of copper in regulation of structural genes of extracellular matrix in fibroblasts
 - Studied molecular mechanism of luteolin in relation to melanor cells

LEADERSHIP ROLES & MENTORING EXPERIENCE:

- 2018 – 2021 Mentor, Rassool Lab, University of Maryland Baltimore
- Direct mentorship role of rotating and incoming graduate students and for volunteer high school students for project development and basic laboratory technical skills
- 2019 – 2020 Volunteer, Molecular Medicine Program recruitment, University of Maryland Baltimore
- 2009 – 2012 Tutor, Center for Academic Student Services, Fairleigh Dickinson University

- Tutored undergraduate level Chemistry, Biology, Physics, and Mathematics to help students improve scientific study skills and empower students to achieve academic goals
- 2010 – 2011 President, Hillel, Fairleigh Dickinson University
 2008 – 2009 Public Relations Officer, Hillel, Fairleigh Dickinson University

PUBLICATIONS:

1. Baer, MR, **Kogan, AA**, Bentzen, SM, Saum, G, Lapidus, RG, Emadi, A, Duong, VH, Niyongere, S, O’Connell, CL, Rassool, FV. (2021). Phase 1 clinical trial of combination therapy with the DNA methyltransferase inhibitor decitabine and the poly ADP ribose polymerase inhibitor talazoparib in adult patients with relapsed/refractory acute myeloid leukemia. Manuscript in prep.
2. **Kogan, AA**, Topper, MJ, McLaughlin, LJ, Creed, TM, Eberly, CL, Kingsbury, TJ, Baer, MR, Kessler, MD, Baylin, SB, Rassool, FV. (2021). Activating STING-dependent immune signaling in acute myeloid leukemia. Manuscript in prep.
3. McLaughlin, LJ, Stojanovic, L, **Kogan, AA**, Rutherford, JL, Choi, EY, Yen, RWC, Xia, L, Zou, Y, Lapidus, RG, Baylin, SB, Topper, MJ, Rassool, FV. Pharmacologic Induction of Innate Immune Signaling Directly Drives Homologous Recombination Deficiency. *Proc Natl Acad Sci U S A*. 2020.
4. Abbotts, R. Topper, MJ, Biondi, C, Fontaine, D, Goswami, R, Stojanovic, L, Choi, EY, McLaughlin, L, **Kogan, AA**, Xia, L, Lapidus, R, Mahmood, J, Baylin SB, Rassool, FV. DNA methyltransferase inhibitors induce a BRCAness phenotype that sensitizes NSCLC to PARP inhibitor and ionizing radiation. *Proc Natl Acad Sci U S A*. 2019.
5. **Kogan AA**, Lapidus RG, Baer MR, Rassool FV. Exploiting epigenetically mediated changes: Acute myeloid leukemia, leukemia stem cells and the bone marrow microenvironment. *Adv Cancer Res*. 2019;141:213-253.
6. Mahmood, J, **Shamah, A** Creed, M, Pavlovic, R, Matsui, H, Kimura, M, Molitoris, J, Shukla, H, Jackson, I, Vujaskovic, Z. Radiation Induced Erectile Dysfunction: Recent Advances and Future Directions. *Advances in Radiation Oncology*. 2016.

SUBMITTED ABSTRACTS:

Oral Presentations:

1. Kogan, AA, DNMTis Sensitize AML Cells to PARPis via Immune Modulation-Dependent Promotion of HRD. Graduate Research Conference, University of Maryland, Baltimore, MD. 2020.
2. Kogan, AA, Mechanisms underlying the efficacy of PARP and DNMT inhibitor combination therapy in Acute Myeloid Leukemia (AML). Graduate Research Conference, University of Maryland, Baltimore, MD. 2019.

3. Kogan, AA, DNA Demethylating Agents Generate a BRCAness Effect: Prediction for sensitivity to PARP inhibitors in AML. Graduate Research Conference, University of Maryland, Baltimore, MD. 2018.

Poster Presentations:

1. Stojanovic, L, McLaughlin, L, **Kogan, A**, Rutherford, J, Topper, M, Baylin, S. B, Rassool, FV. Inflammation signaling is inversely linked to DNA repair signaling in OC and BC. 2020. Graduate Research Conference (GRC). University of Maryland, Baltimore, MD.
2. **Kogan, AA**, McLaughlin, LJ, Baer, MR, Baylin, SB, Topper, MJ, Rassool, FV. DNA methyltransferase inhibitors promote homologous recombination deficiency through induction of immune signaling, sensitizing acute myeloid leukemia cells to PARP inhibitors. 2020. Baltimore Area Research Symposium. University of Maryland, Baltimore, MD.
3. McLaughlin, LJ, Stojanovic, L, **Kogan AA**, Baylin, SB, Topper, MJ, & Rassool, FV. Pharmacologic induction of innate immune signaling via STING directly drives homologous recombination deficiency. 2020. Baltimore Area Research Symposium. University of Maryland, Baltimore, MD.
4. **Kogan, AA**, McLaughlin, LJ, Baer, MR, Baylin, SB, Topper, MJ, Rassool, FV. DNA methyltransferase inhibitors promote homologous recombination deficiency through induction of immune signaling, sensitizing acute myeloid leukemia cells to PARP inhibitors. 2019. ASH, Annual Research Conference. Orlando, FL.
5. **Kogan, AA**, McLaughlin, LJ, Baylin, SB, Topper, MJ, Rassool, FV. Combining PARP and DNMT inhibitors induces STING signaling to drive homologous recombination deficiency in TNBC and AML. 2019. University of Maryland Cancer Biology Retreat. Baltimore, MD.
6. **Kogan, AA**, Topper, MJ, Shissler, SC, Lee, MS, Bollino, DR, Choi, EY, Lapidus, RG, Li L, Small, D, Baer, MR, Webb, TJ, Baylin, SB, Rassool, FV. The combination of PARP inhibitors and DNMT inhibitors modulates immune activity and suggests a role for immune therapy in AML. 2018. ASH, Annual Research Conference. San Diego, CA.
7. McLaughlin, LJ, Kogan, AA, Choi, EY, Lapidus, R, Zou, Y, Li, H, Baylin, SB, Topper, MJ, & Rassool, FV. DNMT and PARP inhibitor combination therapy induces interferon driven homologous recombination defect in triple negative breast cancers. 2018. UMGCCC Annual Cancer Research Day. University of Maryland, Baltimore, MD.
8. **Kogan, AA**, Topper, MJ, Muvarak, NM, Creed, MT, Bentzen, S, Civin, CI, Baer, MR, Kingsbury, TJ, Baylin, SB, Abbotts, RM, Rassool, FV. DNA Demethylating Agents Generate a BRCAness Effect: Prediction for sensitivity to PARP inhibitors in AML. 2018. University of Maryland Cancer Biology Retreat. Baltimore, MD.
9. McLaughlin, LJ, Stojanovic, L, **Kogan, AA**, Lapidus, R, Choi, EY, Zou, Y, Baylin, SB, & Rassool, FV. Impaired homologous recombination by DNA methyltransferase inhibitors induces synthetic lethality in BRCA-proficient ovarian and triple negative breast cancers. 2018. University of Maryland Cancer Biology Research Retreat. University of Maryland, Baltimore, MD.

10. **Kogan, AA**, McLaughlin, LJ, Topper, MJ, Muvarak, NM, Stojanovic, L, Creed, MT, Bentzen, S, Civin, CI, Baer, MR, Kingsbury, TJ, Baylin, SB, Abbotts, RM, Rassool, FV. DNA Demethylating Agents Generate a BRCAness Effect: Prediction for sensitivity to PARP inhibitors in AML. 2018. Baltimore Area Repair Symposium. Baltimore, MD.
11. **Kogan, AA**, McLaughlin, LJ, Topper, MJ, Muvarak, NM, Stojanovic, L, Creed, MT, Bentzen, S, Civin, CI, Baer, MR, Kingsbury, TJ, Baylin, SB, Rassool, FV. DNA demethylating agents generate a Brcaness effect in multiple sporadic tumor types: prediction for sensitivity to PARP inhibitors in AML. 2017. American Society of Hematology. Atlanta, GA.
12. **Shamah AA**, Nidal Muvarak NM, Topper MJ, Baylin SB, Rassool, FV. Mechanisms underlying efficacy of PARP and DNMT inhibitor combination therapy in Acute Myeloid Leukemia. 2017. University of Maryland Cancer Biology Retreat. Baltimore, MD.

Abstract

Title of Dissertation: Activating STING-dependent immune signaling in AML

Aksinija A. Kogan, Doctor of Philosophy, 2021

Dissertation Directed by: Feyruz V. Rassool, PhD, Professor, Radiation Oncology

DNA methyltransferase inhibitors (DNMTis) are an epigenetic therapy for acute myeloid leukemia (AML) patients unfit for or unlikely to respond to intensive chemotherapy. DNMTis transcriptionally activate hypermethylated genes, and have been shown to activate endogenous retroviruses (ERVs) in a viral mimicry-inducing process that drives interferon (IFN) signaling. We previously reported that poly (ADP-ribose) polymerase inhibitors (PARPis) combine with DNMTis to induce an immune response that is mechanistically linked to reduction of DNA double-strand break repair activity in solid tumors. Here, we extend these mechanistic findings by showing that DNMTi+PARPi combination treatment induces a STING-dependent immune response to drive homologous recombination deficiency (HRD) in models of AML. Furthermore, we demonstrate for the first time that DNMTi-mediated ERV reactivation is significantly increased in TP53 mutant AML, and that such activation is the main driver of STING-dependent IFN signaling in this AML subtype. This is of particular importance given the poor

prognosis associated with TP53 mutant AML and the potential relevance to other cancers with TP53 mutations. In contrast, AMLs with wild-type (WT) TP53 require both DNMTi+PARPi, rather than DNMTi alone, for activation of STING-dependent IFN/inflammatory signaling. Finally, we show that the induction of HRD by DNMTi+PARPi combination treatment is STING-dependent in both TP53 mutant and WT AMLs. These findings significantly increase our understanding of the mechanisms that underlie DNMTi+PARPi combination treatment efficacy, and suggest increased efficacy in patients with TP53 mutations.

Activating STING-dependent immune signaling in AML

by
Aksinija A. Kogan

Dissertation submitted to the faculty of the Graduate School of the
University of Maryland, Baltimore in partial fulfillment
of the requirements for the degree of
Doctor of Philosophy
2021

©Copyright 2021 by Aksinija A. Kogan

All rights reserved

Dedication

To my Son, Ronnie.

You are my strength, my courage, and my reason for always persevering.

Acknowledgements

I would like to take this opportunity to express my gratitude to numerous people for their support and encouragement throughout my doctoral studies.

I would first like to thank my advisor, Dr. Feyruz Rassool, for giving me a home in her lab and support over the years. I am grateful for her guidance and the opportunities she has afforded me. I greatly appreciate her expertise and have learned a lot from her about what it means to be a scientist.

To my thesis committee, Dr. Stephen Baylin, Dr. Maria Baer, Dr. Tonya Webb, Dr. Tami Kingsbury, and Dr. Rena Lapidus. Collectively, I would like to thank them for their scientific guidance and contributions to this work. I was incredibly fortunate to work with and learn from each one of them. Individually, I thank Dr. Baylin for his expertise, insights and for consistently encouraging me to think of the bigger picture. I would like to thank Dr. Baer for helping me keep perspective on the clinical relevance of my research and for her attention to detail that has strengthened my work immensely. Thank you to Dr. Webb for her positivity, encouragement, and for teaching me scientific skills I would not have gained otherwise. To Dr. Kingsbury, thank you for making space for me in your lab and for always being willing to provide mentorship and advice. And I would like to thank Dr. Lapidus, who has been a great mentor and friend, for her priceless support, understanding, and guidance both professionally and personally. Additionally, I would like to thank Dr. Stuart Martin for his unconditional willingness to share his wisdom and offer advice. And thank you to Dr. Jeff Winkles and Dr. Toni Antalis for their guidance over the years.

I would like to recognize my lab members, both past and current. Thank you to Dr. Nidal Muvarak for taking me under his wing when I first joined the lab and Dr. Pratik Nagaria for sharing his love for science with me. Also, to Chris Biondi, Ade Adewuyi, Dan Fontaine, and Bryan Pelkey for their positive attitude and enthusiasm, and to Dr. Lena McLaughlin with whom I got to share a bench and all the ups and downs of science during our years together. To Lora Stojanovic, for her friendship and understanding, Dr. Rachel Abbotts, Anna Dellomo, and Julia Rutherford for being more than colleagues – I cannot thank you all enough for being there to share the laughter and the tears, whether they be related to science or life.

Words cannot express how grateful I am to my parents, Darja and Alexander, for all of the sacrifices that they have made on my behalf. I am forever indebted to them for giving me the opportunities and experiences that have made me who I am. Thank you for your unwavering love, help and support. I am thankful to Michael Kessler, my best friend and confidant, for his undying support and his continuous encouragement. Thank you to my brother, Andrej, for always being in my corner, and my wonderful niece, Esther, and nephew, Georg, for their positivity. And to Rachel Lipstein, who has been my family away from home since the day I moved to America – I am incredibly grateful for your friendship and loving support. I am similarly grateful for my childhood friends, Dr. Sophia Ceder and Kamola Silberud, and my close friend Michele Holzwarth Hagen, for their support from across the globe. Most importantly, I am grateful to my son, Ronnie, for his curiosity, for developing a love for science and spending time with me in the lab, and for motivating me every day to finish my thesis. Watching you grow is my greatest joy.

My sincere gratitude to the AML patients from University of Maryland Greenebaum Comprehensive Cancer Center (UMGCCC) for their willingness to donate their samples for the advancement of translational research. In our fight against cancer, they are the real heroes.

Many thanks to the UMGCCC under the leadership of Dr. Cullen, the Translational Laboratory Shared Services under the leadership of Dr. Lapidus, the Flow Cytometry Shared Services under the leadership of Dr. Fan, the Van Andel Genomics Core, and our collaborators at Johns Hopkins University, including the Experimental and Computational Genomics Core under the leadership of Dr. Yu, for their guidance and assistance in the research described in this thesis. In particular, thank you to Dr. Michael Topper for his invaluable scientific contributions, to Dr. Michael Creed and Christian Eberly for their guidance and friendship, and to Brandon Cooper, Kayla Tighe, Andrea Casildo, Dr. Eun Yong Choi and Dr. Ma Xinrong for their contributions to the animal studies.

And lastly, I would like to thank the following funding sources for their support of the research described in this thesis: the Leukemia Lymphoma Society, the Adelson Medical Research Foundation, the National Cancer Institute–Cancer Center Support Grant P30 CA134274 to the University of Maryland Marlene and Stewart Greenebaum Comprehensive Cancer Center, the Molecular Medicine Graduate Program, University of Maryland, and the VanAndel Research Institute - Stand Up to Cancer Epigenetics Dream Team. Stand Up to Cancer is a program of the Entertainment Industry Foundation administered by the AACR.

Table of Contents

Chapter	Page
Dedication	iii
Acknowledgments	iv
List of Tables	xii
List of Figures	xiii
List of Abbreviations	xvi
1. Introduction	
1.1. Acute Myeloid Leukemia	1
1.1.1. Classification	3
1.1.2. Genetic abnormalities	6
1.1.2.1. Translocations in master regulator genes	8
1.1.2.2. Mutations in partner genes	8
1.1.2.3. Role of TP53 mutations in AML	9
1.1.3. Epigenetic dysregulation	12
1.1.3.1. DNA methylation	13
1.1.3.2. Histone modification	14
1.1.3.3. MicroRNAs in epigenetic regulation	15
1.1.4. Immune signaling in AML	15
1.1.4.1. Role of ERVs in AML	16

1.2. Treating AML	17
1.2.1. Current therapy	17
1.2.2. Targeting DNA methylation	19
1.3. PARP inhibitors	23
1.4. Rationale and Aims	27
2. Activating STING-dependent immune signaling in acute myeloid leukemia	
2.1. Introduction	29
2.2. Results	33
2.2.1. DNMTi increases ERV gene expression in TP53 mutant AML	33
2.2.2. PARPi drives cytoplasmic dsDNA increases in AML	35
2.2.3. STING activity is increased in TP53 mutant AML	37
2.2.4. DNMTi increases IFN signaling in TP53 mutant AML	40
2.2.5. DNMTi drives decreases in HR in TP53 mutant AML	43
2.2.6. STING inhibition abrogates IFN signaling and rescues HR activity in AML	46
2.3. Discussion	48
2.4. Methods	51
2.4.1. Cell lines and primary samples	51
2.4.2. Drug reagents and treatments in vitro	52
2.4.3. RNA extraction and quantitative PCR	53
2.4.4. Immunofluorescence staining	53
2.4.5. TCGA analysis	54
2.4.6. Protein extraction and immunoblotting	54

2.4.7. Microarray sample preparation and analysis	55
2.4.8. STRING protein-protein interaction map	56
2.4.9. HR repair analysis	56
2.4.10. Statistical analysis	57
2.4.11. Data availability	57
3. Anti-tumorigenic effects of DNMTi+PARPi combination therapy in an immune-competent AML mouse model	
3.1. Introduction	58
3.2. Results	61
3.2.1. STING inhibition abrogates IFN/inflammasome signaling in TP53 WT and TP53 mutant AML cells	61
3.2.2. DNMTi+PARPi combination therapy results in anti-leukemia responses in an immune-competent AML mouse model	63
3.2.3. DNMTi+PARPi combination therapy enhances immune responses in tumor-bearing mice	65
3.3. Discussion	66
3.4. Methods	68
3.4.1. Cell culture	68
3.4.2. CRISPR-engineered cell lines	68
3.4.3. Drug reagents and treatments in vitro	69
3.4.4. Immune competent mouse model	69
3.4.5. LEGENDplex immunoassay	70
3.4.6. RNA extraction and quantitative PCR	70

3.4.7. Protein extraction and immunoblotting	71
3.4.8. Statistical analysis	71
4. Phase 1 clinical trial of DNMTi+PARPi combination therapy in adult patients with relapsed/refractory AML	
4.1. Introduction	72
4.2. Results	74
4.2.1. Patients	74
4.2.2. Dose escalation	77
4.2.3. Treatment Responses	78
4.2.3.1. Molecular features related to treatment response	80
4.2.4. Pharmacodynamic effects	83
4.3. Discussion	89
4.4. Methods	93
4.4.1. Patient population	93
4.4.2. Pre-treatment studies	94
4.4.3. Treatment	95
4.4.4. Dose escalation	95
4.4.5. Toxicity evaluation	95
4.4.6. Response assessment	96
4.4.7. Management of hematologic toxicity	96
4.4.8. Sample processing	97
4.4.9. RNA extraction and quantitative PCR	97
4.4.10. Immunofluorescence Staining	98

4.4.11. HR repair analysis	99
4.4.12. Construction and sequencing of directional total RNA-seq libraries	99
4.4.13. Statistical analysis	100
4.4.14. Data availability	100
5. Perspectives and Future Directions	101
Appendix	106
References	122

List of Tables

Table	Page
Table 1.1. The FAB classification of AML	4
Table 1.2. The WHO classification of AML	5
Table 1.3. AML classification based on cytogenetics and molecular markers	7
Table 2.1. TP53 mutation status in AML cell lines	33
Table 4.1 Clinical trial patient metadata	75
Table 4.2: Dose escalation schedule	78
Appendix Table S2.1: Cytogenetic and molecular features of AML primary samples treated with DNMTi+PARPi in vitro	106
Appendix Table S2.2: Primers used for qRT-PCR	107
Appendix Table S2.3: TCGA TP53 mutated AML samples identified using Vadakekolathu et al 2020	109

List of Figures

Figure	Page
Figure 1.1: Blood cell development	2
Figure 1.2: Overall survival of patients with TP53 alteration	10
Figure 1.3: Mapping of 168 <i>TP53</i> mutations in 141 CK-AMLs	11
Figure 1.4: Fundamental mechanisms of epigenetic regulation	13
Figure 1.5: DNA methylation and inhibition	20
Figure 1.6: Pathway analysis of changes in gene expression following DNMTi treatment	21
Figure 1.7: Mechanism of PARP inhibition	24
Figure 1.8: Schematic for synthetic lethality	25
Figure 2.1: Model for DNMTi+PARPi mechanism of action	31
Figure 2.2: DNMTi increases ERV gene expression in TP53 mutant AML	34
Figure 2.3: PARPi drives cytoplasmic dsDNA increases in AML	36
Figure 2.4: STING expression is lower in TP53 mutant AML at baseline	38
Figure 2.5: STING activity is increased in TP53 mutant AML	40
Figure 2.6: DNMTi increases IFN signaling in TP53 mutant AML	42
Figure 2.7: Immune and DNA repair pathways are linked	44
Figure 2.8: DNMTi drives decreases in HR in TP53 mutant AML	45
Figure 2.9: STING inhibition abrogates IFN signaling and rescues HR activity	47
Figure 2.10: Schematic of a multifaceted immune response leading to HRD in AML	49

Figure 3.1: MOLM14-Luc mouse model	59
Figure 3.2: Induction of type I IFN and other inflammatory cytokines through STING pathway activation results in potent leukemia-specific immunity, culminating in prolonged survival of mice with AML	60
Figure 3.3: STING inhibition abrogates IFN/inflammasome signaling in C1498 cells	62
Figure 3.4: DNMTi+PARPi combination therapy results in anti-leukemia responses in an immune-competent AML mouse model	64
Figure 3.5: DNMTi and PARPi combination therapy enhances immune responses in tumor-bearing mice	66
Figure 4.1 Swimmer plot for survival for patients on trial	79
Figure 4.2: Network of gene mutations stratified by patient response	81
Figure 4.3: Enrichment score plots of key affected pathways	82
Figure 4.4: Combination treatment generates HRD in patients that show clinical response	84
Figure 4.5: Combination treatment downregulates Rad51 foci formation	86
Figure 4.6 Immune gene upregulation in clinical trial patient samples	87
Figure 4.7: STING expression pre- vs post-treatment grouped by response	89
Figure 4.8: STING expression is notably elevated in AML	92
Figure 4.9: IFI44 expression is notably elevated in AML	93
Appendix Figure S2.1: DNMTi treatment increases ERV gene expression in TP53 mutant AML	110
Appendix Figure S2.2: PARP1 protein levels decrease after DNMTi+PARPi combination treatment	111

Appendix Figure S2.3: STING activity is increased in TP53 mutant AML after DNMTi+PARPi combination treatment	112
Appendix Figure S2.4: DNMTi treatment increases IFN signaling in TP53 mutant AML	113
Appendix Figure S2.5: Immune and DNA repair pathways are linked	114
Appendix Figure S2.6: DNMTi treatment decreases HR gene expression levels in TP53 mutant AML	115
Appendix Figure S2.7: STING inhibition abrogates IFN signaling and rescues HR activity	116
Appendix Figure S3.1: Confirmation of STING CRISPR-Cas9 KO	117
Appendix Figure S3.2: STING inhibition abrogates IFN signaling	118
Appendix Figure S3.3: DNMTi and PARPi combination therapy enhances immune signaling in serum of tumor-bearing mice	119
Appendix Figure S4.1: Hallmark pathway analysis of clinical trial samples	120
Appendix Figure S4.2: Oncogenic pathway analysis of clinical trial samples	121

List of Abbreviations

Abbreviation	Definition
53BP1	p53 binding protein 1
α -KG	α -ketoglutarate
α -MEM	Modified Minimum Essential Medium - alpha
γ H2AX	Histone family member X - gamma
AAALAC	Assessment and Accreditation of Laboratory Animal Care
abn	abnormal
AF9	See MMLT3
ALL	Acute lymphocytic leukemia
ALT-NHEJ	alternative nonhomologous end-joining
AML	Acute myeloid leukemia
ALT (SGPT)	Alanine amino transferase
AML1	Acute myeloid leukemia 1 protein (Runx1/CBFA)
ANC	Absolute neutrophil count
ANOVA	Analysis of variance
APAF1	Apoptotic protease activating factor 1
APCs	Antigen-presenting cells
APL	Acute promyelocytic leukemia
Ara-C	Cytarabine
AST (SGOT)	Aspartate amino transferase

ASXL1	ASXL Transcriptional Regulator 1
ATF-3	Activating transcription factor 3
ATM	ataxia telangiectasia-mutated
ATR	Ataxia telangiectasia and Rad3 related
Aza	Azacitidine
B2M	Beta-2-Microglobulin
BC	Breast cancer
BCA	Bicinchoninic acid
BCR-ABL	breakpoint cluster region – ABL1 proto-oncogene fusion gene (also known as “Philadelphia chromosome”)
BER	Base excision repair
BioCarta	Charting Pathways of Life – database of gene interaction models
BioCyc	Genome database collection
BioGRID	The Biological General Repository for Interaction Datasets
BM	Bone marrow
BMMCs	Bone marrow mononuclear cells
BMN	Other name for Talazoparib
BRCA1/2	Breast cancer type 1/2 susceptibility gene
BRIP1	BRCA1 Interacting Helicase 1
BSA	Bovine serum albumin
BsmBI	Bacillus stearothermophilus B61
C	Control

C17orf70	Also known as UTP6 - U3 small nucleolar RNA-associated protein 6 homolog
C19orf40	Chromosome 19 open reading frame 40 isoform 1
CBF β	Core-binding factor subunit beta (Runx2)
CCD	charge- coupled device
CCL5	C-C Motif Chemokine Ligand 5
CD3	Cluster of differentiation 3
CD8	Cluster of differentiation 8
cDNA	Complementary DNA
CEBP α	CCAAT enhancer-binding protein alpha
CHK1	Checkpoint kinase 1
c-KIT	Mast/stem cell growth factor
CLL	Chronic lymphocytic leukemia
CML	Chronic myelogenous leukemia
CO ₂	Carbon dioxide
Combi	Combination
CpG	Cytosine and guanine only separated by one phosphate in small stretches of DNA
CR	Complete remission
CRi	CR with incomplete count recovery
CRISPR-Cas9	Clustered Regularly Interspaced Short Palindromic Repeats - CRISPR-associated protein 9
crRNA	crisprRNA

CTCAE	Common Terminology Criteria for Adverse Events
CtIP	C-terminal binding protein
CTLA-4	Cytotoxic T-lymphocyte-associated protein 4
Ctrl	Control
D	See “Dac”
Dac	Decitabine
DAPI	4',6-diamidino-2-phenylindole
DBD	DNA binding domain
DCs	Dendritic cells
DDR	DNA damage response
DEK	DEK proto-oncogene
del	Deletion
DIP	Database of Interacting Proteins
DMEM	Dulbecco's Modified Eagle Medium
DMSO	Dulbecco's Modified Eagle Medium
DNMT	DNA methyltransferase
DNMT1	DNA methyltransferase 1
DNMT3a/b	DNA methyltransferase 3a/b
DNMTi	DNA methyltransferase inhibitor
DPBS	Dulbecco's phosphate-buffered saline
DSB	Double strand break
DSBR	Double strand break repair
dsDNA	Double stranded DNA

dsRNA	Double stranded RNA
DT	Decitabine+Talazoparib
DTT	Dithiothreitol
ECL	enhanced chemiluminescence
ECOG	Eastern Cooperative Oncology Group
EDTA	Ethylenediaminetetraacetic acid
EGR1	Early Growth Response 1
EMBRACA	Clinical trial Evaluating Talazoparib (BMN 673), a PARP Inhibitor, in Advanced and/or Metastatic Breast Cancer Patients With BRCA Mutation
ER	Endoplasmatic reticulum
ERV	Endogenous retrovirus
ERV-9	endogenous retrovirus type 9
ERV-Fb1	Endogenous Retrovirus Group FB1 Env Polyprotein
ERV-Fc1	Endogenous Retrovirus Group FC1 Env Polyprotein
ERV-Fc2	Endogenous Retrovirus Group FC2 Env Polyprotein
ERV-FRD1	Endogenous Retrovirus Group FRD Member 1, Envelope
ERV-H1	Endogenous Retrovirus Group histone 1
ERV-K1	Endogenous Retrovirus Group K Member 1
ERV-K10	Endogenous Retrovirus Group K Member 10
ERV-K8	Endogenous Retrovirus Group K Member 8
ERV-W1	Endogenous Retroviral Family W, Env(C7), Member 1
ERV-W2	Endogenous Retroviral Family W, Env(C7), Member 2

ERVFXA34	Endogenous Retroviral pol
ERVMER34-1	Endogenous Retrovirus Group MER34 Member 1, Envelope
ERVV2	Endogenous Retrovirus Group V Member 2 Env Polyprotein
ETO	Runx1 translocation partner 1
ETV6	ETS Variant Transcription Factor 6
EZH2	Enhancer of Zeste 2 polycomb prepressive complex 2 subunit
FA	Fanconi anemia
FAB	French-American-British
FANCA	FA Complementation Group
FANCB	FA Complementation Group B
FANCC	FA Complementation Group C
FANCD2	FA Complementation Group D2
FANCE	FA Complementation Group E
FANCF	FA Complementation Group F
FANCG	FA Complementation Group G
FANCI	FA Complementation Group I
FANCL	FA Complementation Group L
FANCM	FA Complementation Group M
FBS	Fetal Bovine Serum
FDA	Food and Drug Administration
FEN1	Flap endonuclease 1
FLT3	FMS-like tyrosine kinase 3
GADD45A	Growth Arrest And DNA Damage Inducible Alpha

Gal-9	Galectin 9
GAPDH	Glyceraldehyde 3-phosphate dehydrogenase
GATA2	GATA binding protein 2
gDNA	Genomic DNA
GEO	Gene Expression Omnibus
GEPIA	Gene Expression Profiling Interactive Analysis
GM-CSF	Granulocyte-macrophage colony-stimulating factor
GO	Gene Ontology
GSEA	Gene Set Enrichment Analysis
GVHD	Graft versus host disease
HAT	Histone acetyltransferase
HDAC	Histone deacetylase
HDACi	Histone deacetylase inhibitors
HEPES	4-(2-hydroxyethyl)-1-piperazineethanesulfonic acid
HER2	human epidermal growth factor receptor 2
HES1	Hes Family BHLH Transcription Factor 1
HI	hematologic improvement
HiDAC	High-dose cytarabine
HIV	human immunodeficiency virus
HMT	Histone methyl transferase
HPRD	Human Protein Reference Database
HSCT	Hematopoietic stem-cell transplantation
HR	Homologous recombination

HRD	Homologous recombination deficiency
H-151	selective small molecule inhibitor of STING
ICs	Immune-checkpoints
IDH1/2	The isoforms 1 and 2 of isocitrate dehydrogenase
IDT	Integrated DNA Technologies
IF	Immunofluorescence
IFI27	Interferon Alpha Inducible Protein 27
IFI30	Interferon Gamma Inducible Protein 30
IFI44	Interferon Inducible Protein 44
IFI6	Interferon Alpha Inducible Protein 6
IFN	Interferon
IFN α	Interferon Alpha
IFN β (IFN β)	Interferon Beta
IFN γ	Interferon Gamma
IFNAR	IFN α/β receptor
IL-10	Interleukin 10
IL-1 α	Interleukin 1 alpha
IL-1 β	Interleukin 1 beta
IL-2	Interleukin 2
IL-21	Interleukin 21
IL-23a	Interleukin 23 subunit alpha
IL-7R	interleukin-7 receptor
IMDM	Iscove's Modified Dulbecco's Medium

IntACT	Common curation platform for 11 molecular interaction databases
Interm	Intermediate
inv	Inversion
IRF-3	IFN regulatory factor 3
IRF-7	IFN regulatory factor 7
IRF-9	IFN regulatory factor 9
ISG15	Interferon-stimulated gene 15
ITD	Internal tandem duplication
IV	Intravenous
IWG	International Working Group
JAK	JAK
KCl	Potassium Chloride
KEGG	Kyoto Encyclopedia of Genes and Genomes
KMT2A	Lysine Methyltransferase 2A
KO	Knock out
KRAS	Kirsten Rat Sarcoma Viral Proto-Oncogene
LDS	lithium dodecyl sulfate
Luc	Luciferase
MCP-1	Monocyte chemoattractant protein-1
MDS	Myelodysplastic syndrome
MDSCs	Myeloid-derived suppressor cells
MECOM	MDS1 And EVI1 Complex Locus
MgCl ₂	Magnesium chloride

MINT	The Molecular Interaction Database
miRNA	Micro RNA
MKL1	Myocardin-related transcription factor A
MLL	Mixed lineage leukemia
MLLT3	MLLT3 Super Elongation Complex Subunit
MNCs	Mononuclear cells
MPAL	Mixed phenotype acute leukemias
MRE11	meiotic recombination 11
MSigDB	Molecular Signatures Database
MTD	Maximum Tolerated Dose
mut	mutant
MYC	Myc- proto-oncogene
MYH11	Myosin heavy chain 11
NaCl	Sodium Chloride
NCI	National cancer institute
ND	Not determined
NER	Nucleotide excision repair
NFκB	NFκB
NIH	National Institutes of Health
NK	Normal Karyotype
NPM1	Nucleophosmin 1
NR	No response
NRAS	Neuroblastoma RAS Viral Oncogene Homolog

NSCLC	Non-Small Cell Lung Cancer
NUP214	Nucleoporin 214
OASL	2'-5'-Oligoadenylate Synthetase Like
OC	Ovarian cancer
OS	Overall survival
PALB2	Partner And Localizer Of BRCA2
PARP	Poly (ADP-ribose) polymerase
PARP1/2	Poly (ADP-ribose) polymerase 1/2
PARPi	Poly (ADP-ribose) polymerase inhibitor
PB	Peripheral blood
PBMCs	Peripheral blood mononuclear cells
PBS	phosphate-buffered saline
PCNA	Auxiliary protein of DNA polymerase delta
PCR	Polymerase chain reaction
PD-1	Programmed death-1
PD-L1	Programmed death -ligand1
PFS	Progression Free Survival
PFT	Pifithrin- α
PML	Promyelocytic leukemia protein
PMR	Pathogen mimicry response
PMSF	Phenylmethylsulfonyl fluoride
PO	Oral administration
POLB	DNA Polymerase Beta

PRR	pattern recognition receptors
pSTING	Phosphorylated STING
PTPN11	Protein Tyrosine Phosphatase Non-Receptor Type 11
PvDF	Polyvinylidene difluoride membranes
qPCR	Quantitative polymerase chain reaction
RAD18	RING-Type E3 Ubiquitin Transferase RAD18
RAD50	DNA Repair Protein RAD50
RAD51	DNA Repair Protein RAD51 Homolog 1
RAD52	DNA Repair Protein RAD52 Homolog
RAR α	Retinoic acid receptor alpha
RBM15	RNA Binding Motif Protein 15
ref	Refractory
rel	Relapsed
RHOB	Ras Homolog Family Member B
RIPA	Radioimmunoprecipitation assay buffer
RNA	ribonucleic acid
RNAi	RNA interference
RNAseq	RNA-sequencing
RP2D	Recommended Phase II Dose
RPA	Replication protein A
RPMI	Roswell Park Memorial Institute
RT-qPCR	Quantitative reverse transcription PCR
Runx1/2	Runt related transcription factor 2

Runx1T1	RUNX1 Partner Transcriptional Co-Repressor 1
Rux	Ruxolitinib
SCT	Stem cell transplant
SEM	Standard error of the mean
SERPINB8	Serpin Family B Member 8
SDS	sodium dodecyl sulfate
sgRNA	Single guide RNA
SRSF2	Serine And Arginine Rich Splicing Factor 2
SSB	Single strand break
SSBR	Single strand break repair
STAR-EdgeR	Spliced Transcripts Alignment to a Reference – Empirical Analysis of Digital Gene Expression Data in R
STAT	Signal transducer and activator of transcription
STING	Stimulator of interferon genes
STRING	Search Tool for the Retrieval of Interacting Genes/Proteins
SUZ12	SUZ12 Polycomb Repressive Complex 2 Subunit
T	See “Tal”
Tal	Talazoparib
TBK1	TANK Binding Kinase 1
TBST	Tris-buffered saline with tween
TCGA	The Cancer Genome Atlas
TET2	Tet Methylcytosine Dioxygenase 2
TIM-3	T cell immunoglobulin mucin-3

TKD	Tyrosine kinase domain
TMEM173	Gene that encodes STING protein
TNBC	Triple negative breast cancer
TNF	Tumor necrosis factor
TNF α	Tumor necrosis factor alpha
TP53	Tumor protein 53
Tregs	Regulatory T cells
TRIB1	Tribbles homolog 1
TSG	tumor suppressor genes
UMGCC	University of Maryland Greenebaum Comprehensive Cancer Center
UMB	University of Maryland Baltimore
VAI	Van Andel Institute
WHO	World Health Organization
WT	Wild Type
XRCC2	X-Ray Repair Cross Complementing 2

CHAPTER 1: Introduction

1.1 Acute Myeloid Leukemia

Leukemia is a cancer that occurs in blood stem cells that produce the various types of blood cells¹. There are several types of leukemia, which are classified based on the lineage of blood cell affected (myeloid vs lymphoid) (Figure 1.1; green highlight), as well as the degree of differentiation and the speed of disease progression (chronic vs acute) (Figure 1.1; yellow highlight)². **Chronic leukemias** progress slowly, with the majority of the leukemia cells made up of relatively mature, but abnormal, cells³. Chronic leukemias are further subdivided into two subgroups based on the lineage of the leukemia-initiating cell: *Chronic myeloid leukemia* (CML) occurs in primitive myeloid cells that normally develop into granulocytes.¹ The hallmark of CML is the t(9;22) translocation, also known as “Philadelphia chromosome,” which creates the fusion gene BCR-ABL1.¹ *Chronic lymphocytic leukemia* (CLL) is a leukemia that occurs in cells of lymphoid lineage, and results in abnormal accumulation of mature B-lymphocytes.⁴ **Acute leukemias**, on the other hand, are characterized by an abnormal increase of immature white blood cells, or “blasts,” in the bone marrow^{5,6}. In contrast to chronic leukemias, acute leukemias progress rapidly, and are fatal if not treated effectively immediately after diagnosis⁷. Similar to chronic leukemias, acute leukemias can be categorized into two subtypes based on the lineage of the cell initiating the leukemia: *Acute lymphoblastic leukemia* (ALL) is an aggressive leukemia that occurs in immature lymphoid cells that give rise to B- or T-lymphocytes⁸, while *acute myeloid leukemia* (AML) is a bone marrow-based malignancy characterized by accumulation and proliferation of

abnormal immature blood cells of the myeloid lineage, known as myeloblasts.⁹ Given that AML is the focus of this dissertation, it is described in greater detail below.

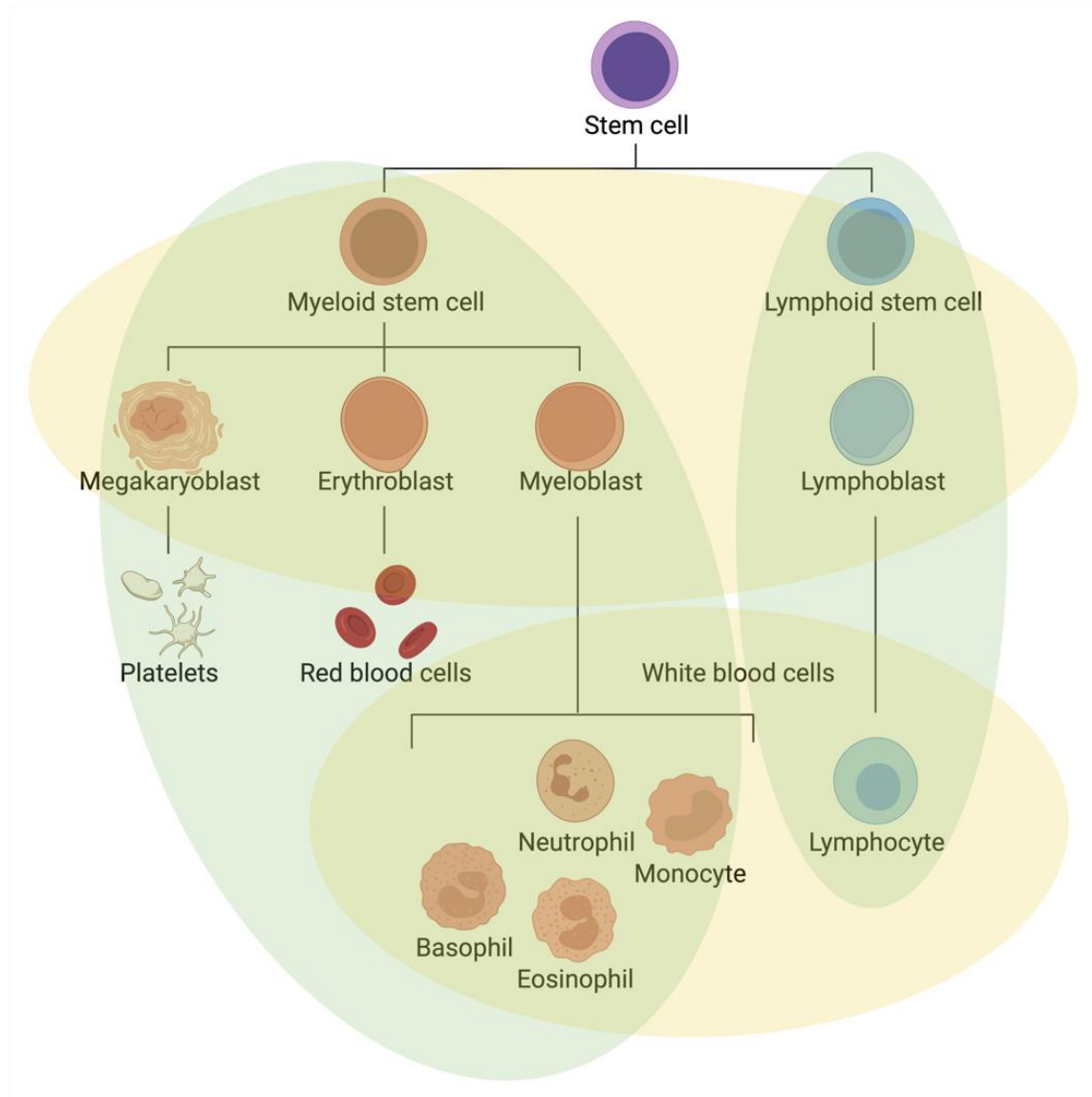


Figure 1.1: Blood cell development. A blood stem cell goes through several steps to become a red blood cell, platelet, or white blood cell. Created with BioRender.com.

There are also **mixed phenotype acute leukemias** (MPALs) which, as the name implies, represent a subtype with blasts with surface markers of both lymphoid and myeloid lineages¹⁰. MPALs are often aggressive and predominantly occur in pediatric patients¹⁰.

AML is diagnosed by an overabundance of myeloid blasts in the bone marrow or the peripheral blood that account for 20% or more of total nucleated cells^{11,12}. AML is the common form of acute leukemia in adults, accounting for approximately 80% of cases¹³. AML most frequently arises de novo, although some patients develop secondary AML from either progression of an antecedent myeloid malignancy or cytotoxic therapy used to treat prior cancers or non-malignant diseases^{14,15}. It is a cytogenetically and molecularly heterogeneous disease, and these alterations have prognostic importance, that will be discussed below¹⁶.

1.1.1 Classification

The two main systems used to classify AML are the French-American-British (FAB) classification and the World Health Organization (WHO) classification. The FAB classification divides AML into nine subtypes, based on the type of myeloid cell from which the AML arises, and the degree of differentiation^{14,17-19}. These subtypes are designated M0 through M7, and are summarized in Table 1.1¹⁸. Subtypes M0 through M5 are initiated in immature white blood cells; M6 occurs in immature forms of red blood cells; and M7 occurs in cells that produce platelets²⁰.

Table 1.1: The FAB classification of AML

Subtype	Morphological description
M0	Undifferentiated acute myeloblastic leukemia
M1	Acute myeloblastic leukemia with minimal maturation
M2	Acute myeloblastic leukemia with maturation
M3	Acute promyelocytic leukemia (APL)
M4	Acute myelomonocytic leukemia
M4 _{EO}	Acute myelomonocytic leukemia with bone marrow eosinophilia
M5	Acute monocytic leukemia
M6	Acute erythroid leukemia
M7	Acute megakaryoblastic leukemia

A more recent AML classification is the World Health Organization (WHO) classification, which mainly classifies AML based on genetic abnormalities, myelodysplasia-related changes, therapy-related AML, and other AMLs that do not fall in the aforementioned categories²¹⁻²³. A summary of the WHO classification of AML is found in Table 1.2^{21,23}.

Table 1.2: The WHO classification of AML

Subtype	Morphological description
AML with recurrent genetic abnormalities	AML with t(8;21)(q22q22.1); <i>RUNX1-RUNX1T1</i>
	AML with inv(16)(p13.1q22) or t(16;16)(p13.1;q22); <i>CBFB-MYH11</i>
	APL with t(15;17)(q22;q21), (PML/RAR α) and variants
	AML with t(9;11)(p21.3;q23.3); <i>KMT2A-MLLT3</i>
	AML with t(6;9)(p23;q34.1); <i>DEK-NUP214</i>
	AML with inv(3)(q21.3q26.2) or t(3;3)(q21.3;q26.2); <i>GATA2, MECOM</i>
	AML (megakaryoblastic) with t(1;22)(p13.3;q13.1); <i>RBM15-MKLI</i>
	AML with mutated <i>NPM1</i>
	AML with biallelic mutation of <i>CEBPA</i>
AML with multilineage dysplasia	Following MDS or MDS/MPD
	Without antecedent MDS or MDS/MPD, but with dysplasia in at least 50% of cells in 2 or more myeloid lineages
AML and MDS, therapy-related	Alkylating agent/radiation-related type
	Topoisomerase II inhibitor-related type (some may be lymphoid)
	Others
AML, not otherwise specified	AML, minimally differentiated
	AML, without maturation
	AML, with maturation
	Acute myelomonocytic leukemia
	Acute monoblastic/acute monocytic leukemia
	Acute erythroid leukemia (erythroid/myeloid and pure erythroleukemia)
	Acute megakaryoblastic leukemia
	Acute basophilic leukemia
	Acute panmyelosis with myelofibrosis
Myeloid sarcoma	
Myeloid proliferations associated with Down syndrome	Transient abnormal myelopoiesis (TAM) associated with Down syndrome
	Myeloid leukemia associated with Down syndrome

1.1.2 Genetic abnormalities

One of the hallmarks of AML is the degree of heterogeneity with respect to cytogenetic abnormalities. Additionally, over 50% of newly diagnosed cases of AML also exhibit molecular aberrations²⁴. As mentioned above, cytogenetic and molecular changes are of greatest importance in determining prognosis, including likelihood of relapse and overall survival (OS), in AML patients⁹ and cytogenetic and molecular data are increasingly being used to inform clinical care of patients²⁴. The European LeukemiaNet (ELN) has developed a classification based on genetic abnormalities that includes three risk stratification groups: favorable, intermediate and adverse. The favorable risk group includes translocations such as those that result in the AML-ETO fusion protein, inversion of chromosome 16, and mutations in NPM1 and CEBPA. The intermediate risk group typically includes patients presenting with normal karyotype, and those with cytogenetic abnormalities that have not been classified as either favorable or adverse. The adverse risk group is the largest of the three risk stratification groups and includes various chromosomal aberrations such as translocations, inversion and monosomy and complex karyotypes (three or more unrelated chromosomal abnormalities), as well as various mutations in genes such as FLT3, RUNX1 and TP53 (Table 1.3)²⁵.

Table 1.3: AML classification based on cytogenetics and molecular markers

Abnormality	Risk
t(8;21)(q22;q22.1); AML-ETO (RUNX1-RUNX1T1)	Favorable
inv(16)(p13.1q22) or t(16;16)(p13.1;q22); CBFB-MYH11	
NPM1 mutation	
CEBPA mutation	
t(9;11)(p21.3;q23.3); MLLT3-KMT2A	Intermediate
Normal karyotype	
Cytogenetic abnormalities not classified as favorable or adverse	
t(6;9)(p23;q34.1); DEK-NUP214	Adverse
t(v;11q23.3); KMT2A rearrangement	
t(9;22)(q34.1;q11.2); BCR-ABL1	
inv(3)(q21.3q26.2) or t(3;3)(q21.3;q26.2); GATA2, MECOM(EV11)	
-5 or del(5q); -7; -17/abn(17p)	
Monosomy 5	
Monosomy 7	
Complex karyotype	
FLT3-ITD	
RUNX1 mutation	
ASXL-1 mutation	
TP53 mutation	

Genetic abnormalities in AML can be divided into two main groups: 1. Chromosomal translocations that most often result in loss-of-function of transcription factors that are required for normal hematopoietic development, known as *master regulators*²⁶. 2. Activating translocations that result in overexpression of *partner genes*, conferring a proliferative advantage to hematopoietic progenitors²⁷. The two genetic alterations cooperate to cause an acute leukemia phenotype characterized by proliferation and impaired differentiation^{9,26}.

1.1.2.1 Translocations in master regulator genes

A common translocation observed in AML is t(8;21), resulting in the AML1-ETO fusion protein²⁸. AML1, also known as RUNX1, is a transcription factor involved in regulating hematopoietic differentiation; when it is fused with ETO, ETO causes transcriptional repression at target sites of AML1^{28,29}. Nevertheless, AML with t(8;21) has a favorable prognosis, as it responds well to therapy³⁰. Another common subtype of AML with favorable prognosis is AML with inversion in chromosome 16 [inv(16)], which results in the expression of the CBF β -MYH11 fusion protein, and disrupts the interaction of CBF β with AML1, leading to similar consequences as in the case of AML1-ETO⁹. MLL rearrangements, which are less frequent, result from translocations involving chromosome 11 (11q23), resulting in more than 30 MLL fusion genes³¹⁻³⁴. The most common MLL fusion gene in AML is MLL-AF9 resulting from t(9;11) translocation^{34,35}. Some MLL rearrangements in acute leukemias occur secondary to topoisomerase II therapy and are often associated with poor prognosis^{33,36}. Other chromosomal abnormalities that are present in AML include deletions in chromosomes 5 and 7, inversion of chromosome 3 [inv(3q)], trisomy 8 and complex karyotype³⁷.

1.1.2.2 Mutations in partner genes

Despite the fact that over 700 chromosomal abnormalities have been identified in AML, nearly 50% of AML patients have normal karyotypes (NK) while still exhibiting variable responses to chemotherapy^{9,38}. This variation in treatment response can be explained by the presence of recurrent mutations that influence the response to therapy⁹. Similar to chromosomal abnormalities, these gene mutations can serve as prognostic factors. For example, AMLs with mutations in the *NPM1* and *CEBPA* genes have a

favorable outcome, while mutations in *DNMT3A*, *IDH1/2*, *TET2*, *FLT3*, and *TP53* genes are associated with an unfavorable outcome²⁴. *DNMT3A* mutations result in hypomethylation of genes involved in hematopoiesis, and the aberrant chromatin remodeling results in anthracycline therapy resistance³⁹. *IDH1/2* and *TET2* mutations are linked, as *IDH1/2* catalyze the conversion of isocitrate in the Krebs cycle to α -ketoglutarate (α -KG), which is essential for *TET2* activity⁴⁰. Mutations in *IDH1/2* result in the production of 2-hydroxyglutarate, leading to impairment of *TET2* function and abnormal DNA methylation^{41,42}. Mutations in *FLT3* occur in about 30% of AML patients⁴³ and include internal tandem duplications (ITD) in the juxtamembrane domain of *FLT3*, known as *FLT3/ITD*, as well as mutations in the tyrosine kinase domain (TKD), referred to as *FLT3/TKD* mutations^{44,45}. Given that my thesis explores the effect of *TP53* mutations on immune responses in AML, the role of *TP53* mutations in AML is expanded on below.

1.1.2.3 Role of *TP53* mutations in AML

TP53 is one of the most frequently mutated genes in human malignancies^{15,46}. Unlike in many other cancers, *TP53* alterations comprise a small percentage of abnormalities in AML⁴⁶. While mutations in *TP53* are observed in only 5–10% of AML cases, they are highly associated with poor prognosis and poor long-term survival (Figure 1.2)^{47,48}. In fact, median overall survival (OS) is significantly reduced in patients with *TP53* mutations compared with wild-type (WT)^{48,49}.

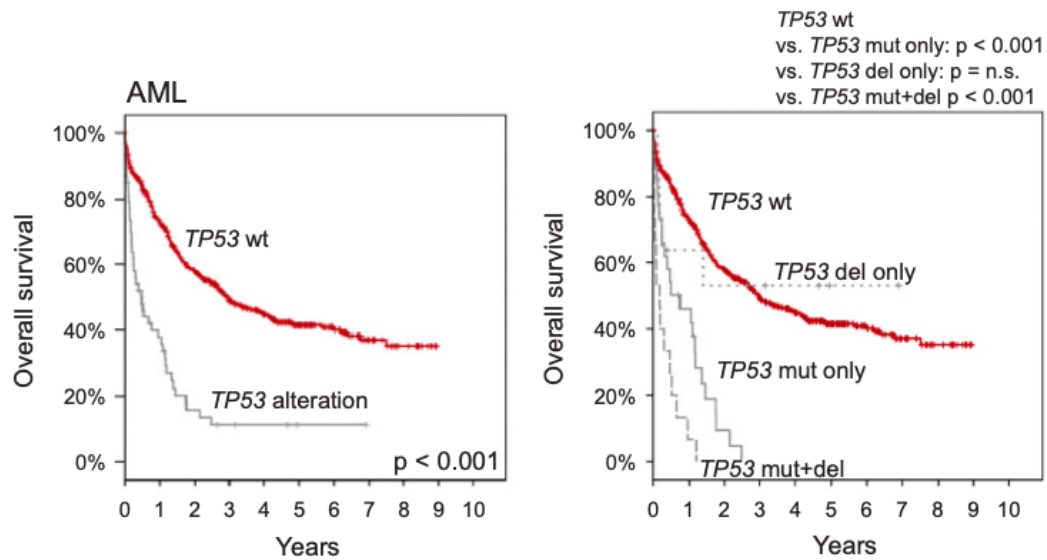


Figure 1.2: Overall survival of patients with TP53 alteration. In the left panel, OS was analyzed in AML patients with (gray line) and without (red line) TP53 alteration. In the right panel, the OS was analyzed in patients with TP53 mutation only (TP53mut only, continuous gray line), with TP53 deletion only (TP53del only; dotted gray line) in patients that showed alterations in both alleles (TP53mut +del, broken gray line) and in patients without aberrations in TP53 (TP53wt; red line). Figure adapted from Stengel et. al, 2017⁴⁸.

While in some studies TP53 deletions have less dismal outcomes in terms of OS⁴⁸, it has not yet been elucidated whether outcomes vary across distinct types of TP53 mutations (non-sense, missense, deletions, insertions, splice site mutations)⁵⁰. In fact, numerous studies have shown no differences in terms of OS between AML patients with TP53 missense mutations and truncating aberrations^{15,51-53}. Recently, a synthetic TP53 mutation dataset was created to calculate the functional impact of DNA-binding domain (DBD) TP53 alterations in human cells in culture and *in vivo*⁵⁴. Unlike for other tumor suppressor genes, the majority of p53 mutations are missense mutations

occurring in the DBD (Figure 1.3)⁵⁴⁻⁵⁶. These mutations lead to the loss of its tumor suppressive activity and may lead to gain of novel oncogenic functions⁵⁷.

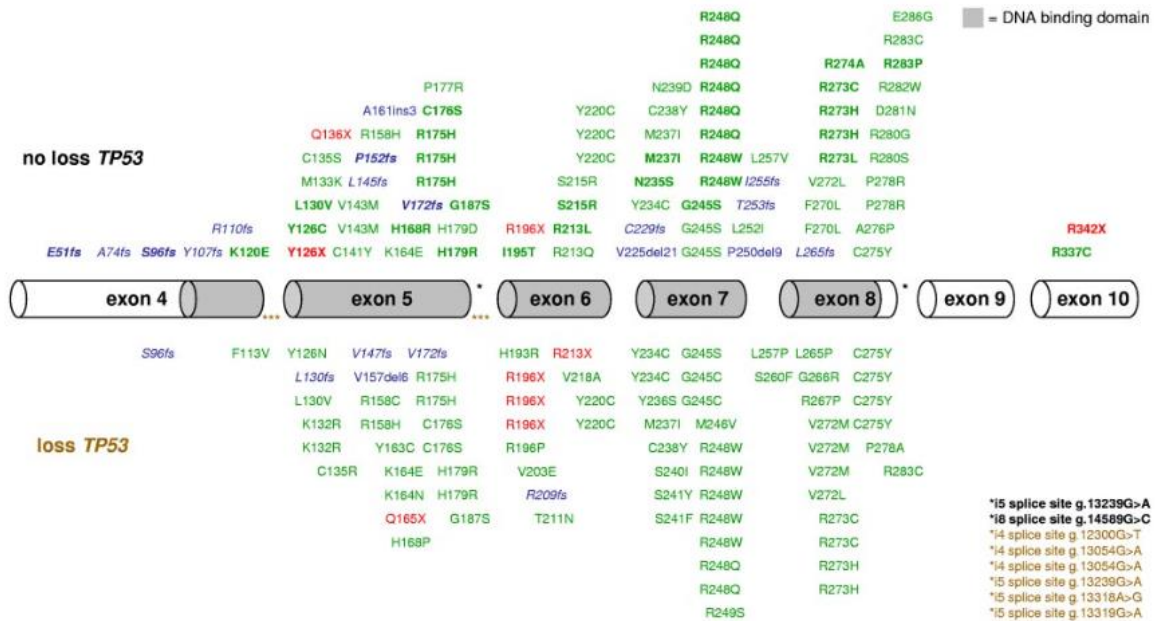


Figure 1.3: Mapping of 168 *TP53* mutations in 141 CK-AMLs. Hemizygous mutations are indicated in the bottom panel, heterozygous, and/or homozygous mutations are marked in the top panel. Exons 4 to 10 are drawn to relative scale; missense mutations (green), nonsense mutations (red), and insertion/deletion mutations (blue) are shown at their approximate location along the exons. Bold represents homozygous mutations, and blue italics, frameshift mutations leading to a premature stop codon. Figure from Rucker et. al, 2012⁵⁸.

1.1.3 Epigenetic dysregulation¹

While cytogenetic and genetic alterations play key roles in AML biology and prognosis (as discussed above), epigenetic changes that induce heritable changes without changing the DNA sequence⁵⁹⁻⁶¹ also contribute to the pathogenesis of AML^{60,62}. The two main mechanisms of epigenetic regulation in the cell are DNA methylation and post-translational histone modification (Figure 1.4)⁶³. Additionally, there is growing evidence that microRNAs are another dimension to epigenetic control of hematopoiesis and leukemogenesis contributing to the epigenetic landscape⁵⁹⁻⁶¹.

¹ Kogan AA, Lapidus RG, Baer MR, Rassool FV. Exploiting epigenetically mediated changes: Acute myeloid leukemia, leukemia stem cells and the bone marrow microenvironment. *Adv Cancer Res.* 2019;141:213-253. doi: 10.1016/bs.acr.2018.12.005. Epub 2019 Jan 21. PMID: 30691684.

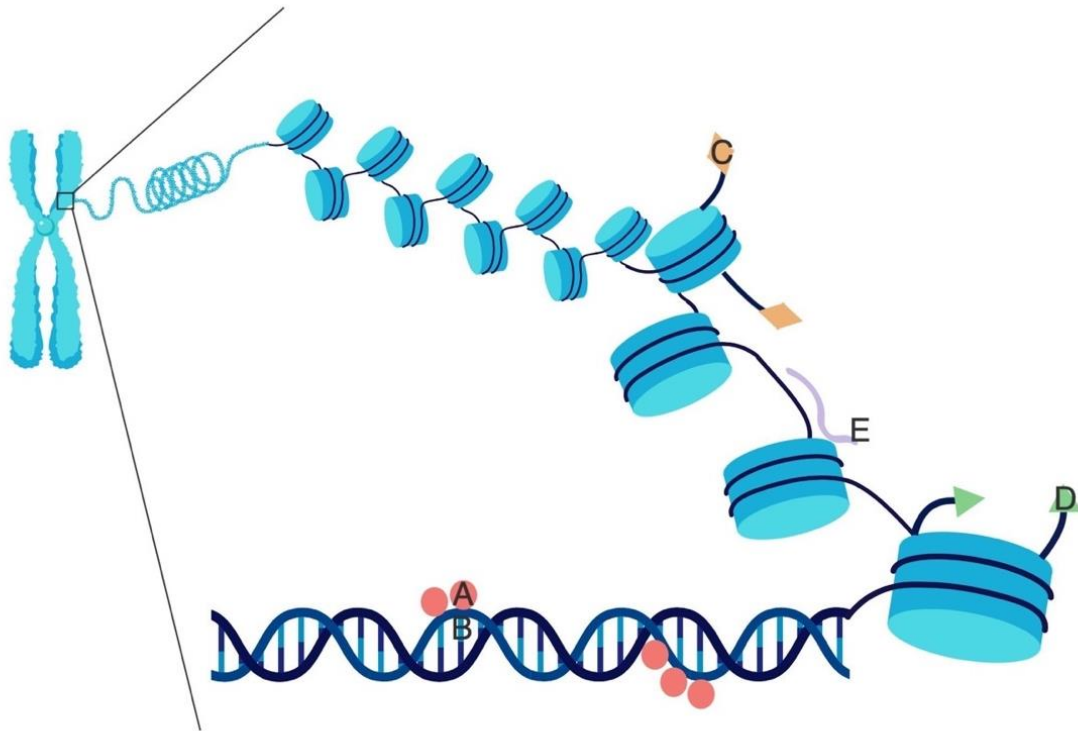


Figure 1.4: Fundamental mechanisms of epigenetic regulation. (1) DNA methylation by the addition of a methyl group (A) to cytosine (B) at CpG sites. (2) Histone modifications via the binding of enzymes and proteins (C) to histone tails (D). (3) RNA based mechanisms modulate gene expression via non-coding RNA (E). Created with BioRender.com.

1.1.3.1 DNA Methylation

Cytosines in the CpG motif are methylated by enzymes called DNA methyltransferases (DNMTs). DNMT1 is the most abundant DNMT in mammalian cells and is considered to be the key maintenance methyltransferase in mammals. In contrast, DNMT3a and DNMT3b are responsible for de novo DNA methylation patterns, which are then copied to daughter cells during S-phase by DNMT1⁵⁹. Control of gene expression is derived through methylation of cytosine residues in areas high in CpG density, termed CpG

islands(Figure 1.4)^{64,65}. While non-CpG island methylation is reversible, methylation of CpG islands persists through mitosis and is only physiologically reversible in the embryo. In normal cells, methylation of CpG sites is consistent; genes that are highly expressed generally have hypomethylated CpG islands, while genes whose CpG islands are hypermethylated usually are not expressed⁶⁶. DNA methylation alterations are a common feature in hematological malignancies. Hypermethylation of cytosines in CpG islands is directly associated with silencing of tumor suppressor genes^{67,68}. While the focus of DNA methylation research, particularly as it relates to cancer, has been CpG island promoter methylation, leukemogenesis has been associated with both hypo- and hypermethylation of CpG islands at different loci as well as global methylation changes, although the pathological mechanisms remain unclear^{63,67}.

1.1.3.2 Histone modifications

The amino-terminal tails of histones are subjected to a variety of post-translational modifications (Figure 1.4)⁶⁹. These modifications are reversible to accommodate cellular requirements for gene expression⁶⁰. Histone methyltransferases (HMTs) are responsible for methylation of histones, while acetylation is catalyzed by histone acetyltransferases (HATs) and deacetylation by histone deacetylases (HDACs)⁶⁹. The complex interplay between HMTs, DNMTs, HATs and HDACs in epigenetic pathways contributes to aberrant gene expression in cancer cells⁶⁹. Despite lack of specificity, targeting histone modifications has been clinically successful. For example, the HDAC inhibitor (HDACi) valproic acid induces differentiation of leukemic blasts and decreases tumor growth in vivo⁷⁰. The development of therapeutics that target specific histone-modifying enzymes will potentially increase their therapeutic success while decreasing side effects due to the

lack of specificity. On the other hand, targeting individual histone-modifying enzymes may decrease clinical efficacy due to compensation by other histone-modifying enzymes, potentially leading to resistance. Designing personalized cocktails of inhibitors based on an individual's tumor epigenetic profile may help overcome the potential problems of compensation and resistance.

1.1.3.3 MicroRNAs in epigenetic regulation

MicroRNAs (miRNAs) are a family of small, non-coding RNAs that regulate gene expression and play an important role in hematopoietic cell fate^{71,72}. They can regulate multiple target genes, and modulate the expression of oncogenes as well as tumor suppressors⁷². There is growing evidence that microRNAs provide another dimension to epigenetic control of hematopoiesis and leukemogenesis⁶¹. miRNAs are interesting therapeutic targets because one miRNA can alter several pathways, and restoring the function of a misregulated miRNA may be more effective than identifying different misregulated pathways and proteins and targeting them separately⁵⁹. However more research is needed to better understand miRNA profiles in healthy and diseased tissues in order to develop better therapeutic strategies.

1.1.4 Immune signaling in AML

AML cells have genetically and epigenetically dysregulated genes, which can be recognized as foreign antigens and targeted by the immune system^{73,74}. The immune system is regulated by an essential balance between inhibitory and stimulatory immune-checkpoints (ICs) which determine the antigen-specific immune responses⁷⁵. However, similar to solid tumors, AML cells can activate immune evasion mechanisms to escape from host immune responses in order to avoid immune-mediated elimination⁷⁶⁻⁷⁸. These regulatory mechanisms include

expression of negative costimulatory ligands, such as programmed death-ligand 1 (PD-L1), cytotoxic T-lymphocyte-associated protein 4 (CTLA-4), and galectin 9 (Gal-9) on AML cells, as well as stimulating the expansion of regulatory T cells (Tregs) and myeloid-derived suppressor cells (MDSCs)^{78,79}. Furthermore, previous studies have shown that DNA methylation and histone modification play an important role in the dysregulation of ICs^{79,80}. The interactions between ICs and their ligands lead to disruption of antigen-presenting cell (APC) function which, in turn, leads to the reduction of T-cell proliferation and cytokine release resulting in T cell apoptosis and associated increased activity of Tregs and MDSCs⁷⁹. More recently, Zhang et al. have shown that leukemia-specific CD8⁺ T cells were deleted from the host animal with AML⁹. The deletional T cell tolerance in these AML-bearing hosts seemed to be regulated by host APCs, as administration of an agonistic anti-CD40 antibody resulted in increased anti-leukemia T cell immunity and prolonged survival⁹. Further investigation of this has implicated a subset of host dendritic cells (DCs), called CD8 α ⁺ DCs, in the observed T cell tolerance suggesting a role for innate immunity in the initiation of this process^{6,10}.

Type I interferon (IFN) are rapidly produced after the activation of pattern-recognition receptors (PRRs) as part of the antiviral innate immune response and its role in anti-tumor immunity has been well characterized^{11,12}. Type I IFN signaling is critical to the generation of T cell responses that lead to tumor elimination^{13,14}. Woo et. al showed that cytosolic DNA from dying tumor cells may induce type I IFN production through the activation of a cytosolic DNA-sensing receptor called stimulator of interferon genes (STING)¹⁵. Subsequent studies have expanded on this and shown that upregulation of endogenous retroviral transcripts (ERVs) and sensing of cytoplasmic double-stranded RNA (dsRNA) can also lead to STING-mediated type I IFN signaling^{16,17}. Upon its activation, STING translocates from the endoplasmic reticulum

(ER) to the Golgi, where it recruits tank binding kinase 1 (TBK1), resulting in its phosphorylation and activation of the transcription factor interferon regulatory factor-3 (IRF-3) which then translocates to the nucleus to activate transcription of type I IFN^{6,18}. Studies by Curran et al. in C1498 AML-bearing mice have shown that administration of STING agonists results in expansion of functional leukemia antigen-specific T cells and improved survival¹⁸. Studies in solid tumors have shown that other agents, such as DNA methyltransferase inhibitors (DNMTis), can induce a similar effect centered on potentiation of STING-mediated interferon IFN signaling^{17,19}. These data suggest that the STING pathway may be an effective target for the treatment of AML which will be explored throughout this body of work.

1.2 Treating AML

While standard chemotherapy for AML has not changed significantly since the 1970s, progress is now being made in the development of targeted therapies⁸⁴⁻⁸⁶. Research efforts in the last decade have expanded our knowledge at cytogenetic and molecular levels and has enabled the development of targeted therapies based on AML subtype⁸⁶. In the last five years alone, numerous agents have been approved for different indications in AML, including the BCL-2 inhibitor venetoclax, FLT-3 inhibitors, and IDH inhibitors⁸⁶. The heterogeneity of AML makes its management complicated and underscores the need for optimal targeted therapies to achieve better outcomes^{85,86}.

1.2.1 Current Therapy

Treatment of AML currently consists of two phases: 1) induction chemotherapy, and 2) post-remission therapy⁸⁷. Patients are initially treated with a combination chemotherapy regimen commonly referred to as 7+3^{87,88}. This conventional induction chemotherapy consists of the nucleoside analog cytarabine (Ara-C) administered by intravenous infusion for 7 days,

combined with an anthracycline (commonly daunorubicin or idarubicin) administered by bolus intravenous injection daily for 3 days⁸⁸⁻⁹⁰. Cytarabine, or cytosine arabinoside, is incorporated into DNA during replication as a cytosine, then is converted to cytosine arabinoside triphosphate, leading to inhibition of DNA synthesis⁹¹. Daunorubicin is a member of the topoisomerase II inhibitor family that intercalates into DNA and stabilizes topoisomerase II-DNA complexes, leading to impaired DNA replication⁹². Idarubicin is a daunorubicin alternative that was introduced in the 1980s⁹³. These anthracyclines are critical components of chemotherapy regimens used to treat AML⁸⁸. Induction chemotherapy aims to induce complete remission (CR) by causing cytotoxicity in AML cells. CR is achieved in 60-80% of adults less than 60 years, but only 40-60% of adults over 60 years of age^{9,87}. When patients do not respond to the standard regimen, salvage chemotherapy regimens are administered, or patients are enrolled in clinical trials of novel agents⁹⁴. When patients achieve CR, a second phase of treatment, post-remission therapy, is highly important in preventing relapse⁹⁵.

Standard post-remission strategies include consolidation chemotherapy consisting of high-dose cytarabine (HiDAC) or hematopoietic stem cell transplantation (HSCT)⁸⁷. The genetic risk profile of patients and the risk of transplant-related morbidity and mortality determine which post-remission treatment strategy will be recommended⁹⁶. AML patients 60 years and younger with favorable genetic risk typically receive 4 cycles of HiDAC as consolidation chemotherapy^{95,97}. Patients with adverse genetic risk typically undergo HSCT⁹⁸. For adults with intermediate genetic risk, however, both HiDAC and HSCT are acceptable options⁹⁹. DNA demethylating agents are frequently used instead of intensive chemotherapy to treat older patients with comorbidities, poor performance status and/or adverse genetic risk¹⁰⁰. This older and more unfit patient population may also be recommended to participate

in clinical trials of investigational therapies, when available¹⁰¹. Given both the incidence of refractory disease and the high relapse rate in AML, research on novel agents and treatment combinations is ongoing to improve treatment outcome and prolong OS¹⁰².

1.2.2 Targeting DNA methylation²

As discussed above, hypermethylation of promoters of CpG-island-containing DNA regions lead to transcriptional silencing of tumor suppressor genes (TSGs) in cancers and leukemias, and DNA methyltransferase inhibitors (DNMTis) have been developed that can reverse these effects¹⁰³. 5-Azacytidine (AZA) is a nucleoside analog that incorporates into RNA and is subsequently transcribed into DNA. 5-Aza-2- deoxycytidine (decitabine; DAC) is the deoxy derivative of AZA?? and is incorporated directly into DNA¹⁰⁰. AZA and DAC sequester and inhibit methylation enzymes after their incorporation into RNA and DNA, respectively (Figure 1.5)¹⁰⁴. Both AZA and DAC are approved by the United States Food and Drug Administration (FDA) to treat high-risk MDS patients. Successful clinical results have also been reported in AML^{100,105,106}, so both drugs are also commonly used to treat AML.

² Kogan AA, Lapidus RG, Baer MR, Rassool FV. Exploiting epigenetically mediated changes: Acute myeloid leukemia, leukemia stem cells and the bone marrow microenvironment. *Adv Cancer Res.* 2019;141:213-253. doi: 10.1016/bs.acr.2018.12.005. Epub 2019 Jan 21. PMID: 30691684.

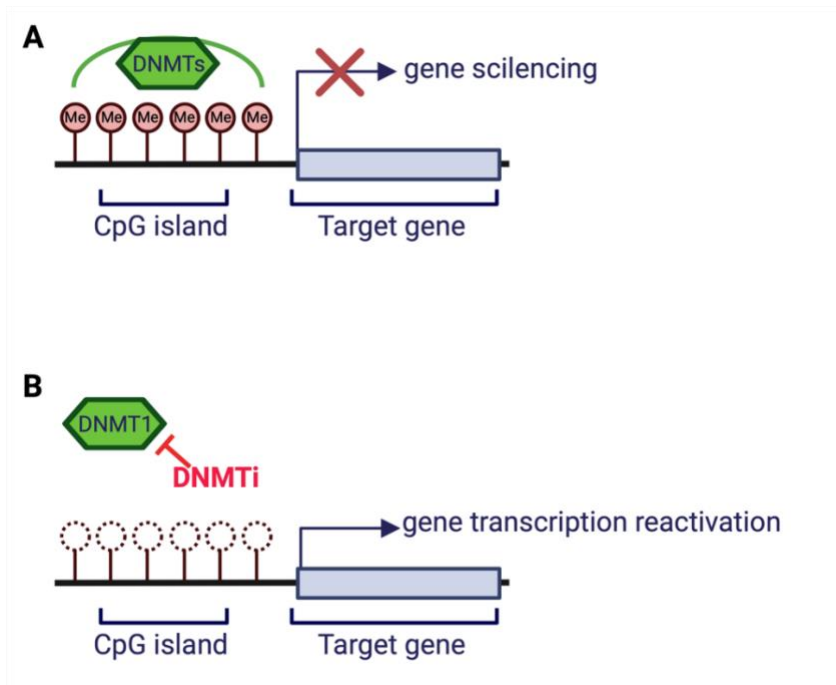


Figure 1.5: DNA methylation and inhibition. (A) DNMTs promote methylation of CpG-island containing promoters and subsequent gene silencing. (B) DNMTis prevent methylation from occurring resulting in gene transcription reactivation. Figure modified from Gravina et al. (2010)¹⁰⁷. Created with BioRender.com.

While these drugs used at high concentrations produce direct DNA damage and cytotoxicity, these effects are not the primary mechanisms responsible for clinical efficacy in patients with MDS or AML. The Baylin group reported that transient exposure of cultured and primary leukemia and epithelial tumor cells to epigenetic drugs at nanomolar concentrations can reprogram multiple cancer pathways in the Hanahan and Weinberg “cancer wheel”¹⁰⁸ (Figure 1.6).

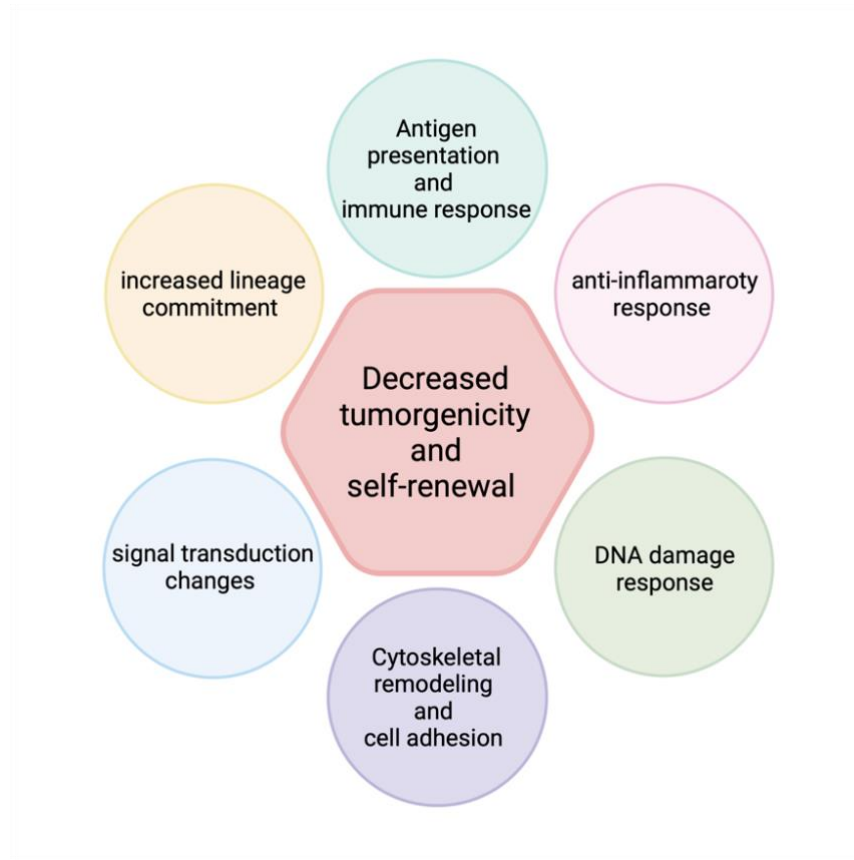


Figure 1.6: Pathway analysis of changes in gene expression following DNMTi treatment.

Microarray analyses post DNMTi treatment show stable changes in the expression of multiple genes, also known as transcriptional reprogramming, in cancer pathways defined by Weinberg and Hanahan. Figure modified from Tsai, et al. (2012)¹⁰⁴. Created with BioRender.com.

Low doses of these epigenetic drugs can lead to re-sensitization of cancer cells to cytotoxic chemotherapy, and combination treatments with epigenetic plus traditional drugs may be a promising approach^{109,110}. Since cytotoxic chemotherapy kills cells by activating pro-apoptotic genes, and DNA methylation of these pro-apoptotic genes can block cell death from occurring, reactivation of epigenetically silenced apoptotic genes by DNMTis can increase the efficacy of chemotherapy¹¹⁰. For example, APAF1 is silenced in metastatic melanoma cells

and treatment with AZA restores APAF1 expression and chemosensitivity¹¹¹. Conversely, methylation-induced silencing of DNA repair genes can be detrimental by leading to microsatellite instability, or even beneficial by preventing the repair of genes targeted by chemotherapy, causing cells to undergo apoptosis rather than repair¹¹².

Continued work is aimed at understanding how DNMTs function, and at identifying biomarkers of response. Overall, it is possible that effective therapy may require agents that target other aspects of the epigenome, and that synergize more effectively with a variety of combination treatments. For example, there are ongoing studies testing combinations of hypomethylating agents and biological agents such as retinoic acid, and promising results have also been described for the combination of DAC with IL-2 in melanoma. Reversal of DNA methylation using DNMTs can also overcome chemoresistance induced by gene silencing, and suggests additional combination options^{59,106}.

Despite the clinical successes achieved with DNA methylation inhibitors, there is still much room for improvement. Currently available DNA methylation inhibitors block DNA methylation at the enzymatic level, leading to global DNA methylation inhibition. This is therapeutically beneficial as tumor suppressor genes are hypermethylated in cancer, but global hypomethylation may lead to activation of oncogenes and/or increased genomic instability¹⁰⁶. Furthermore, DNA methylation inhibitors act during S-phase of the cell cycle, and thus they preferentially affect dividing cells. This is advantageous when treating cancers that grow rapidly, but may be less clinically useful in treating cancers that are not characterized by rapid cell cycling¹⁰⁶. Additionally, upon DNMTi withdrawal, DNA methylation returns to pre-treatment levels, resulting in a need for continuous DNMT inhibition^{59,113}. Thus, while DNA methylation inhibitors are clinically successful, their lack of specificity, cell cycle dependency

and need for continuous administration leave room for the development of other targeted therapies or novel combination therapies⁶⁶. Since my thesis work focuses on a novel combination of DNMTis and poly ADP-ribose polymerase inhibitors (PARPis) in AML, the next section discusses PARPis.

1.3 PARP inhibitors

Poly(ADP-ribose) polymerase 1 (PARP1) is a nuclear protein that plays a key role in DNA single-strand break (SSB) repair through poly-(ADP-ribosyl)ation, or PARylation, of itself, histones and other target proteins^{114,115}. PARPs have been classically linked to base excision repair (BER, single-strand break repair), by binding to the site of damage and recruiting DNA repair machinery¹¹⁶. However, it has also been shown to be involved in nucleotide excision repair (NER, repair of bulky DNA adducts) and there is increasing evidence for its role in double-strand break (DSB) repair, including alternative non-homologous end-joining (ALT NHEJ)^{117,118}. Though essential for maintaining genome integrity, PARP1 over-activity has been linked to several types of cancers, leading to the development of PARP1 inhibitors (PARPis)^{115,116}.

The mechanism of action of the majority of early PARPis was via catalytic inhibition of PARP by blocking its PARylation activity^{115,119}. More recently, another mechanism of PARP inhibition was revealed. The primary cytotoxic effects of a new generation of PARPis have been correlated with trapping of cytotoxic PARP1-DNA complexes at sites of SSBs and DSBs (Figure 1.7)^{120,121}. The potent PARPi talazoparib (Tal), which mainly exerts its cytotoxic effects through trapping PARP in DNA, is used in our studies in the next chapters. Importantly, the trapped PARP1-DNA complexes lead to stalling and collapsed replication forks, which require additional mechanisms to repair^{122,123}.

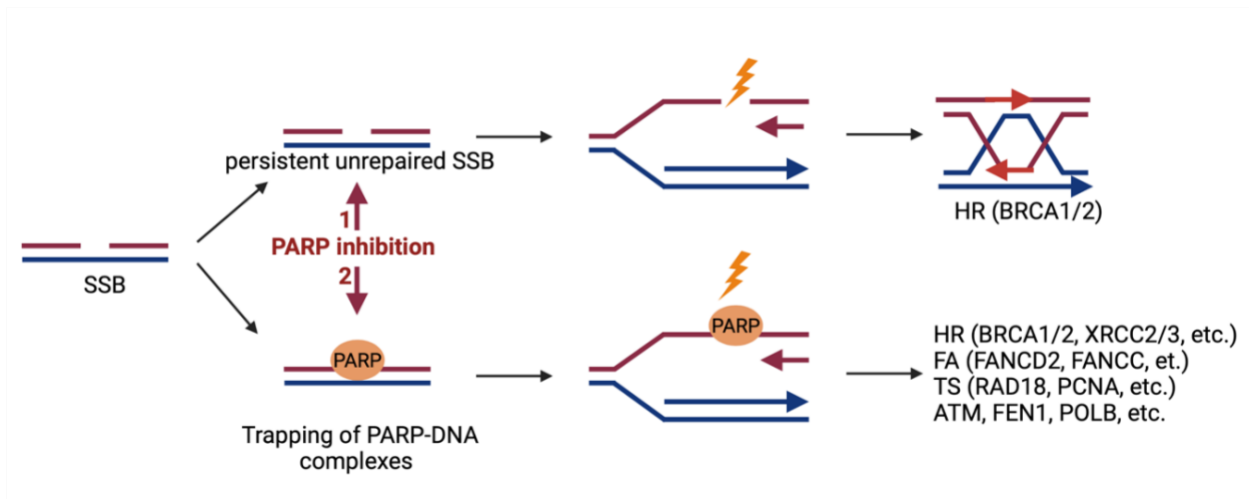


Figure 1.7: Mechanism of PARP inhibition. PARPis act via two major mechanisms: either by inhibiting the catalytic function (1) or by affecting the DNA binding of PARP thereby trapping and creating PARP-DNA complexes (2). Figure modified from Murai et al. (2012)¹¹⁹. Created with BioRender.com.

One of the first studies to highlight the promising potential of PARPis in cancer was work by Bryant et al, demonstrating synthetic lethality of PARPis in breast cancer with homologous recombination deficiency (HRD) (Figure 1.8)¹²⁴. In normal conditions, during DNA damage, PARP1 recognizes SSBs and initiates BER repair to properly repair the damage¹²⁵. Use of PARPi in normal cells with intact BRCA1/2 genes, leads to generation of DSBs from the unrepaired SSBs, but this can be repaired by HR in an error prone free manner¹²³. In contrast, tumors that have BRCA1/2 deficiencies are unable to repair the DSB break that results from treatment with PARPi, leading to tumor cell death via synthetic lethality¹²².

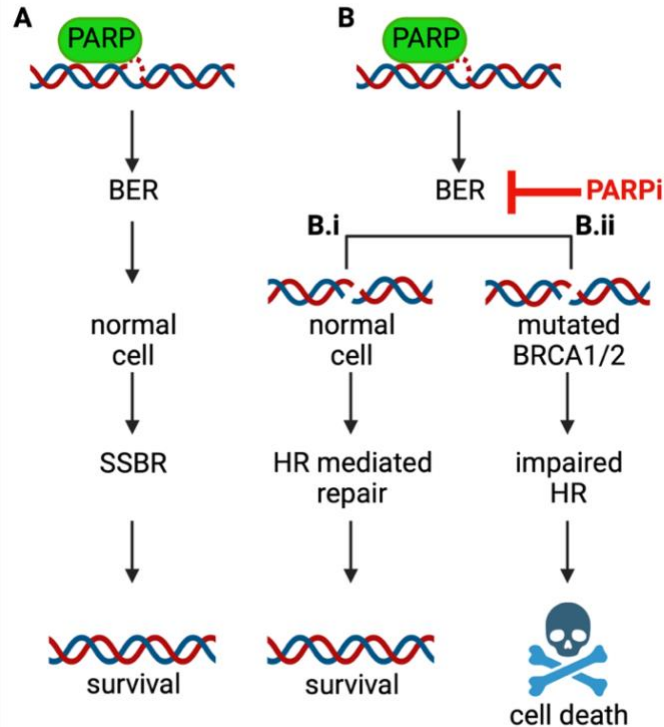


Figure 1.8: Schematic for synthetic lethality. (A) When DNA is damaged, SSBR is initiated and mediated by PARP. (B) PARPis prevent SSBR which results in accumulation of DSBs. (B.i) Normal cells can repair DSBs through HR-mediated repair leading to cell survival. (B.ii) Cancer cells with mutated BRCA1/2 have defects in HR and are unable to repair the accumulated DSBs leading to cell death. Created with BioRender.com.

PARPis prevent SSB repair, increase DSBs, and depend on HR to mediate repair. Thus when used in cancers with BRCA1/2 mutations, PARPis led to cell death through synthetic lethality¹²³. The basis of synthetic lethality is understanding the molecular underpinnings of cancer and using drug targets that would be lethal for cancer cells but leave normal cells unharmed¹²⁶. Numerous studies have investigated other potential mutations in cancer that would sensitize cancer cells to PARPi therapy^{123,127-129}. Recent studies have shown that disruptions of expression and/or function of other HR-related pathway components, such as disruption of Fanconi anemia (FA) and

ATM genes, referred to as BRCAness genes, can lead to HRD, and can therefore predict sensitivity to PARPis^{128,129}. However, PARPis have failed to show long-term clinical benefit for patients with intact BRCAness genes, underscoring the necessity of developing new strategies to maximize the efficacy of these inhibitors.

1.4 Rationale and Aims

AML accounts for 80% of adult acute leukemia, with only a 25% 5-year survival rate¹³⁰. Diverse cytogenetic and molecular abnormalities predict treatment outcomes, enable treatment stratification, and, increasingly, provide therapeutic targets¹³¹. DNMTis are effective in treating AML in patients who are unfit for, or unlikely to respond to, intensive chemotherapy, with responses even in AMLs with unfavorable karyotypes or mutations in *TP53*^{85,132}. However, DNMTi responses are not durable^{133,134}, and novel therapy combinations are needed.

Studies in solid tumors have shown that DNMTis induce an immune signature centered on potentiation of interferon (IFN) signaling that is facilitated in part by upregulation of endogenous retroviral transcripts (ERVs) and sensing of cytoplasmic double-stranded RNA (dsRNA)^{81,82}. This phenomenon, termed DNMTi-induced “viral mimicry”, stimulates production of cytokines and attraction of activated CD8⁺ T lymphocytes to tumor sites, accompanied by antitumor responses^{82,83}.

Poly ADP-ribose polymerase inhibitors (PARPis) induce synthetic lethal cell death in BRCA-mutant and homologous recombination-deficient (HRD) breast and ovarian cancer (BC and OC)^{123,135}. In our published work in BRCA wild-type (WT) BC and OC, we showed that DNMTi and PARPi combination treatment upregulates both cytosolic dsRNA and dsDNA in a “pathogen mimicry” response (PMR), leading to broad innate immune and inflammasome-like signaling, driven in part by stimulator of interferon signaling (STING), unexpectedly directly generating decreased DNA DSB repair and HRD¹²⁹. This study will explore this signaling paradigm in AML. Our overall hypothesis is that **activating STING increases IFN signaling and induces HRD, leading to anti-leukemia innate immune responses in AML**. Furthermore, as discussed in subsequent chapters, given the role that TP53 plays in maintaining silencing of repeat

sequence elements in the genome, including ERVs, we aim to study the impact of TP53 mutations on the DNMTi+PARPi combination treatment-mediated immune response. The following specific aims were investigated to elucidate this mechanism:

Specific Aim 1: Determine the role of STING in induction of IFN signaling and HRD by DNMTi+PARPi combination treatment in *TP53* mutant versus WT AML.

Specific Aim 2: Test the role of STING signaling and TP53 abrogation in DNMTi+PARPi combination treatment-driven anti-leukemia responses in immune-competent mice.

Specific Aim 3: Explore immune and HR-related changes in patients treated with DNMTi+PARPi combination in a phase 1 clinical trial.

Overall, our findings significantly increase our understanding of the mechanisms that underlie DNMTi+PARPi combination treatment efficacy and suggest differential use of these therapies based on TP53 status to induce potential immune activation of STING in AML and other cancers.

CHAPTER 2: Activating STING-dependent immune signaling in AML³

2.1. Introduction

As discussed in the Introduction (Chapter 1), AML is a genetically heterogeneous disease characterized by malignant clonal proliferation of immature myeloid cells in the bone marrow^{63,136}. AML has diverse cytogenetic and molecular abnormalities that predict treatment outcomes, enable treatment stratification, and, increasingly, provide therapeutic targets¹³⁷. *TP53* alteration or loss is one of the most powerful predictors of poor outcome in AML^{58,138,139}, suggesting the need for alternative therapies. Herein, we present data with translational significance for AML involving a lesser investigated role of p53 as a guardian of the genome for prevention of unwanted transcription of repeat sequences¹⁴⁰. Furthermore, our data link this role with a similar, long-recognized guardian role for the process of DNA methylation in DNA¹⁴¹.

DNMTis are approved for treatment of MDS and are also used for treatment of AML in patients unfit for intensive chemotherapy¹⁴²⁻¹⁴⁵. These epigenetic agents are primarily thought to exert their efficacy by reversing gene expression changes that are associated with DNA methylation abnormalities commonly found in AML^{106,146,147}. In preclinical studies, *TP53*-deficient neoplastic fibroblasts treated with DNMTis showed increased apoptosis compared to

³ Kogan, AA, Topper, MJ, McLaughlin, LJ, Creed, TM, Eberly, CL, Kingsbury, TJ, Baer, MR, Kessler, MD, Baylin, SB, Rassool, FV. (2021). Activating STING-dependent immune signaling in acute myeloid leukemia. Manuscript in prep.

cells with WT *TP53*^{148,149}. These findings link to clinical data demonstrating that AML patients with *TP53* mutations had robust responses to DNMTi treatment¹⁵⁰. In contrast, in other studies there was no significant association between *TP53* mutations and response to treatment with DNMTis^{24,132}. Although DNMTis are widely used for the treatment of AML, and patients achieve remission, remissions are not durable and efficacy is less than was hoped given the strength of preclinical data¹⁴⁷. Fennell et. al. describe a number of possibilities for why this may be the case, including the fact that AML has historically never been cured by single-agent therapy¹⁴⁷. Therefore, in order to increase efficacy, researchers have pursued drug treatments that can synergize with the favorable epigenetic reprogramming induced by DNMTis.

We have been exploring the combinatorial approach of adding PARPis to DNMTis¹²¹. PARPis are approved for use in the clinic to treat BRCA-deficient or HR-deficient BC and OC^{122,124,135}. PARPis inhibit repair of SSBs and DSBs both by inhibiting PARylation and by trapping PARP1/2 in DNA¹¹⁹. BRCA mutations render cells deficient in HR, and therefore potentially lethal DSBs formed during replication in PARP-inhibited cells cannot be repaired, leading to subsequent cell death by synthetic lethality^{119,121,128,151,152}. We reported that combining PARPi with DNMTi increased PARP trapping and produced synergistic cytotoxicity in AML and triple-negative BC (TNBC) cells³⁴. Extending these anti-tumor effects to non-small cell lung cancer (NSCLC), we also showed that DNMTis downregulate a subset of DNA damage response genes, inducing HRD, which mimics the BRCA-mutant phenotype and sensitizes cells to PARPis (Figure 2.1)¹²⁸. Similar findings were also demonstrated in our recent study in TNBC and OC¹²⁹.

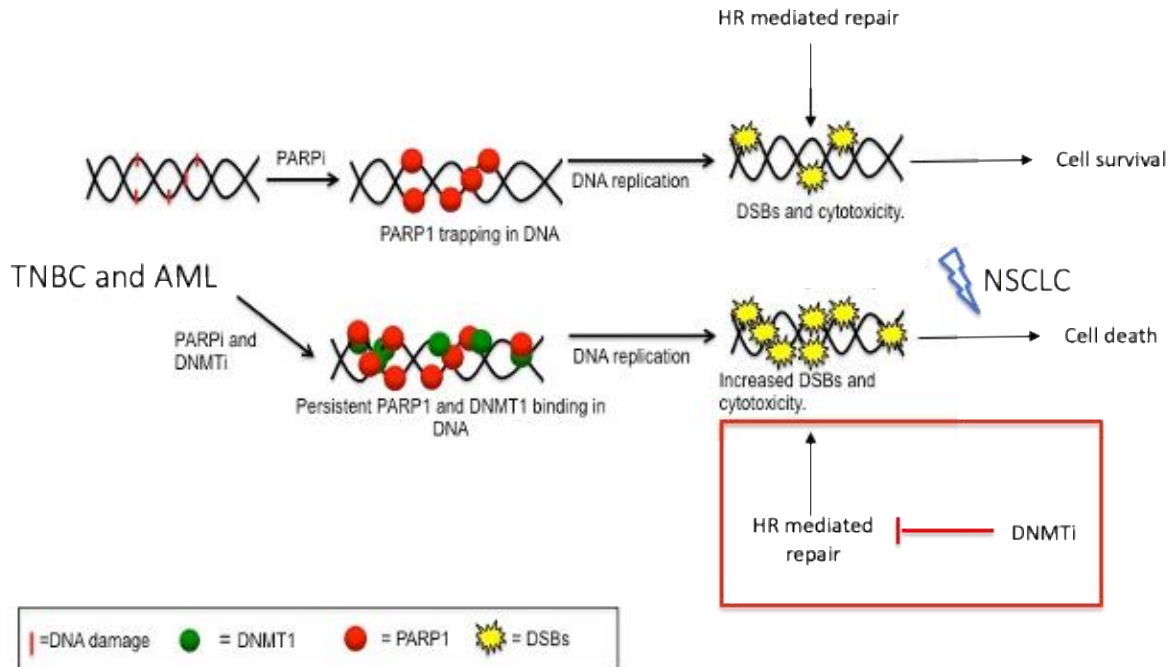


Figure 2.1: Model for DNMTi+PARPi mechanism of action. With PARPi alone, these protein-DNA adducts can be repaired through HR during replication (top). When PARPi is combined with DNMTi there is increased persistent PARP1 and DNMT1 binding in the DNA. With the additional DNMTi priming of the epigenome resulting in inhibition of HR-mediated repair (red box), these protein-DNA adducts cannot be repaired, thus the DSBs persist (including the addition of IR in NSCLC) and promote cell death (bottom). Figure modified from Muvarak et al. (2016)¹²¹.

DNMTis have also been shown to transcriptionally reprogram immune signaling, with significant relevance to immune therapy strategies seeking to exploit immunological modulation^{104,153-155}. This reprogramming includes induction of an IFN response via transcriptional activation of ERV genes⁸¹. These ERV genes form RNA and DNA intermediates by reverse transcription, which in turn drive immune signaling through the STING gene and other cytoplasmic dsRNA sensors^{81,156-158}. DNA damage induced by PARPi has been reported to activate

STING signaling^{159,160}, via cytosolic double-stranded DNA (dsDNA)¹⁶¹. In our recent study in TNBC and OC, we reported a broadened response with DNMTi+PARPi combination treatment, termed PMR, encompassing activation of STING-dependent IFN signaling leading to downregulation of HR, thus generating an HRD phenotype in BRCA-proficient cells¹²⁹.

Herein, in studies of leukemia models, we define new mechanistic insights linking the role of TP53 to STING-dependent IFN signaling responses in AML. Specifically, we examine ERV gene expression levels in cells treated with DNMTis. Interestingly, we identify differential ERV gene transcriptional responses between TP53 WT and mutant models and stratify our mechanistic experiments on the basis of TP53 mutation status. The rationale for this stratification is built on previous reports that TP53 plays a significant role in the maintenance of epigenetic silencing^{162,163}. Mutations in TP53, including those with loss of function and dominant negative function, relieve this transcriptional repression¹⁶³. Since cytosolic dsDNA is known to drive STING signaling¹⁶⁴, and PARPis are known to increase cytosolic dsDNA¹⁶⁵, we also determine how PARPi treatment affects cytosolic dsDNA fragment formation and subsequent STING signaling. After characterizing how DNMTi+PARPi treatment alters STING-mediated immune signaling and HRD induction, and whether any such changes differ with respect to TP53 mutation status, we finally determine whether these effects are STING-dependent. Thus, in this chapter of the thesis, we bring a new synthesis of events for STING activation and IFN signaling with DNMTis and PARPis that is dependent on TP53 mutation status. This work is translationally relevant to AML and may be extrapolated to other cancers.

2.2. Results

2.2.1. DNMTi treatment increases ERV gene expression in TP53 mutant AML

In solid tumor models, DNMTis were previously shown to activate STING-mediated IFN signaling through transcriptional activation of ERVs^{81,82,129}. We used qPCR analysis to test the depth of this response in DNMTi-treated AML cell lines (DAC, 10nM, 72h). Given that TP53 has been shown to suppress transcription and to play a direct role in epigenetic silencing^{150,162,166}, we also hypothesized that TP53 mutant AML cell lines would be more susceptible to DNMTi induction of viral mimicry via ERV transcriptional increase. We tested this hypothesis in TP53 mutant (Kasumi-1, KG-1a, and U937) and WT (MOLM-14, OCI-AML2 and OCI-AML3) AML cell lines (Table 2.1).

Table 2.1: TP53 mutation status in AML cells lines

Cell line	TP53 status	Location		cDNA	protein
MOLM-14	WT				
OCI/AML2	WT				
OCI/AML3	WT				
Kasumi-1	MUT - Hom	exon 7	DBD	c.743G>A	p.R248Q
KG-1	MUT - Hom	exon 7	DBD	c.673G>A	p.V225I
U-937	MJT - Hom	intron 5	DBD	c.559+1G>A	p.?

TP53 mutant AML cell lines exhibited a 2- to 8-fold increase ($p < 0.005$) in ERV gene expression following DNMTi treatment, whereas TP53 WT AML cell lines showed no increases (Figure 2.2 A, Figure S2.1A; $P < 0.01$). To test whether these ERV-activating effects are directly mediated by TP53, we used the TP53 inhibitor pifithrin (50 μ M, 72h), which specifically inhibits transactivation of p53-responsive genes¹⁶⁷. TP53 WT MOLM-14 AML cells cultured with pifithrin as a single agent demonstrated significant increases in 4/13 ERVs

tested (Figure 2.2B; $P < 0.05$). This effect was dependent on the presence of WT TP53, as treatment of the TP53 mutant cell line Kasumi-1 with pifithrin resulted in no change in ERV expression (Figure S2.1B). Given our interest in DNMTi treatment in combination with PARPi^{121,129}, we tested whether PARP inhibition with talazoparib (Tal, 5nM, 72 h) could similarly drive ERV activation. PARPi alone resulted in no significant changes in ERV gene expression in WT or mutant TP53 AML cells (Fig S2.1C-H), and DNMTi+PARPi drug combination treatment had similar effects on ERV gene expression as DNMTi treatment alone (Fig S2.1C-H).

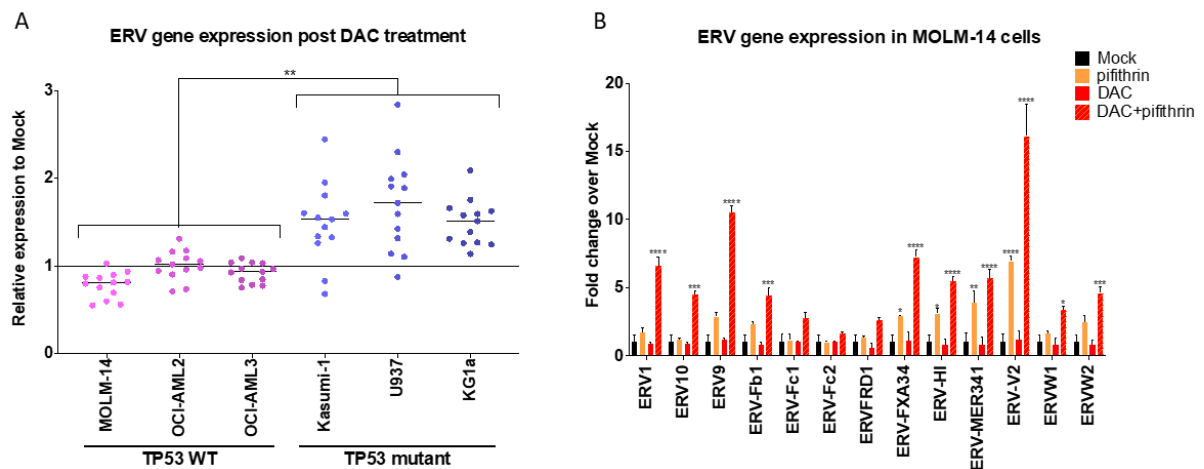


Figure 2.2: DNMTi treatment increases ERV gene expression in TP53 mutant AML. (A) Relative RNA expression for a subset of ERV genes after mock or 10 nM DAC treatment in MOLM-14, OCI-AML2, OCI-AML3, Kasumi-1, KG-1a, and U937 cell lines (72hrs, $n = 3$). **(B)** Relative RNA expression for a subset of ERV genes after mock or 10 nM DAC treatment \pm 50 μ M pifithrin in MOLM-14 cells (72hrs, $n = 3$).

2.2.2. PARPi drives cytoplasmic dsDNA increases in AML

Given these TP53-specific ERV findings, as well as previous reports that PARPi increases cytosolic dsDNA and drives STING signaling^{129,160}, we compared the impact of PARPi on cytosolic dsDNA expression in TP53 WT and mutant cell lines. Interestingly, we first found that levels of cytosolic dsDNA are increased in TP53 WT MOLM-14 cells compared with TP53 mutant Kasumi-1 cells (Figure 2.3A). Moreover, there was a distinct correlation between TP53 mutation status and PARP1 protein expression levels, which are significantly lower in TP53 WT, compared with TP53 mutant, cell lines (Figure 2.3B; $P < 0.05$). Importantly, these differences in PARP1 levels between TP53WT vs mutant AML seem to be universal for AML, as we observed them in primary samples from the Cancer Genome Atlas database (TCGA)¹⁶⁸ (Figure 2.3C; $P=0.002$). Treatment of AML cell lines with the PARPi Tal at a low concentration (5nM) caused reductions in PARP1 protein levels only in TP53 WT cell lines, and not in mutant TP53 cells, which is consistent with these cell lines having lower levels of PARP1 at baseline (Figure 2.3B, Figure S2.2A-F). Increasing Tal concentrations (10-20nM) in TP53 mutant Kasumi-1 cells, with a high baseline level of PARP1 protein, led to a decrease in PARP1, consistent with a concentration-dependent PARPi effect on PARP1 (Figure 2.3D). Furthermore, increasing the Tal concentration led to a concordant increase in cytoplasmic dsDNA in TP53 mutant Kasumi-1 cells similar to levels seen using lower concentrations of Tal concentrations in WT TP53 cells (Figure 2.3A).

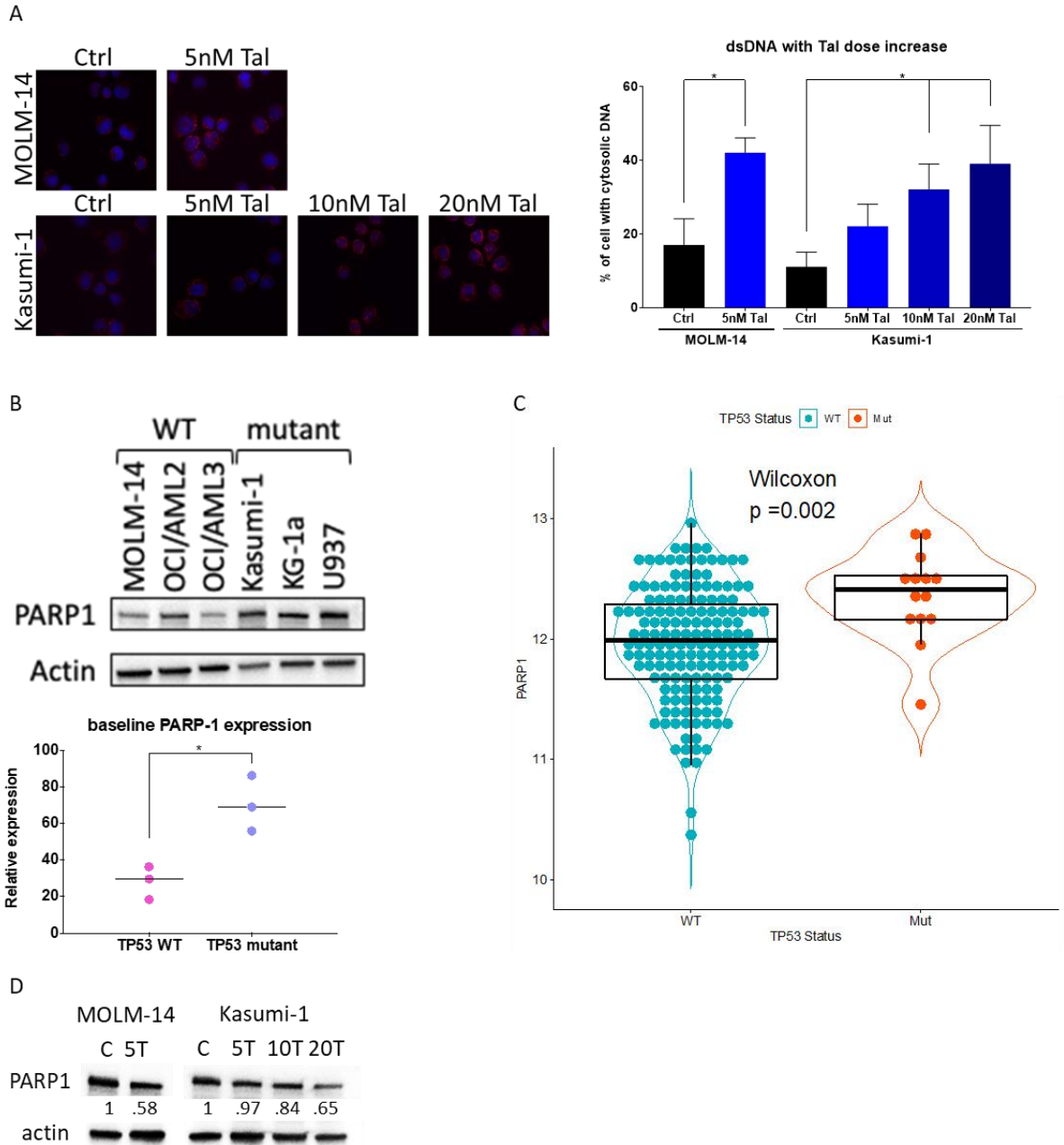


Figure 2.3: PARPi drives cytoplasmic dsDNA increases in AML. (A) Representative immunofluorescence images for dsDNA (left) and quantified (right) in MOLM-14 and Kasumi-1 cells after mock, or 5 nM, 10nM, and 20nM Tal treatment (72hrs, n = 3). (B) Immunoblot for PARP1 in TP53 WT (MOLM-14, OCI/AML2, and OCI/AML3) and TP53 mutant (Kasumi-1, KG-1a, and U937) cell lines at baseline with β -actin used as a loading

control (n = 3). (C) Violin plots for PARP1 mRNA expression in TCGA AML samples grouped by TP53 status. All data are presented as mean \pm SEM with statistical significance derived from two-tailed unpaired Student's t test (or ANOVA), or Wilcoxon signed-rank test. (D) Immunoblot for PARP1 after mock, or 5 nM, 10nM, and 20nM Tal treatment in MOLM-14, and Kasumi-1 cell lines with β -actin used as a loading control (72hrs, n = 3).

2.2.3. STING activity is increased in TP53 mutant AML

We found that the status of STING expression basally, and with our drug treatments, is crucial to the increases in ERV expression and cytoplasmic dsDNA observed above. In a recent study we showed that DNMTi+PARPi treatment increases STING expression in TNBC and OC¹²⁹. To evaluate whether this mechanism explains DNMTi+PARPi efficacy in AML¹²¹, we first characterized basal STING expression in primary AML TCGA samples and in AML cell lines. Indeed, AML samples with WT TP53 from TCGA have significantly higher levels of STING than samples with TP53 mutations (Figure 2.4A; P=0.00021). Western blot analysis of STING protein levels in AML cell lines is consistent with these data, with TP53 WT cell lines showing higher baseline protein levels than TP53 mutant cell lines (Figure 2.4B).

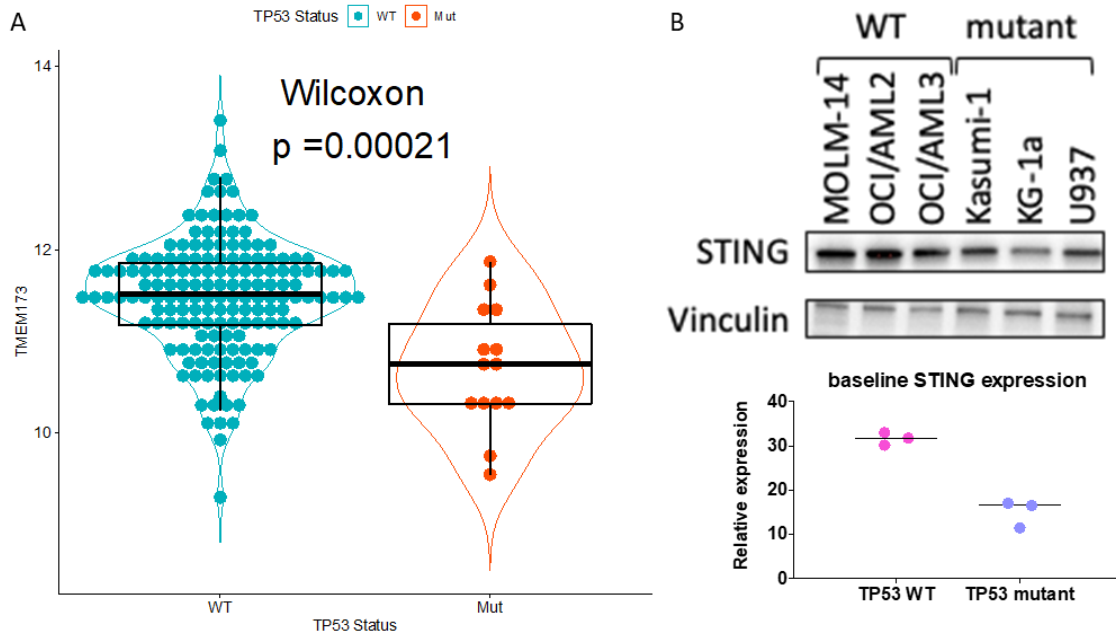


Figure 2.4: STING expression is lower in TP53 mutant AML at baseline. (A) Violin plots for STING mRNA expression in TCGA AML samples grouped by TP53 status. (B) Immunoblot for STING in TP53 WT (MOLM-14, OCI/AML2, and OCI/AML3) and TP53 mutant (Kasumi-1, KG-1a, and U937) cell lines at baseline with vinculin used as a loading control (n = 3).

We then evaluated whether STING protein levels increase more significantly in TP53 mutant cell lines after DNMTi+PARPi combination treatment, as compared to WT. Surprisingly, we found that STING protein levels did not change after DNMTi, PARPi, or combination treatment in any of the cell lines tested (Figure 2.5A,B, Figure S2.3A-D). We therefore considered whether STING protein activation (via phosphorylation) may vary with TP53 mutation status. Indeed, while basal STING expression is lower in TP53 mutants, STING phosphorylation, and therefore its activity, is approximately 2-fold increased at baseline in

TP53 mutant Kasumi-1 cells (Figure 2.5B,D) compared to TP53 WT MOLM-14 cells (Figure 2.5A,C). Furthermore, in TP53 mutant cells, phospho-STING protein levels increase following DNMTi treatment, but increase even further with DNMTi+PARPi combination treatment (Figure 2.5B,D Figure S2.3,C,D,G,H). In contrast, in TP53 WT AML cells phospho-STING levels are not altered by single-agent DNMTi or PARPi treatment, but increase with the drug combination (Figure 2.5A,C Figure S2.3A,B,E,F). These results suggest that TP53 mutants not only have increased baseline STING activation, but also have the capacity to further increase STING activity compared with WT TP53 AML cells, though WT increases with the DNMTi+PARPi combination.

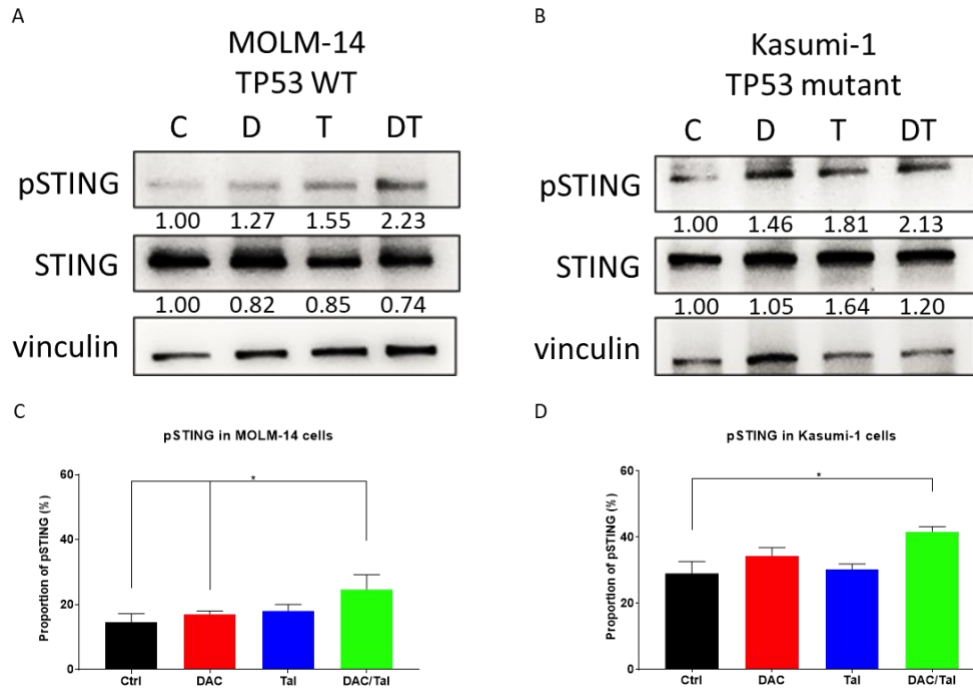


Figure 2.5: STING activity is increased in TP53 mutant AML. (A-B) Immunoblot for pSTING and STING in MOLM-14 (A) and Kasumi-1 (B) cells after mock, 10 nM DAC, 5 nM Tal, or DAC/Tal combination: 10 nM DAC + 5 nM Tal treatment with vinculin used as a loading control, quantified values below each respective protein (72hrs, n = 3). (C-D) Quantification of proportion of pSTING in MOLM-14 (C) and Kasumi-1 (D) cells after mock, 10 nM DAC, 5 nM Tal, or DAC/Tal combination: 10 nM DAC + 5 nM Tal treatment (72hrs, n = 3). All data are presented as mean \pm SEM with statistical significance derived from two-tailed unpaired Student's t test (or ANOVA), or Wilcoxon signed-rank test.

DNMTi treatment increases IFN signaling in TP53 mutant AML

Given this increased STING activity in AML, and our previous reports that DNMTi+PARPi combination treatment induced STING and IFN signaling in TNBC and OC¹²⁹, we next examined whether DNMTi and/or PARPi combination treatment also drives

IFN signaling in AML. Hallmark and KEGG (Kyoto Encyclopedia of Genes and Genomes) pathway analysis of genome-wide expression data from MOLM-14 cells with WT TP53 supported the transcriptional activation of multiple immune response pathways by DNMTi+PARPi combination treatment, whereas single-agent DAC or Tal treatment showed a markedly less robust response (Figure 2.6A). To validate these data, we performed qPCR analysis on a panel of immune genes that were selected based on our genome-wide expression data and previous data from our laboratory¹²⁹ (Figure 2.6B). In MOLM-14 cells, DNMTi treatment alone led to modest increases in expression in only 3 of the 24 immune genes tested (Figure S2.4A; $P < 0.05$). In contrast, DNMTi+PARPi combination treatment significantly increased expression of 13 of these tested genes (Figure S2.4A; $P < 0.01$). Investigation of two additional TP53 WT AML cell lines (OCI-AML2 and OCI-AML3) revealed similar gene expression changes (Figure S2.4B, C). The pattern of IFN gene expression is quite different in TP53 mutant Kasumi-1 cells, as DNMTi treatment alone drives pronounced increases in expression of IFN genes ($P < 0.05$ in 7/24 genes) (Figure 2.6B, Fig S2.4D) and DNMTi+PARPi combination treatment increases the magnitude of IFN-related gene expression ever further. Investigation of additional mutant TP53 AML cell lines (KG-1a and U937) revealed a similar pattern of IFN gene expression differences (Figure S2.4E-F). Importantly, these results were replicated in AML primary samples (Table S2.1, Figure 2.6C,D, Figure S2.4G-L).

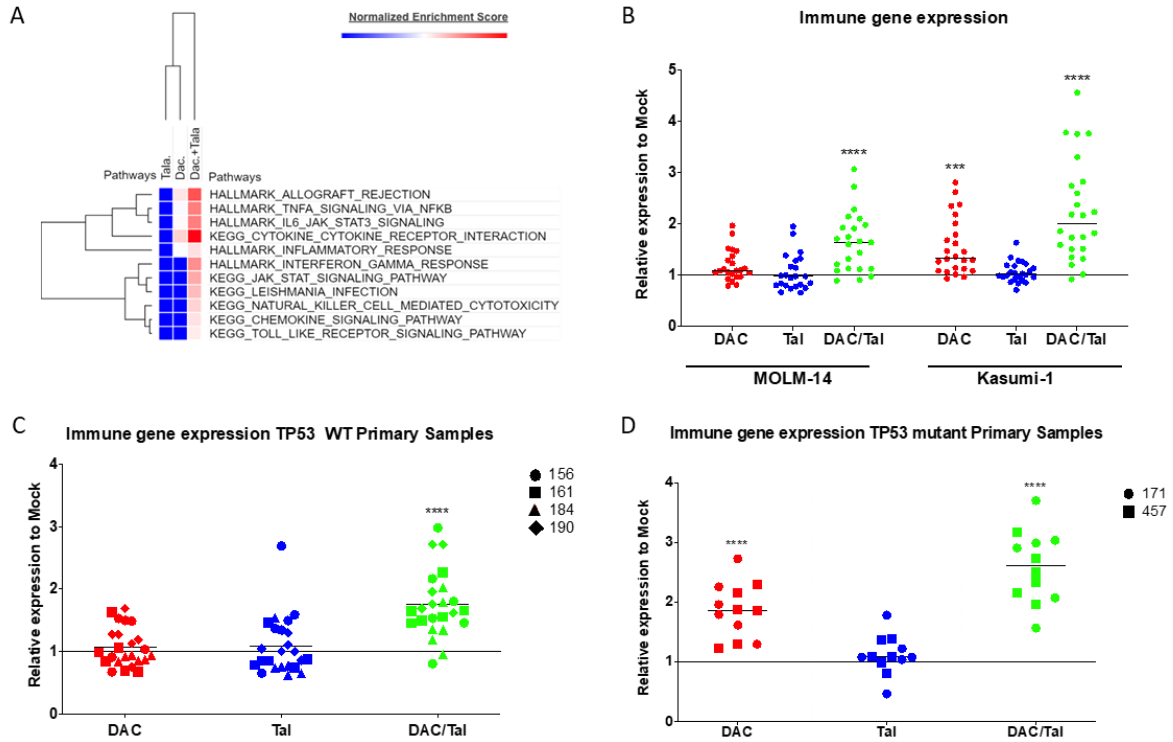


Figure 2.6: DNMTi treatment increases IFN signaling in TP53 mutant AML. (A) Normalized enrichment scores for MOLM-14 after 10 nM DAC, 5 nM Tal, or DAC/Tal combination: 10 nM DAC + 5 nM Tal treatment, cDNA microarray data. Blue: downregulated, red: upregulated Hallmark and KEGG pathways Log2 fold change relative to mock (72hrs, n = 3). (B) Relative RNA expression for a subset of immune genes after mock, 10 nM DAC, 5 nM Tal, or DAC/Tal combination: 10 nM DAC + 5 nM Tal treatment in MOLM-14 and Kasumi-1 cell lines (72hrs, n = 3). (C-D) Relative RNA expression for a subset of immune genes after mock, 10 nM DAC, 5 nM Tal, or DAC/Tal combination: 10 nM DAC + 5 nM Tal treatment in TP53 WT (C) and mutant (D) primary samples (72hrs, n = 3). All data are presented as mean \pm SEM with statistical significance derived from two-tailed unpaired Student's t test (or ANOVA).

DNMTi treatment drives decreases in HR in TP53 mutant AML

In our previous studies we have shown that DNMTi+PARPi combination treatment leads to increased DNA damage and reduced HR capacity^{121,128}, and we most recently connected this HRD to immune signaling in solid tumors¹²⁹. To examine the connection between immune signaling and HR in AML, we used the STRING database and computational tool¹⁶⁹ to perform network analysis for known protein interactions between targets of interest. This analysis revealed TP53 as a new potential basal central node intersection for genes in the IFN pathway and DNA damage genes including HR-related factors (Figure 2.7A, Fig S2.5A). In support of this predicted protein network interaction, treatment of TP53 WT MOLM-14 cells with IFN β or TNF α /IL-1 β showed increases in downstream IFN gene expression levels, decreases in DNA repair gene expression and downregulation of HR activity as measured via an *in vitro* plasmid reporter assay^{128,129} (Figure S2.7B,D). Furthermore, IFN β (Figure 2.7B) and TNF α /IL1- β (Figure S2.5C) treatment each decreased HR activity. In further validation of the predicted direct relationship between IFN signaling and HR activity, treatment of MOLM-14 AML cells with the JAK inhibitor ruxolitinib (Rux), which inhibits IFN pathway signaling¹⁷⁰, rescues HR activity (Figure 2.7B).

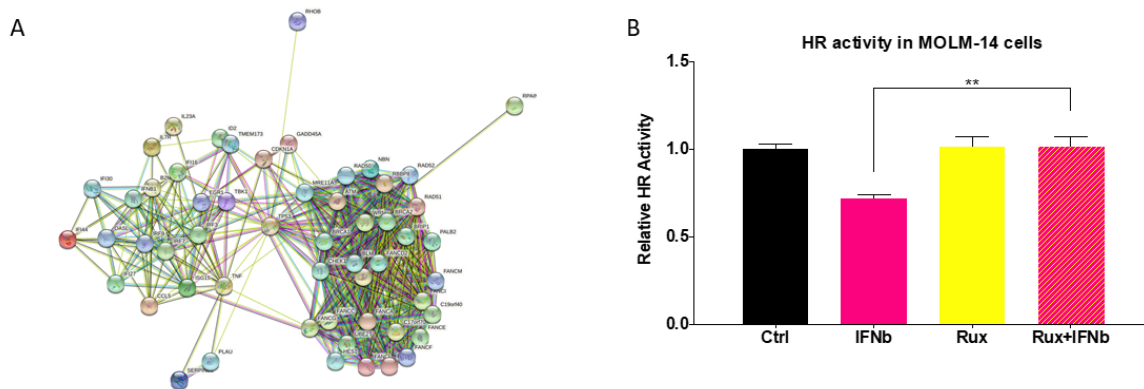


Figure 2.7: Immune and DNA repair pathways are linked. (A) STRING protein–protein interaction map of homologous recombination and IFN genes of interest. See Fig. S5A for an expanded version (B) Relative HR activity analysis 24h after 5 μ M ruxolitinib, 100 ng/mL IFN β , or 5 μ M ruxolitinib + 100 ng/mL IFN β treatment in MOLM-14 cells (n = 3).

Given the above central role of TP53 in the interactions between IFN and DNA repair, we hypothesized that the expression and activity of HR-related genes following DNMTi and/or PARPi treatment would differ between TP53 WT and mutant AML cell lines. Indeed, while DNMTi or PARPi treatment alone had no significant effect on HR gene expression in TP53 WT MOLM-14 cells, DNMTi treatment alone resulted in a decrease in expression of HR-related genes (Figure 2.8A; $P < 0.0001$) in TP53 mutant Kasumi cells, and the DNMTi+PARPi combination treatment further decreased expression of these genes (Figure 2.8A; $P < 0.001$, Figure S2.6A,D). Importantly, study of additional AML cell lines (Figure S2.6B,C,E,F) and primary samples with WT (N=4) and mutant (N=2, Table S2.1) TP53 treated with DNMTi, PARPi, and DNMTi+PARPi combination revealed similar HR gene expression patterns (Figure 2.8C,D, Fig S2.6G-L).

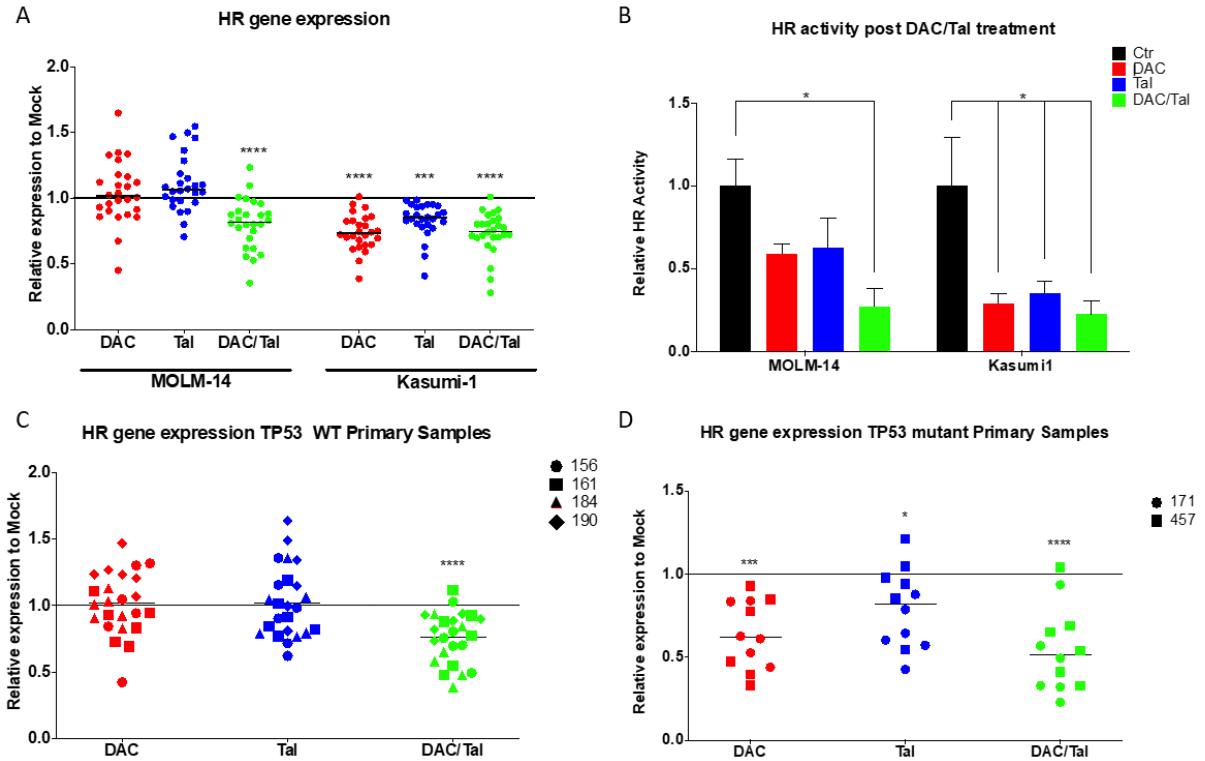


Figure 2.8: DNMTi treatment drives decreases in HR in TP53 mutant AML. (A) Relative RNA expression for a subset of HR genes after mock, 10 nM DAC, 5 nM Tal, or DAC/Tal combination: 10 nM DAC + 5 nM Tal treatment in MOLM-14 and Kasumi-1 cell lines (72hrs, n = 3). (B) Relative HR activity analysis in MOLM-14 and Kasumi-1 cell lines after mock, 10 nM DAC, 5 nM Tal, or DAC/Tal combination: 10 nM DAC + 5 nM Tal treatment (72hrs, n = 3). (C-D) Relative RNA expression for a subset of HR genes after mock, 10 nM DAC, 5 nM Tal, or DAC/Tal combination: 10 nM DAC + 5 nM Tal treatment in TP53 WT (C) and mutant (D) primary samples (72hrs, n = 3). All data are presented as mean \pm SEM with statistical significance derived from two-tailed unpaired Student's t test (or ANOVA).

STING inhibition abrogates IFN signaling and rescues HR activity in TP53 WT and TP53 mutant AML

We next found that a direct connection between IFN signaling and HR activity in AML cells treated with DNMTi and/or PARPi is STING-dependent. We used H-151, which is a highly potent and covalent antagonistic inhibitor of STING¹⁷¹. The increases in IFN gene expression seen with DNMTi+PARPi combination treatment in TP53 WT MOLM-14 cells were significantly decreased with the addition of H-151 (Figure 2.9A; 500nM, $P < 0.001$, Figure S2.7A). Similarly, in TP53 mutant Kasumi-1 cells, H-151 treatment significantly decreased the altered IFN gene expression seen in cells treated with either DNMTi ($P < 0.05$) or DNMTi+PARPi combination ($P < 0.0001$) (Figure 2.9A, Figure S2.7B). With respect to effects of STING inhibition on HR gene expression in WT TP53 MOLM14 cells, H-151 treatment rescued the decreased expression of HR genes that is driven by DNMTi+PARPi combination treatment (Figure 2.9B, Figure S2.7C, D; $P < 0.001$). Notably, H-151 co-treatment also resulted in robust rescue of HR gene expression in TP53 mutant Kasumi-1 cells treated with DNMTi or with DNMTi+PARPi (Figure 2.9B; $P < 0.0001$, Figure S2.7D). H-151 also rescued the DNMTi+PARPi combination treatment-induced reduction in HR activity in WT TP53 MOLM-14 cells (Figure 2.9C; $P < 0.001$) as well as in TP53 mutant Kasumi-1 cells (Figure 2.9D; $P < 0.0001$), further supporting the mechanistic role of STING in HRD induction.

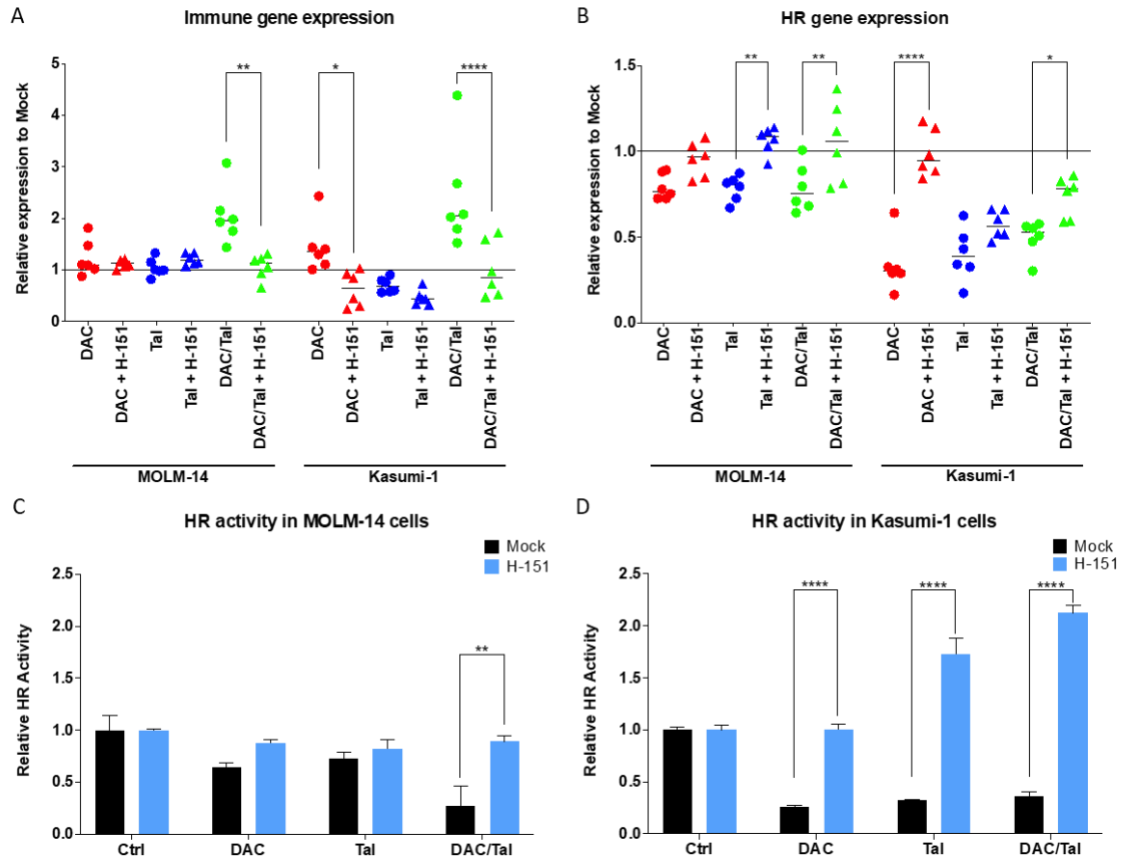


Figure 2.9: STING inhibition abrogates IFN signaling and rescues HR activity in TP53 WT and TP53 mutant AML. (A) Relative RNA expression for a subset of immune genes after mock, 10 nM DAC, 5 nM Tal, or DAC/Tal combination: 10 nM DAC + 5 nM Tal treatment \pm 500 nM STINGi for all conditions in MOLM-14 and Kasumi-1 cell lines (72hrs, n = 3). (B) Relative RNA expression for a subset of HR genes after mock, 10 nM DAC, 5 nM Tal, or DAC/Tal combination: 10 nM DAC + 5 nM Tal treatment \pm 500 nM STINGi for all conditions in MOLM-14 and Kasumi-1 cell lines (72hrs, n = 3). (C-D) Relative HR activity analysis of MOLM-14 (C) and Kasumi-1 (D) cells after 72hr treatment with mock, 10 nM DAC, 5 nM Tal, or DAC/Tal combination: 10 nM DAC + 5 nM Tal \pm 500 nM STINGi for all conditions (n = 3).

2.3. Discussion

In this mechanistic study, we show for the first time that DNMTs drive activation of ERVs and STING-dependent IFN signaling in AML in a TP53-dependent fashion. Notably, enhanced ERV activation is linked to presence of mutant versus WT TP53 in AML cell lines and patient samples. A similar pattern was seen for IFN signaling, which is consistent with previous studies that have shown STING activation via ERV transcript-generated dsRNA^{81,172}. Our findings provide new and translationally relevant insights into the importance of the presence of widespread TP53 binding sites near genomic repeat elements and a suggested guardian role in the genome for promoting the silencing of such elements¹⁷³. The findings bring a therapy paradigm into juxtaposition with previous suggestions that mutation or abrogation of TP53 in cancer cells may impact how DNMTs transcriptionally relieve the silencing of repeat elements present in normal somatic cells^{163,173-175}. Our direct link between TP53 and DNMTs demonstrates why TP53 mutant AML cells may be significantly more sensitive, and poised to be immunologically reactive to, DNMTi treatment. This has potential implications for the treatment of AML, and suggests approaches for strategically activating immune signaling in TP53 mutant AML, where TP53 alteration or loss is one of the most powerful predictors of poor treatment outcomes^{58,138,139} (schematic model, Fig 2.10).

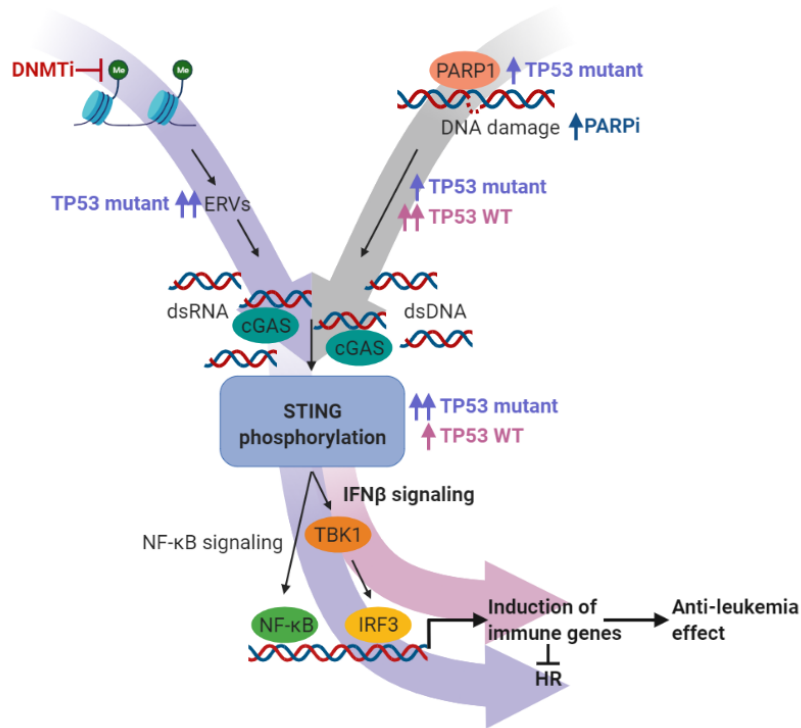


Figure 2.10: Schematic of a multifaceted immune response leading to HRD in AML. In the proposed model for the combination therapy, the DNMTi induction of viral mimicry via cytosolic dsRNA combined with the PARPi increase of cytosolic dsDNA, converge to the activation of STING signaling. This activated response leads to transcriptional increase in IFN β and TNF α /NF- κ B signaling, which facilitates the transcriptional repression of HR genes and leads to anti-leukemia effects.

In addition to relevance of data to DNMTi's, our present findings have implications for PARPis for inducing synthetic lethality in BRCA-wild-type TNBC and OC cells^{135,176}. This paradigm is also dependent upon activation of IFN signaling by increasing cytosolic dsDNA levels^{129,165,177}. Our data further reveal that production of cytosolic dsDNA by PARPi treatment is observed in TP53 WT AML cells, but this mechanism is minimally operative for immune

signaling in TP53 mutant AML cells. One possible explanation for this is that we find that PARP1 levels are significantly increased in TP53 mutant samples, and so higher PARPi concentrations are required to disrupt PARP1 activity. Indeed, others have reported elevated PARP1 levels in many therapy-resistant cancers, which is understood to reflect increased selective pressure toward DNA repair activity and genomic instability^{116,178-180}. All of these findings suggest that PARP expression levels may be useful as a biomarker of both PARPi efficacy and potential response to immune therapies.

The role of STING activation in our findings bears special mention as a critical factor for activating anti-cancer immune responses not only in AML, but in cancer in general. Notably, STING expression is reduced in many tumors, and researchers are actively pursuing ways of driving STING-dependent immune signaling¹⁸¹⁻¹⁸⁴. After recently reporting that DNMTi treatment in TNBC and OC can transcriptionally activate STING¹²⁹, we now show that AML cells with TP53 mutations have higher STING activity at baseline, with even further increases following DNMTi treatment. Moreover, STING activity in TP53 WT AML models increases only after DNMTi+PARPi combination therapy, but even these increases are more modest than those seen in AML cells with TP53 mutations. Therefore, while induction of IFN signaling and HRD in both TP53 mutant and WT cells is STING-dependent, TP53 mutant AMLs seem to be particularly amenable to STING activation via epigenetic reprogramming, and may be good candidates for other novel STING pathway activation strategies.

Overall, our work has implications for therapy strategies reliant on activating innate immune pathways. For example, AMLs with TP53 mutations may define a group of patients in whom DNMTis can be used to activate immune signaling to prime for combination with immune checkpoint therapy. DNMTi treatment has also been shown to increase the expression of immune

checkpoint molecules such as PD-L1 and CTLA-4, which may present additional synergistic potential^{133,185-187}. In fact, recent reports describe encouraging preliminary results in which DNMTi+anti-CTLA-4 combination therapy leads to decreased tumor burden and improved survival in melanoma and OC mouse models^{81,187,188}. Additional clinical and preclinical research will increase our understanding of immune responses in TP53 mutant AML, and will further enable increasingly effective combination treatments. Given the current limitations with regard to predicting immuno-oncological treatment response, our findings hold particular promise in their identification of a specific molecular subset with sensitivity to immune-modulatory treatment⁸⁵. Finally, our findings, as revealed in our present studies of TCGA samples, may extend to other cancers with TP53 mutations, and may support the use of epigenetic treatments in a wider range of malignancies.

2.4. Methods

2.4.1 Cell lines and primary samples

Human AML cell lines KASUMI-1 and KG-1a (both harboring TP53 mutations) were cultured in RPMI1640 + L-Glutamine and 20% Fetal Bovine Serum; U937 (TP53 mutant) and MOLM14 (TP53 WT) were cultured in RPMI1640 + L-Glutamine supplemented with 10% FBS; OCI/AML2 and OCI/AML3 (both TP53 WT) were cultured in α -MEM + L-Glutamine and 20% Fetal Bovine Serum. All cell lines were cultured and maintained in 37°C incubators with 5% CO₂ and passaged every 3- 5 days.

Primary AML patient samples were obtained with informed consent on a protocol approved by the institutional review board of the University of Maryland School of Medicine (IRB H25314). Mononuclear cells (MNCs) from AML primary samples were isolated by density centrifugation over Ficoll-Paque (Sigma-Aldrich) and were cultured in IMDM with

20% FBS, without cytokine supplementation. MNCs were cultured in 37°C incubators with 5% CO₂.

2.4.2 Drug reagents and treatments in vitro

The DNTMi decitabine (DAC, Sigma-Aldrich) was prepared as a stock solution of 10 mM in DMSO, aliquoted, and stored at -80°C for single use. Cell lines were treated daily with 10nM DAC. The PARPi talazoparib (Tal, Pfizer) was prepared as a stock solution of 50 mM in DMSO, aliquoted and stored at -80°C. Tal was further diluted to 5 mM in 1µL single-use aliquots in DMSO and stored at -80°C. Cell lines were treated with 5 nM Tal every 72 hours. For combination treatments, cells were treated with the combination of 10 nM DAC and 5 nM Tal on day 1 and new DAC at the appropriate concentration for a final concentration of 10nM was added to cells on days 2 and 3. Cells were harvested after 72 hours.

The TP53 inhibitor Pifithrin- α (PFT, Selleckchem) was prepared as a stock solution of 50 mM in DMSO and stored at -20°C in single-use aliquots. Cells were treated with 50 uM PFT on day 1 of the 72 hr treatment cycle. Interferon- β (IFN β , PeproTech) was prepared as a stock solution of 1 mg/mL in water and aliquoted and stored at -20°C for single use. Cells were treated with IFN β at a final concentration of 100ng/mL on day 1 of the 72 hr treatment cycle. The JAK/STAT inhibitor ruxolitinib (Rux, Invivogen) was prepared as a stock solution of 10 mM in DMSO and stored at -20°C in single-use aliquots. Cells were treated with 2 uM Rux on day 1 of the 72 hr treatment cycle. Tumor necrosis factor α (TNF α , PeproTech) was prepared as a stock solution of 200ng/µL in water and stored at -20°C. Cells were treated with 50 ng/mL TNF α on day 1 of the 72 hr treatment cycle. Interleukin 1- β (IL1- β , PeproTech) was prepared as a stock solution of 40 ng/µL in water and stored at -20°C. Cells were treated with 1 ng/mL IL1- β on day 1 of the 72 hr treatment cycle. The STING inhibitor H-151

(Invivogen), was prepared as a stock solution of 150 mM in DMSO and stored at -20°C in single-use aliquots. Cells were treated with 500 nM H-151 on day 1 of the 72 hr treatment cycle.

2.4.3 RNA extraction and quantitative PCR

Total RNA was isolated from cultured cells using the NucleoSpin RNA Plus kit (Macherey-Nagel) according to manufacturer protocol. cDNA was synthesized by converting 1-2ug of RNA using the High Capacity cDNA Reverse Transcription kit (Applied Biosystems). Quantitative real-time PCR was performed using Power Sybr Green PCR Master Mix (Applied Biosystems) in a CFX384 Touch Real-Time PCR system (BioRad). The sequences of primers used are listed in supplemental materials and methods.

2.4.4 Immunofluorescence staining

AML cells were cytopun onto glass slides for 5 min at 200 rpm in PBS in a Shandon Cytospin 4. Cells were fixed for 10 min in 4% paraformaldehyde, washed 3 times in DPBS, permeabilized for 10 min in permeabilization solution (50 mM NaCl, 3 mM MgCl₂, 10 mM HEPES, 200 mM Sucrose and 0.5% Triton X-100 in PBS 1X), washed 3 times in DPBS + 1% BSA, then blocked overnight in 10% FBS. After incubation with mouse monoclonal anti-double stranded DNA antibody (1:100, Millipore) for 1 hr at 37°C, cells were washed and incubated with Dylight 594-anti-mouse and/or Dylight 488-anti mouse antibody (1:200, KPL, Inc.) for 1 hr at 37°C. After washing, slides were sealed in mounting solution containing DAPI (Cell Signaling). Images were examined and acquired using a Nikon fluorescent microscope Eclipse 80i (100×/1.4 oil, Melville, NY). Images were captured using a CCD (charge-coupled device) camera and the imaging software NIS Elements (BR 3.00, Nikon).

2.4.5 TCGA analysis

To evaluate STING gene expression values (labeled "TMEM173" in processed TCGA legacy data) between samples with and without TP53 mutations, we used the TCGA bioinformatics R package¹⁸⁹ to leverage transcriptomics data from The Cancer Genome Atlas¹⁶⁸. Using samples from the 'TCGA-LAML' TCGA leukemia cohort, we quantified and compared normalized expression values from legacy data (i.e. hg19) derived from RNA-seq experiments. For this comparative analysis, we defined 16 samples as TP53 mutation carriers (Table S2) using TP53 mutation carrier status data from Vadakekolathu et al.¹⁹⁰. We used The Wilcoxon Rank Sum Test as implemented in the `stat_compare_means` function of the `ggpubr` package to evaluate the statistical significance of log-transformed STING gene expression distributional differences.

2.4.6 Protein extraction and immunoblotting

Cell pellets were harvested at the indicated time points and were stored in -80°C prior to protein extraction. Cells were lysed in RIPA buffer (Sigma) supplemented with 1% phosphatase inhibitor (Thermo scientific) and 1% protease inhibitor (Thermo scientific) and incubated for 45 minutes on ice with periodic vortexing. Supernatants were collected after centrifugation at 16,000xg at 4°C for 20 minutes. Protein was quantified using Pierce BCA assay (Thermo scientific). Whole cell extracts (20µg) in NuPAGE LDS Sample Buffer with 10% β-mercaptoethanol were boiled for ten minutes and loaded onto 4-20% SDS-PAGE gels (Bio-Rad laboratories), transferred to polyvinylidene difluoride membranes (PVDF, GE Life Sciences) and blocked in TBST-5% bovine serum albumin (BSA) for 1hr at room temperature. Primary antibodies were applied overnight at 4°C. Blots were washed 3 times in Tris Buffered Saline-0.1% Tween 20 (TBST) and secondary antibodies were added for 1 hr at room

temperature, followed by 3 additional washes. Blots were developed using a Hi/Lo Digital-ECL Western blot detection kit and Kwik Quant Imager in the 1:10 ratios. Band densitometry was quantified using ImageJ software (NIH). Antibodies used were PARP1 rabbit monoclonal (1:1000, Cell Signaling), anti- β -actin mouse monoclonal (1:10000), pSTING (TMEM173) rabbit monoclonal (1:1000, Cell Signaling), STING (TMEM173) rabbit monoclonal (1:1000, Cell Signaling), and vinculin rabbit monoclonal (1:1000, Cell Signaling).

2.4.7 Microarray sample preparation and analysis

Total RNA was isolated using the NucleoSpin RNA extraction kit. RNA was quantified with NanoDrop ND-1000, followed by quality assessment with 2100 Bioanalyzer (Agilent Technologies). Sample amplification and labeling procedures were carried out using the Quick RNA Amplification and Labeling Kit (Agilent Technologies) with minor modifications. Briefly, 400 ng total RNA was reverse-transcribed into cDNA by MMLV-RT using oligo dT primers (System Bioscience). The cDNA was then used as a template for in vitro transcription in the presence of T7 RNA polymerase and cyanine-labeled CTP (Perkin Elmer). The labeled cRNA was purified using the RNeasy mini kit (Qiagen). RNA spike-in controls (Agilent Technologies) were added to RNA samples before amplification and labeling according to the manufacturer's protocol. Agilent human GE 4x 44K v2 microarrays containing 41,000 unique probes targeting 27,958 Entrez gene RNAs were used. 825ng of each cyanine-labeled sample was used for hybridization at 65°C for 17 hours in a hybridization oven with rotation. After hybridization, microarrays were washed and dried according to the Agilent microarray processing protocol in a walk-in ozone-controlled enclosure. Microarrays were scanned using an Agilent G2505C Scanner controlled by Agilent Scan Control 7.0 software. Data were extracted with Agilent Feature Extraction 9.5.3.1

software. The R/Bioconductor package limma was then used to process expression data files. Within- and between-array normalizations were performed using the loess and aquantile methods, respectively. The normexp option was used for background correction. Raw files were read in using the read.maimages function. Log₂-fold change in transcription for drug-treated conditions over mock-treated was obtained for each sample at the day 3 time point studied.

2.4.8 STRING protein-protein interaction map

Homologous recombination and Interferon Alpha Response/TNF α via NF- κ B genes of interest were used as input for exploratory analysis using string-db (<https://string-db.org>), a computational resource which summarizes known and predicted protein-protein interactions culled from experimental data from several databases: DIP, BioGRID, HPRD, IntACT, MINT, and PRB; and curated data from: Biocarta, Biocyc, GO, KEGG, and Reactome. The comparisons selected for input were specific for Homo Sapiens and included all genes used for RT-qPCR analysis. Interaction scores are assigned based on probabilities derived from various evidence channels and normalized for random associations as described in von Mering et al. (2005)¹⁹¹.

2.4.9 HR repair analysis

Nuclear extracts were prepared using the Cell Lytic NuCLEAR Extraction Kit (Sigma-Aldrich). Nuclear extracts were dialysed for two hours using the Plus One Mini Dialysis Kit 1kDa (GE Healthcare) in dialysis solution (20 mM HEPES pH9, 100 mM KCl, 0.2 mM EDTA, 20% glycerol, 0.5 mM DTT, 0.1 mM PMSF). Protein content was quantified by Nanodrop and diluted to 0.5 μ g/ μ l in DNase/RNase-free water. Diluted nuclear extracts were incubated with 5 μ l each of dl-1 and dl-2 plasmid (Homologous Recombination Assay Kit, Norgen

Biotek) in reaction buffer for 2 hours at 30 °C. Plasmid DNA was recovered with the QIAamp DNA mini kit (Qiagen), and the relative quantity of recombined product was determined by quantitative real-time PCR CFX384 Real Time System (BioRad) using PCR primers spanning the repair site, normalized against amplification of a distant site (primers supplied by Norgen Biotek).

2.4.10 Statistical analysis

Unless otherwise defined, all data are presented as mean \pm SEM. Statistical analysis for biological assays and mouse studies was performed using Graphpad Prism software to calculate 2-tailed unpaired t test or 1-way or 2-way ANOVA, as appropriate.

2.4.11 Data Availability

Raw and processed data files related to gene expression microarray will be made available through the Gene Expression Omnibus (GEO) database repository with the publication of the associated manuscript.

CHAPTER 3: Anti-tumor effects of DNMTi+PARPi combination therapy in immune-competent AML mouse models

3.1. Introduction

As discussed in the preceding chapters, AML has diverse cytogenetic and molecular abnormalities that predict treatment outcomes, enable treatment stratification, and, increasingly, provide therapeutic targets¹³⁷. While DNMTis are used to treat AML patients unfit for intensive chemotherapy, responses are not durable. This suggests the need for novel DNMTi therapy combinations. Our in vitro results in AML cell lines and primary cells presented in Chapter 2 show that DNMTis in combination with PARPis induce an IFN/inflammasome response that is dependent on STING and is mechanistically linked to generation of HRD. Differences in signaling were noted in TP53 mutant vs WT AMLs. IFN/inflammatory signaling is mainly mediated by the transcriptional activation of ERVs by DNMTi treatment. In contrast, in AMLs with WT TP53, DNMTis require combination with PARPis for activation of STING-dependent IFN/inflammatory signaling. Nevertheless, in both TP53 mutant and WT AMLs, induction of signaling leading to HRD is STING-dependent. These results led to validation studies in AML mouse models treated with DNMTi and PARPis.

Our previous studies in AML mouse xenografts treated with the drug combination showed significantly decreased leukemia burden, as measured by photon intensity (Figure 3.1A,B), and increased survival (0.1 mg/kg dose of talazoparib paired with 0.5 mg/kg of AZA (Figure 3.1C)¹²¹. The dosing regimen was well tolerated, as measured by mouse weights over the course of the study (Figure 3.2D). However, these mouse models lacked immune systems. Therefore, in this chapter

we validate efficacy of this drug combination in immune-competent AML mouse models and study alterations in expression of key cytokines and IFNs in the leukemia microenvironment.

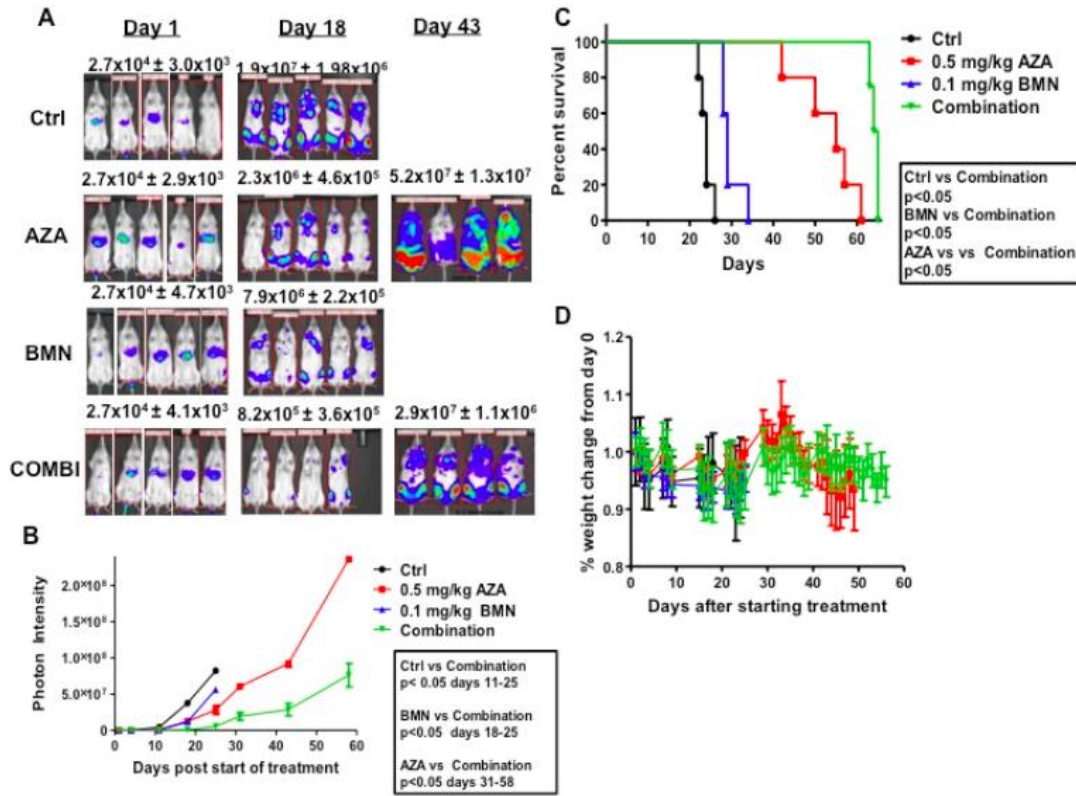


Figure 3.1: MOLM14-Luc mouse model. (A) Bioluminescence measurements of photon intensity showing leukemia burden for duration of the experiment. Measurements represent mean \pm SEM. (B) Graph of photon intensity with time post drug treatment up to 61 days and euthanasia. Measurements represent mean \pm SD (C) Graph of % survival with time post therapy. (D) % body weight change vs time. Measurements represent mean \pm SEM. In all of the above, error bars represent the SEM. Figure from Muvarak et. al (2016)¹²¹.

Several studies examining immune function in AML patients¹⁹² and mouse models¹⁹³ have reported defects in T cell function, as well as an immunosuppressive phenotype. Importantly, it has been well established that tumor-associated immune suppression can lead to impaired anti-

tumor responses and ultimately poor outcomes. Similarly, Zhou and colleagues recently characterized a unique population of exhausted T cells (CD8+Tim3+PD-1+) in mice with advanced AML¹⁹³. Work has also implicated antigen-presenting cells (APCs), producers of type I IFN, in generating a unique T cell tolerant state in AML-bearing animals¹⁹⁴, suggesting that the host type I IFN response through STING may not be activated in this disease¹⁹⁵, and that therapeutic strategies that enhance immune function could be effective in AML (Figure 3.2).

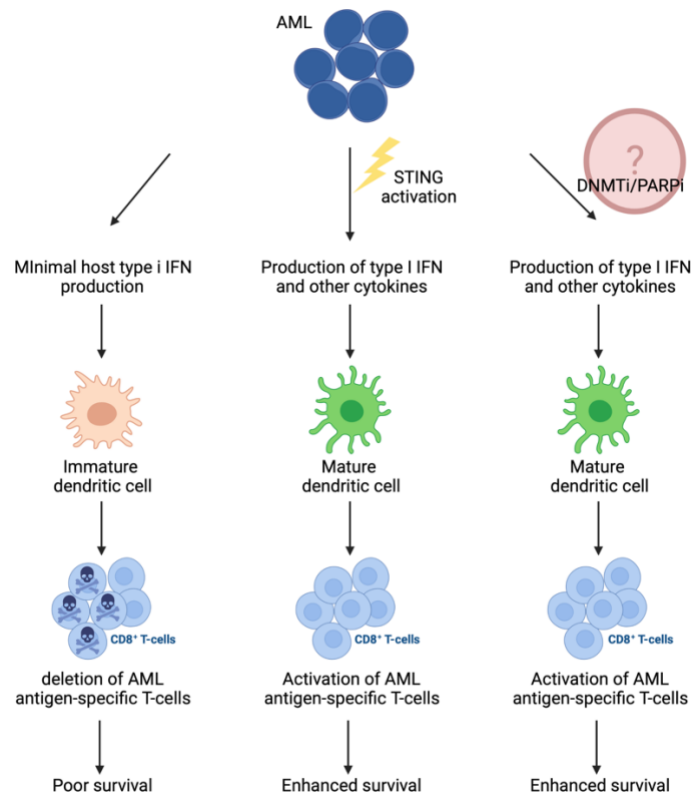


Figure 3.2: Induction of type I IFN and other inflammatory cytokines through STING pathway activation results in potent leukemia-specific immunity, culminating in prolonged survival of mice with AML. Figure modified from Curran et al. (2012)¹⁹⁵. Created with BioRender.com.

As discussed in earlier chapters, DNMTs have been shown to induce genome-wide transcriptional changes resulting in a sustained anti-tumor memory response and inhibition of tumor cell growth and stem-like cancer properties^{104,156}. They also upregulate and enrich immunomodulatory pathways in multiple cancer types and reverse tumor-mediated immune evasion. DNMTs can induce an IFN $\alpha\beta$ response, reestablish antigenicity, and activate and recruit CD8⁺ T effector cells to the tumor microenvironment^{196,197}. Induction of these immune events is modulated by upregulation of dsRNA from ERVs^{81,82}. These DNMTi-induced ERVs are associated with a cytosolic dsRNA antiviral response that is potentiated by the activation of PRRs, which in turn initiate an innate immune response¹⁹⁸. The link between inflammation and DNA damage has been extensively studied, although the exact effects of inflammation on DNA repair still remain largely unknown. In this chapter, we will use the immune-competent orthotopic murine AML model C1498^{199,200} to corroborate the established model for induction of innate immune signaling and provide an additional layer to the positive feedback loop between inflammation and DNA damage which can then be exploited for cancer therapy.

3.2. Results

3.2.1. STING inhibition abrogates IFN/inflammasome signaling in TP53 WT and TP53 mutant AML cells

Given the STING-mediated immune response that we observed in our in vitro studies (described in Chapter 2), we wanted to confirm that IFN/inflammasome signaling with DAC-Tal treatment is STING-dependent in these murine cells as well. In order to study this effect more directly, we developed STING knock-out (KO) cells using CRISPR/CAS9 technology (Figure S3.1). We were successful in creating bulk KO with nearly complete abrogation of STING protein levels and a danger sequencing KO score of 90. We then treated our parental

C1498 cell line with either DNMTi, PARPi or the combinations thereof \pm the addition of the STINGi described in Chapter 2, and our STING KO cells with DNMTi, PARPi or combination. Our studies confirm that both STINGi treatment and STING knock-out (KO) similarly abrogate induction of IFN/inflammasome gene expression changes by the drug combination (Figure 3.3A, Figure S3.2A). Furthermore, HR gene expression, downregulated by our combination treatment, is restored by STING inhibition via exogenous treatment as well as by CRISPR KO (Figure 3.3B, Figure S3.2B).

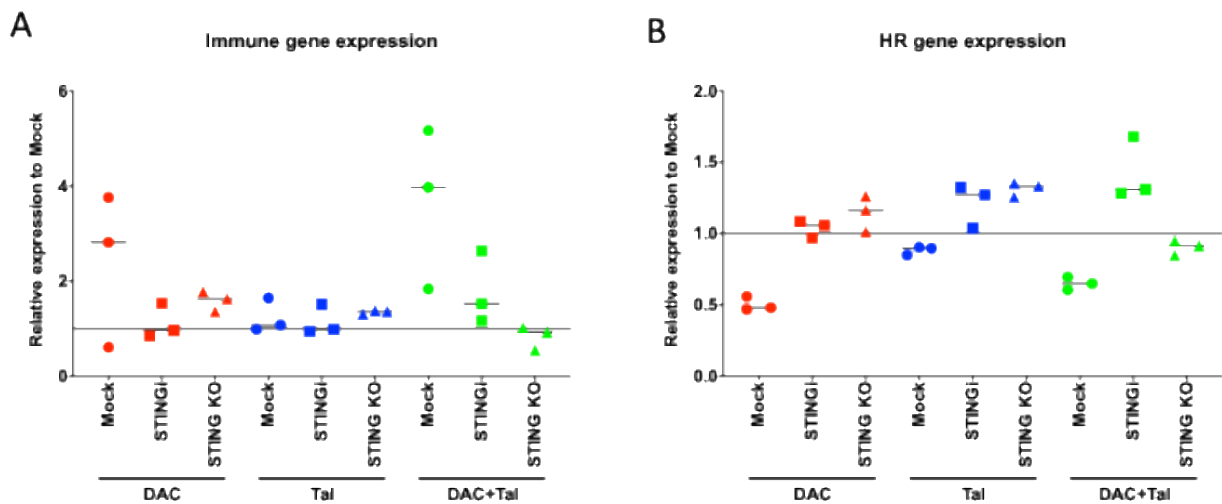


Figure 3.3: STING inhibition abrogates IFN/inflammasome signaling in C1498 cells. (A-B) Relative expression of immune (A) and HR (B) genes after CRISPR KO of STING, or co-treatment with 500nM STINGi in C1498 cells treated with vehicle, 10 nM DAC, 5 nM Tal, or DAC/Tal combination: 10 nM DAC + 5 nM Tal \pm 500 nM STINGi for all conditions (72hrs, n = 3). All data are presented as mean \pm SEM with statistical significance derived from two-tailed unpaired Student's t test (or ANOVA).

3.2.2. DNMTi+PARPi combination therapy results in anti-leukemia responses in an immune-competent AML mouse model

To test the extent to which treatment with DNMTi+PARPi drives an anti-leukemia immune response, we used the above-described immune-competent murine AML model C1498L^{199,200}. To enable imaging of this cell line and measurement of leukemia burden in C57B16 mice, we performed lentiviral transduction of the luciferase gene, creating C1498L-luc cells. Thereafter, 1×10^6 C1498L-luc cells were injected intravenously into C57B16 mice. Three days post injection, mice were imaged and sorted into 4 groups so that mean tumor burdens were similar. Given that DAC or AZA combined with the PARPi TAL gave similar *in vivo* results¹²¹, and AZA had been optimized in *in vivo* mouse models¹⁰⁴, we used AZA in this set of experiments. Dosing was started on the day of sorting, and groups of treated mice were as follows: vehicle, DNMTi (0.3 mg/kg AZA, PARPi 0.3mg/kg Tal), and DNMTi+PARPi, dosed for 5 days with 2 days rest. Disease burden was monitored by longitudinal luminescence imaging. Mice were observed daily and weighed 5 days/week and were euthanized immediately when they became moribund. AZA-Tal was well tolerated, as shown by mouse body weights throughout the study (Figure 3.4D). Leukemia burden was lower in the AZA/Tal drug combination-treated mice, compared with other treatment groups (Figure 3.4A,B). AZA-Tal combination treatment also prolonged survival compared with other treatment groups (Figure 3.4C; $P < 0.05$).

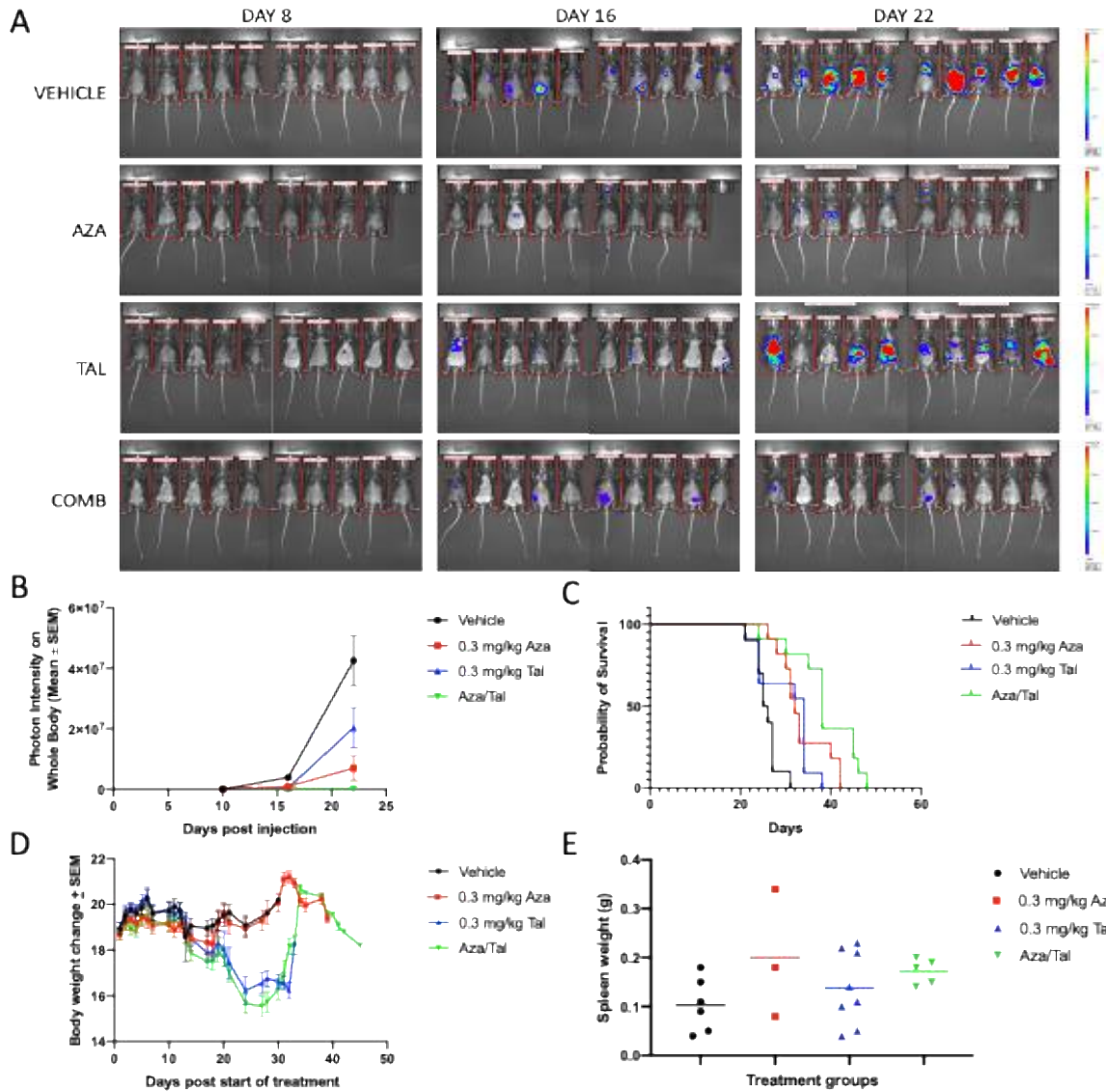


Figure 3.4: DNMTi+PARPi combination therapy results in anti-leukemia responses in an immune-competent AML mouse model. (A) Bioluminescence measurements (mean \pm SEM) of photon intensity showing relative leukemia burden. (B) Graph of photon intensity with time post drug treatment up to 22 days. (C) Graph of % survival with time post therapy. (D) % body weight change vs time. (E) Graph of spleen weight in different treatment groups post euthanasia. In all of the above, error bars represent the SEM.

3.2.3. DNMTi+PARPi combination therapy enhances immune responses in tumor-bearing mice.

To confirm our finding of increased expression of IFN/inflammasome genes following DNMTi+PARPi combination treatment *in vitro*, we next determined whether C1498 mice treated with the drug combination showed increased immune responses *in vivo*. First, serum prepared from blood extracted from the mice after 14 days of study treatment was analyzed for cytokine expression using flow cytometry. Mice from the combination drug-treated group showed increases in cytokines, including, IL-1 α , IL-10, IFN- γ , TNF α , MCP-1 and GM-CSF, compared with single-agent treatments (Figure 3.5A)¹⁹³. In contrast, other cytokines tested showed no significant differences (Figure S3.3). Second, the combination-treatment group showed increases in expression of STING, IRF3 and IRF7, compared with either AZA or Tal treatment groups (Figure 3.45). Interestingly, IFN β expression was driven by the PARPi treatment, while increases in IRF3 and IRF7 were DNMTi-mediated.

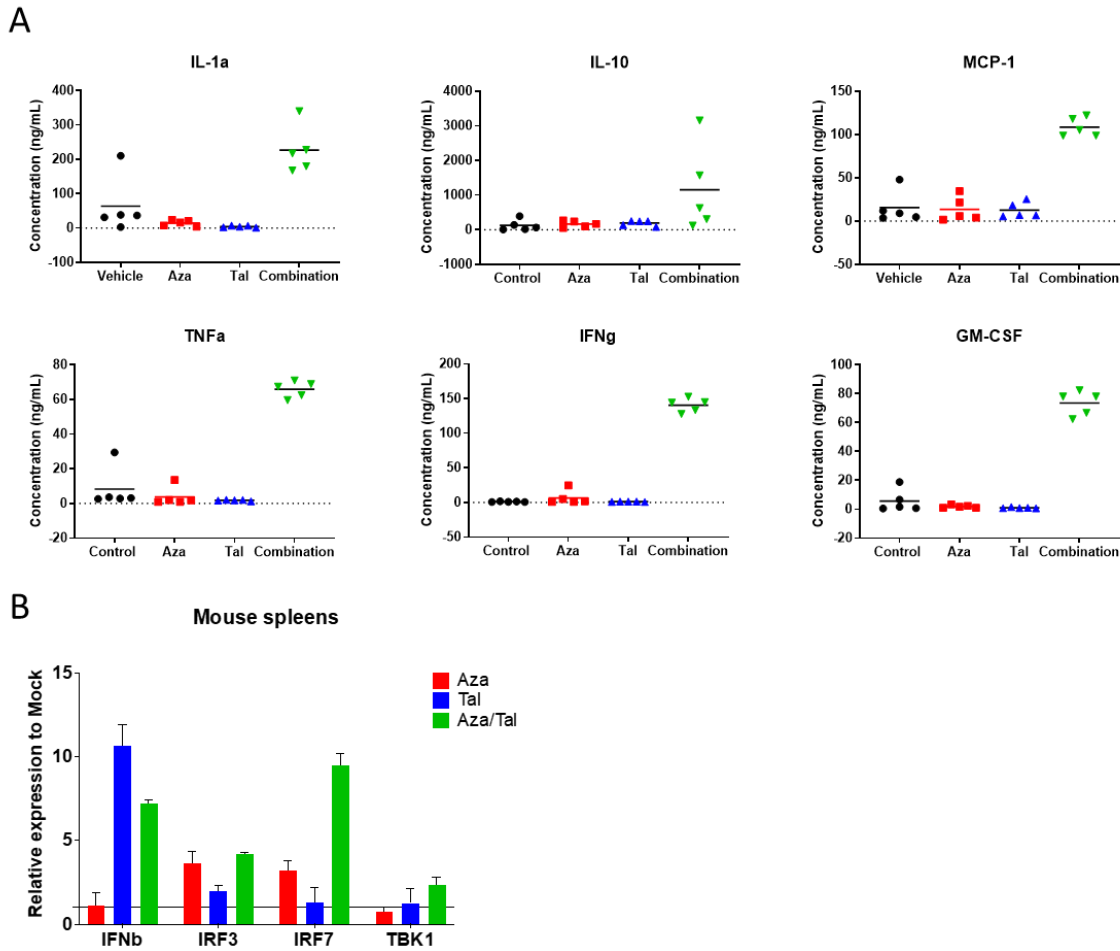


Figure 3.5: DNMTi+PARPi combination therapy enhances immune responses in tumor-bearing mice. (A) Cytokine expression measured via flow cytometry using serum extracted from mice after 14 days of treatment. **(B)** Relative expression of immune genes in spleen samples from mice treated with Aza, Tal, or the combination.

3.3. Discussion

Immunotherapy has revolutionized treatment for many cancers, but in AML the ability to predict the groups of patients and the types of AML that may respond to immune targeting remains limited. In this study, we show that IFN/inflammasome signaling is driven by DNMTi in combination with PARPi therapy *in vivo*. We have previously shown that low doses of DNMTis

can transcriptionally activate epigenetically silenced repeat elements, including ERVs, resulting in a cytoplasmic dsRNA response, known as viral mimicry, leading to IFN signaling^{81,156,157}.

How IFN type I immune signaling leads to anticancer changes in the tumor microenvironment is not well understood in hematologic malignancies, including AML²⁰¹⁻²⁰³. Our results show that DNMTi+PARPi combination treatment of immune-competent AML mice can significantly increase release of cytokines, including IFN γ , that may contribute to anti-leukemia immune responses. Previous studies have shown that conventional T cells could be activated to release IFN γ in the presence of AML cells, leading to anti-leukemic effects^{204,205}. Another cytokine upregulated by the combination therapy is GM-CSF, which can promote differentiation of AML cells²⁰⁶⁻²⁰⁸. IL-1 α is also upregulated by the drug combination and has been shown to increase anti-tumor immunity in AML^{204,209}. Future study of how these drugs functionally activate T-cell and macrophage responses in vivo will expand our knowledge of their effects on the tumor microenvironment in AML.

STING activation is critical for activating anti-cancer immune responses in solid tumors, but less is known about its role in hematologic malignancies, including AML^{177,183,184}. Notably, STING expression is low in many tumors, compared to normal tissues, and research on activation of STING-dependent immune signaling is actively being pursued¹⁸¹⁻¹⁸⁴. Accordingly, we recently reported that DNMTi treatment of TNBC and OC can transcriptionally activate STING¹²⁹. TANK-binding kinase-1 (TBK1) phosphorylates STING and leads to the recruitment of interferon regulatory factor-3 (IRF3)^{210,211}. This leads to IRF3 phosphorylation, dimerization, and translocation into the nucleus, where it induces transcription of genes encoding various cytokines, interferons, and chemokines²¹¹. TBK1 is also known to contribute to NF- κ B activation via phosphorylation of I κ B α , providing a synergistic response against invading pathogens^{211,212}. In

concordance with this, we report increased expression levels of TBK1, IRF3, and IRF7, an interferon regulatory factory that is involved in innate immune response to DNA and RNA viruses²¹³, in mouse spleens post DNMTi+PARPi combination treatment. Therefore, our data suggest that AMLs may be particularly poised for STING activation using novel STING activation strategies.

3.4. Methods

3.4.1 Cell culture

The murine cell line C1498 was cultured in DMEM+ L-Glutamine supplemented with 10% Fetal Bovine Serum (FBS). Cells were cultured and maintained in 37 °C incubators with 5% CO₂ and passaged every 3- 5 days.

3.4.2 CRISPR-engineered cell lines

STING sgRNA targeting exon 3 was expressed from lentiCRISPR v2 (Addgene plasmid #52961 (<http://n2t.net/addgene:52961>)) to generate C-1489 STING KO cells. Targeting crRNA (CAGTAGTCCAAGTTCGTGCG) was designed using the BROAD GPP Web portal (<https://portals.broadinstitute.org/gpp/public/>), synthesized by Integrated DNA Technologies (IDT), and cloned into plentiCRISPRvsPuromycin BsmB1 site. Non-targeting vs STING-targeting lentiviruses were transduced into C-1489 cells using Kolliphor (1ng/ml). After 72hrs cells were pelleted and rinsed to remove Kolliphor prior to resuspension in medium supplemented with 5 µg/mL puromycin for 5days to select for transduced cells. Following selection and cell expansion, PCR amplification of the gDNA encompassing the targeted domain followed by amplicon sequencing (Genewiz) and ICE Analysis (Synthego) revealed 90% KO.

3.4.3 Drug reagents and treatments in vitro

The DNTMi decitabine (DAC, Sigma-Aldrich) was prepared as a stock solution of 10 mM in DMSO, aliquoted, and stored at -80 °C for single use. Cell lines were treated daily with 10 nM DAC. The PARPi talazoparib (Tal, Pfizer) was prepared as a stock solution of 50 mM in DMSO, aliquoted and stored at -80 °C. Tal was further diluted to 5 mM in DMSO in single-use 1 µL aliquots and stored at -80 °C. Cell lines were treated with 5 nM Tal every 72 hours. For combination treatments, cells were treated with the combination of 10 nM DAC and 5 nM Tal on day 1 and new DAC was added to of cells on days 2 and 3 at the appropriate concentration for a final concentration of 10 nM. Cells were harvested after 72 hours.

The TP53 inhibitor pifithrin- α (PFT, Selleckchem) was prepared in DMSO as a stock solution of 50 mM and stored at -20 °C in single-use aliquots. Cells were treated with 50 μ M PFT on day 1 of the 72 hr treatment. STING inhibitor H-151 (Invivogen) was prepared as a stock solution of 150 mM in DMSO and stored at -20 °C in single-use aliquots. Cells were treated with 500 nM H-151 on day 1 of the 72 hr treatment.

3.4.4 Immune-competent mouse model

C57BL/6 female mice (6–8 weeks old) from Envigo (Frederick, MD) were housed under pathogen-free conditions in the University of Maryland Baltimore (UMB) AAALAC-accredited facility. All experiments with these mice were conducted in compliance with PHS guidelines for animal research and approved by UMB IACUC. Exponentially growing C1498-luciferase-expressing murine AML cells (1×10^5) were injected into tail veins. Mice were arbitrarily sorted into 4 groups of 10 mice on day 3 after injection, prior to treatment initiation. Mice were observed daily, weighed 5 days per week, and imaged once per week beginning on day 10. Mice were bled on days 14 and 28 for serum isolation.

Mice were treated with 0.3 mg/kg AZA, 0.1 mg/kg Tal, the combination of both, or vehicle. AZA was prepared as a stock solution of 0.03 mg/ml, aliquoted, and stored at -80 °C for single use. Tal was prepared weekly at 0.03 mg/mL in 10% DMAc, 6% Solutol, and 84% PBS and stored at 4 °C in the dark. AZA was administered by subcutaneous injection daily and Tal was administered by oral gavage 5 days per week for the duration of the study. The endpoints of the study were disease burden by imaging and survival. Spleens were harvested when mice were euthanized.

3.4.5 LEGENDplex immunoassay

Serum was isolated from mouse blood collected at day 14 and stored at -20. LegendPlex mouse cytokine panel 2 (Biologend) was used per manufacturers instruction to look at changes in cytokine levels with treatment. Briefly, Matrix C, and diluted standards were added to the standard wells of a 96 well plate. Assay Buffer and 25ul of diluted serum sample were added to the sample wells. Mixed beads and detection antibodies were added to all plates, and plate was incubated while covered on a shaker for 2 hr at room temperature. SA-PE was added and plate was incubated for another 30min. Plate was then centrifuged and supernatant removed. Samples were washed once using 1X wash buffer and then resuspended in wash buffer to be read on flow cytometer. BD Canto was used to read the samples and set up performed according to the user manual.

3.4.6 RNA extraction and quantitative PCR

Total RNA was isolated from cultured cells using the NucleoSpin RNA Plus kit (Macherey-Nagel) according to manufacturer protocol. cDNA was synthesized by converting 1-2 ug of RNA using the High Capacity cDNA Reverse Transcription kit (Applied Biosystems). Quantitative real time PCR was performed using Power Sybr Green PCR Master Mix (Applied

Biosystems) in a CFX384 Touch Real-Time PCR system (BioRad). The sequences of primers used are listed in Supplementary Materials and Methods.

3.4.7 Protein extraction and immunoblotting

Cell pellets harvested at the indicated time points were stored in -80°C prior to protein extraction. Cells were lysed in RIPA buffer (Sigma) supplemented with 1% phosphatase inhibitor (Thermo scientific) and 1% protease inhibitor (Thermo scientific) and incubated for 45 minutes on ice with periodic vortexing. Supernatants were collected after centrifugation at $16,000\times g$ at 4°C for 20 minutes. Proteins were quantified using Pierce BCA assay (Thermo Scientific). Whole cell extracts ($20\mu\text{g}$) in NuPAGE LDS Sample Buffer with 10% β -mercaptoethanol were boiled for ten minutes and loaded onto 4-20% SDS-PAGE gels (BioRad Laboratories), transferred to polyvinylidene difluoride membranes (PVDF, GE Life Sciences) and blocked in TBST-5% bovine serum albumin (BSA) for 1hr at room temperature. Primary antibodies were applied overnight at 4°C . Blots were washed 3 times in Tris Buffered Saline-0.1% Tween 20 (TBST) and secondary antibodies were added for 1 hr at room temperature followed by 3 additional washes. Blots were developed using a Hi/Lo Digital-ECL Western blot Detection kit and Kwik Quant Imager at 1:10 ratios. Band densitometry was quantified using ImageJ software (NIH). GAPDH mouse monoclonal (1:10000) and STING (TMEM173) rabbit monoclonal (1:1000, Cell Signaling) antibodies were used.

3.4.8 Statistical analysis

Unless otherwise stated, all data are presented as mean \pm SEM. Statistical analysis for biological assays and mouse studies was performed using GraphPad Prism software to calculate 2-tailed unpaired t test or 1-way or 2-way ANOVA as appropriate.

CHAPTER 4: Phase 1 clinical trial of DNMTi+PARPi combination therapy in adult patients with relapsed/refractory AML⁴

4.1. Introduction

The standard therapeutic approaches for AML for the last 50 years has been combination cytotoxic chemotherapy including the nucleoside analogue cytarabine and an anthracycline, usually daunorubicin or idarubicin^{214,215}. Post-remission therapy generally consists of high-dose cytarabine or HSCT⁹⁵. While roughly 70% of adults under age 60 years achieve CR and survival has improved in younger adults overall, less than 40% of patients with prognostically unfavorable AML cell karyotypes or molecular abnormalities (discussed in Chapter 1) or with advanced age or significant comorbidities²¹⁶ achieve CR and long-term survival is less than 10%^{217,218}. New therapies are needed for patients in groups with poor responses to cytotoxic chemotherapy and for those resistant to, or relapsing after, initial therapy. These patients are currently often treated with DNMTis.

Decitabine, or 5-aza-2'-deoxycytidine, is a DNMTi that becomes incorporated into replicating DNA as an altered cytosine base and covalently binds DNMTs, creating a cytotoxic DNMT-DNA complex, while simultaneously triggering the degradation of soluble DNMT's²¹⁹. Decitabine has also been found to induce cellular differentiation at low concentrations by reversing DNA methylation-induced gene silencing²²⁰. Decitabine was FDA-approved for treatment of MDS

⁴ Baer MR, Kogan AA, Bentzen SM, Saum G, Lapidus RG, Emadi A, Duong VH, O'Connell CL, Rassool FV. Phase 1 study of combination therapy with the DNA methyltransferase inhibitor decitabine and the poly ADP ribose polymerase inhibitor talazoparib in adult patients with relapsed/refractory acute myeloid leukemia. Manuscript in prep.

and the regimen in use is 20 mg/m² intravenously (IV) daily for five days every 4 weeks^{145,221}. Decitabine is well tolerated and has also shown efficacy in AML, and therefore is also currently in widespread use to treat AML in patients who are previously untreated and “unfit” for chemotherapy or who have refractory or relapsed AML with low likelihood of response to intensive chemotherapy²²²⁻²²⁷. The CR rate for previously untreated AML patients who receive the 5-day decitabine regimen is in the range of 25% with median survival in the range of 7 months²²²⁻²²⁴. Decitabine has also been used in a 10-day regimen for AML, with a higher response rate and longer duration in some reports²²⁵⁻²²⁹. To improve responses, combinations of DNMTis and novel agents are being tested in clinical trials²¹⁴.

While PARP inhibitors have been mainly applied toward creating synthetic lethality in homologous recombination-deficient tumors, primarily breast and ovarian cancer patients with BRCA mutations, combinations with DNMTis are being explored in sporadic cancers. Using *in vitro* and *in vivo* models of BRCA-proficient AML and TNBC, we have shown that DNMTis in combination with the PARPi talazoparib increase PARP trapping and anti-tumor activity¹²¹. Extending these anti-tumor effects to NSCLC, we also showed that DNMTis downregulate a subset of DNA damage response (DDR) genes that induce homologous recombination deficiency (HRD), which mimics the BRCA-mutant phenotype and sensitizes cells to PARPis¹²⁸. Similar findings were also demonstrated in our recent study in TNBC and OC²³⁰. These preclinical studies suggested that combining talazoparib with a DNMTi may be an attractive therapeutic strategy in AML.

Talazoparib has been evaluated in clinical trials in solid tumors. A phase 1 clinical trial of talazoparib in patients with solid tumors demonstrated good tolerability and established a dose of 1 mg orally (PO) daily as the recommended phase 2 dose²³¹. Talazoparib was subsequently

approved at this dose for germline BRCA-mutated, HER2-negative locally advanced or metastatic breast cancer based on the EMBRACA phase 3 clinical trial²³². The only previously completed clinical trial of talazoparib in hematologic malignancies was a phase 1 trial testing doses of 0.1 to 2 mg daily and showing limited activity as a single agent^{233,234}. While no responses were seen, stable disease was reported in 13 of 25 patients with AML/MDS²³⁴. Given limited single-agent activity, other clinical trials focus on combining PARPis with other AML therapy. Veliparib has been evaluated in two combinatorial regimens in AML patients. The first involves combination therapy with temozolomide, and the second with topotecan and carboplatin^{235,236}.

We designed and implemented a phase 1 clinical trial combining decitabine and talazoparib in relapsed and refractory AML, with correlative laboratory studies. The objectives were to determine the recommended phase 2 doses of decitabine and talazoparib in combination, to test for response to therapy, to explore pharmacodynamic effects, and to explore cytogenetic and molecular predictors of response.

4.2. Results

4.2.1. Patients

A total of 25 patients with relapsed or refractory AML were enrolled on the study (Table 4.1). Median age was 70 years (range, 37 to 89 years). Fifteen were male and ten were female. Karyotypes were complex in 7 of 24 patients, and two had t(3;3). TP53 mutations were present in 5 of 22 patients with molecular studies, and ASXL1 mutations in 5 others. AML was relapsed in 14 patients and refractory in 11. Importantly, 22 of 25 patients had been previously treated with decitabine or azacitidine; median number of courses received by these 22 patients was 8 (range, 2-40). Thirteen had been previously treated with decitabine; median number of courses was 3 (range, 2-32).

Table 4.1: Clinical trial patient metadata

Cohort	Patient	Age/ Sex	Karyotype	Mutations	Status	Prior DNMTi	WBC*	Cycles received	Response	Survival (mos)
1	002	75F	Normal	N-RAS	Ref	AZAx7 DACx3	2.5	2	No	2
	003	64F	Complex	TP53	Rel	DACx9	3.4	4	No	3.2
	005	78M	Normal	FLT3-ITD NPM1 SF3B1 WT1	Ref	AZAx12 DACx3	6.2	2	No	2.3
2	006	75F	Complex	ASXL1 IDH2 RUNX1 SRSF2	Ref	AZA x 5	1.4	6	HI	5.4
	007	69M	Normal	ASXL1 FLT3-ITD RUNX1 SRSF2	Ref	DACx3	12.2	7	HI	6.9
	008	89M	del(16)	DNMT3A ETV6 PTPN11 SF3B1	Ref	AZAx37 DACx3	41.8	3	No	2.3
3	012	37F	Complex	CEPBA TP53	Rel	None	5.9	5	HI	8.3
	013	69M	Normal	ASXL1 IDH2 MPL U2AF1	Ref	DACx32	34.6	3	No	3.6
	015	70M	Near- tetraploidy, t(3;3)	TP53	Ref	AZAx7	1	17	No	19.2
4	020	87M	Normal	FLT3-ITD NPM1 TET2	Rel	AZAx3	2.3 (HU)	2	No	3.2
	023	73M	Normal	TP53 ASXL1 DNMT3A	Rel	DACx16	1.8	1	Died (sepsis)	1
	025	45F	Complex	EED SUZ12	Rel	DACx2	18.2	2	No	5.2
	026	73M	Complex	TP53	Ref	DACx2	0.6	2	No	5
	029	78M	t(4;7)	ASXL1 GATA2 TET2	Rel	DACx16	2.0	2	No	2.8

Table 4.1: Clinical trial patient metadata (continued)

Cohort	Patient	Age/ Sex	Karyotype	Mutations	Status	Prior DNMTi	WBC* (HU)	Cycles received	Response	Survival (mos)
4	030	53F	t(3;3), -7	PTPN11 GATA2 ETV6 SF1	Rel	DACx4	48.1 (HU)	1	Died (sepsis)	1
	031	86M	Normal	ASXL1 ZRSR2 STAG2 TET2 NRAS KRAS ASXL2	Ref	AZAx4	22.6 (HU)	7	No	7.9
5	033	74M	del(5q)	ASXL1 RUNX1 CEPBA SRSF2 TET2	Rel	AZAx9	4	4	No	7.2
	034	63F	inv(1)	NPM1 DNMT3A NRAS	Rel	DACx10	2.3	3	CRi	4.2
6	036	63F	Normal	ND	Rel	AZAx?	0.3	1	ND	2.4
	038	57F	Complex	None	Rel	AZAx6	1.6	2	No	14
	040	55M	Complex	U2AF1, ETV6	Ref	AZAx8	1.0	3	No	6.9
	041	73M	del(20q)	ND	Rel	DACx2	0.4	1	No	2.1
7	042	71M	Normal	NPM1, DNMT3A, FLT3 TET2 KRAS NRAS	Rel	None	4.2	6	CRi	13.8
	043	55M	t(8;21)	RAD21 TET2 CEBPA	Ref	AZAx9	9.8	2	No	4.2
	USC- 004*	53F	?	?	Ref	None	0.23	1	No	3

*x106/ml Ref=Refractory; Rel=Relapsed; DNMTi=DNA methyltransferase inhibitor; AZA=azacitidine; DAC=decitabine

4.2.2. Dose escalation

Decitabine and talazoparib doses were successfully escalated from Cohort 1 to Cohort 7, using the 3+3 design (Table 4.2). The standard algorithm of the 3+3 design was applied. The ‘outer layer’ of this nested dose escalation trial escalated the dose of the two drugs by sequentially going through dose levels 1-7 (corresponding to cohort nomenclature in the Table). If the *provisional* MTD for decitabine in combination with talazoparib had been dose level 1 or 2, one or the other of the ‘inner layers’ of the trial would have been activated. For instance, if the provisional MTD had corresponded to level 2, the dose of decitabine would have been fixed at 15 mg/m² and the dose of talazoparib would have been escalated through steps 2a-c, again using the algorithm of the 3+3 design. If the tolerance had not been exceeded at level 2c, then the RP2D of decitabine would have been 15 mg/m² combined with a dose of talazoparib of 1.0 mg. The MTD had not been reached at dose level 6, so the RP2D of decitabine was 20 mg/m² combined with a dose of talazoparib of 1.0 mg daily for 28 days. Since Cohort 6, with 20 mg/m² decitabine daily for 5 days and talazoparib 1 mg daily for 28 days, was completed without dose-limiting toxicity, cohort 7, consisting of decitabine 20 mg/m² daily for 10 days and talazoparib 1 mg daily for 28 days, was added.

Table 4.2: Dose escalation schedule

		Talazoparib po x 28 days			
		0.25 mg	0.50 mg	0.75 mg	1.0 mg
Decitabine IV X 5 days	10 mg/m ²	1	1a	1b	1c
	15 mg/m ²	2	2a	2b	2c
	20 mg/m ²	3	4	5	6
Decitabine IV X 10 days	20 mg/m ²				7

In Cohort 4, Patient 2 died of sepsis, and the cohort was expanded, although death was attributed to AML, rather than to treatment. Patient 6 also died of sepsis, attributed to AML, and a seventh patient was added. All other cohorts included only three patients. The final dose level was decitabine 10 mg/m² IV daily for 10 days and talazoparib 1 mg orally daily for 28 days.

There were no non-hematologic toxicities. Hematologic toxicities could not be assessed in the presence of persistent AML.

4.2.3. Treatment responses

Responses can be defined as complete remission (CR), CR with incomplete count recovery (CRi), hematologic improvement (HI), not determined (ND), and no response (NR). Responses to decitabine-talazoparib treatment included CRi in one patient in Cohort 5 and one in Cohort 7, who received 3 and 6 cycles, respectively, and HI in two patients in Cohort 2 and one in Cohort 3, who received 6, 7 and 5 cycles of treatment, respectively. The Cohort 7 patient who achieved CRi and the Cohort 3 patient who achieved HI were two of the three patients in

the study who were DNMTi-naïve. One patient in Cohort 3 did not meet criteria for response, but had stable disease and received 17 cycles of treatment. A swimmer plot for all patients is shown in Figure 4.1.

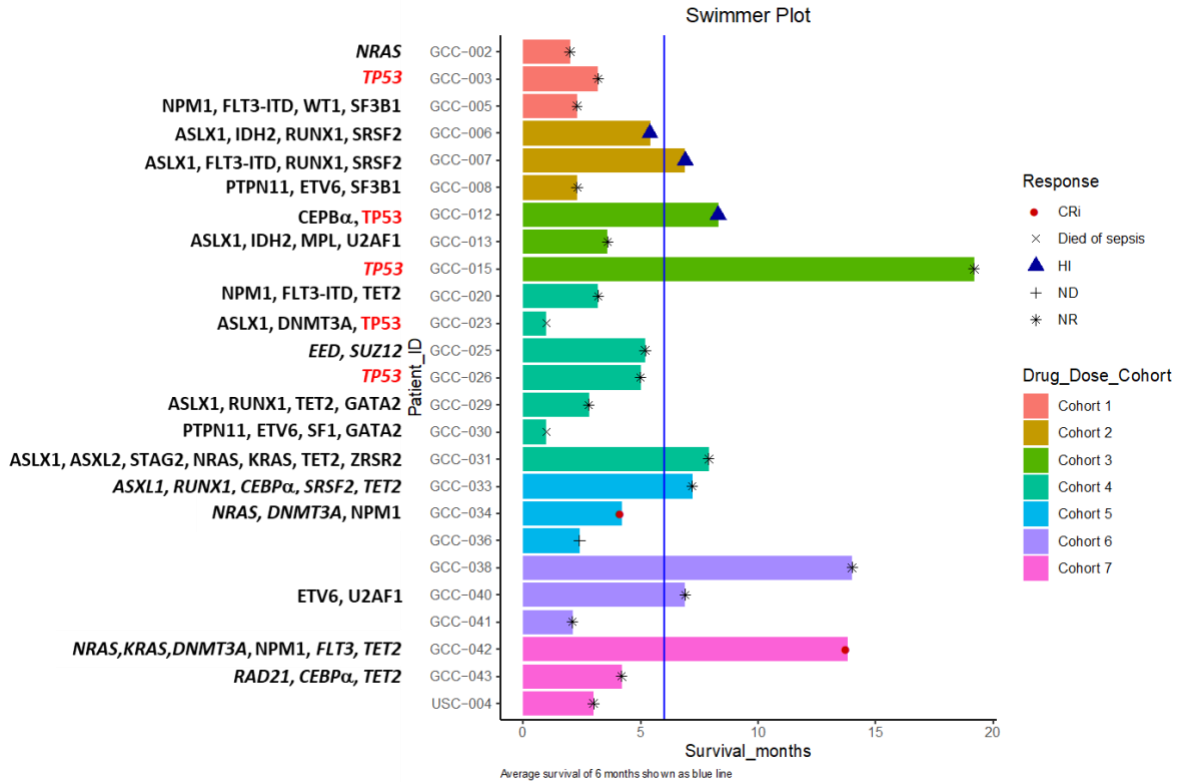


Figure 4.1 Swimmer plot for survival for patients on trial. Left to right: patient mutation status, patient ID, survival (in months), bars color coded by cohort, blue line is the current average survival time for AML patients, and responses at end of each bar (see key on right for description of symbols).

The two patients in Cohorts 5 and 7 who achieved CRi received 3 and 6 cycles of treatment, respectively. The patient in Cohort 5 achieved CRi after 3 cycles, but had repeated infections while pancytopenic and opted to stop treatment. The patient in Cohort 7 achieved CRi after 2 cycles. He relapsed after completing 6 cycles.

4.2.3.1. Molecular features related to treatment response

As part of standard care, the DNA from AML cells from each patient is sequenced for common mutations found in AML (Figure 4.1). To identify mutations that correlated with patient responses, we analyzed the network of gene mutations stratified by patient response, using igraph. Analysis of gene mutation profiles was performed in patients with at least two total mutated genes (Fig 4.2). NRAS, KRAS, TET2, NPM1 and DNMT3 mutated gene pairs were found to be enriched among complete responders. In contrast, SRSF2, RUNX1, FLT3-ITD and IDH2 mutated gene pairs showed enrichment among HI responders.

Given our data showing that AML cell lines and primary cells with TP53 mutations have increased immune signaling with decitabine-talazoparib treatment (Chapter 2), it is of interest that patient 015, with a mutation in TP53, had the longest survival.

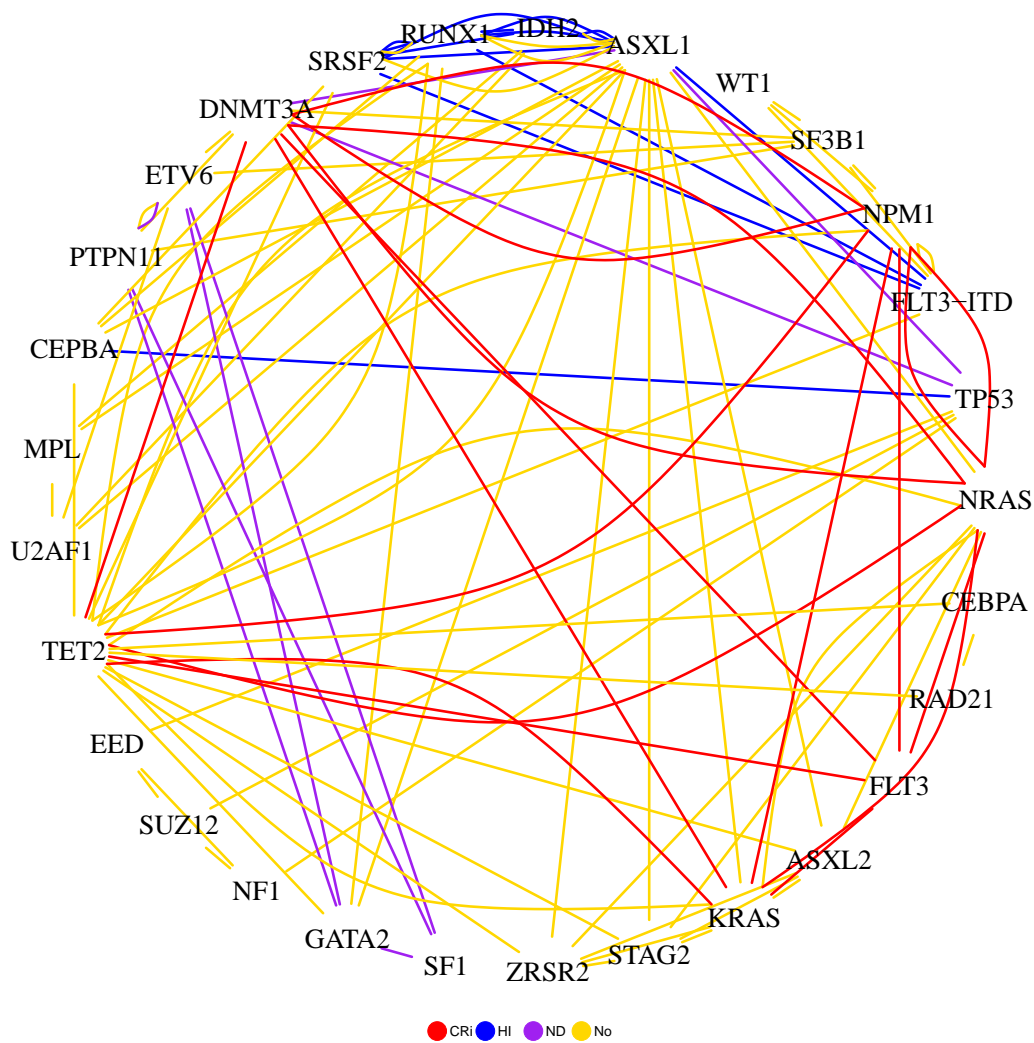


Figure 4.2: Network of gene mutations stratified by patient response. All genes identified with at least one mutation in any patient are shown along the outer ring of the network. Lines then connect all mutation pairs within each patient, and are colored according response: complete response (red), Hi response (blue), or no response (yellow).

To identify differential gene expression that characterized decitabine-talazoparib treatment, RNA sequencing (RNA-seq) was performed on clinical trial samples collected prior to treatment begin on cycle 1 day 1 and at the end of cycle 1. 24 bone marrow and 36 whole

blood RNAseq library samples were processed by the Van Andel Institute (VAI) Genomics Core using the STAR-EdgeR analysis pipeline. These processed data were evaluated for differential expression and pathway analyses. We performed Gene Set Enrichment Analysis (GSEA) using the Molecular Signatures Database (MSigDB) Hallmark gene sets, canonical pathways in Kyoto Encyclopedia of Genes and Genomes (KEGG), and oncogenic signatures (C6). Using an $\text{fdr-based padj} = 0.1$, we see an overall predominance of pathways showing significant negative enrichment as opposed to positive enrichment (Figure S4.1). Hallmark pathways analysis shows enrichment for genes that are downregulated in myc and DNA repair-related pathways in post-treatment samples, compared with pretreatment samples (Figure 4.3).

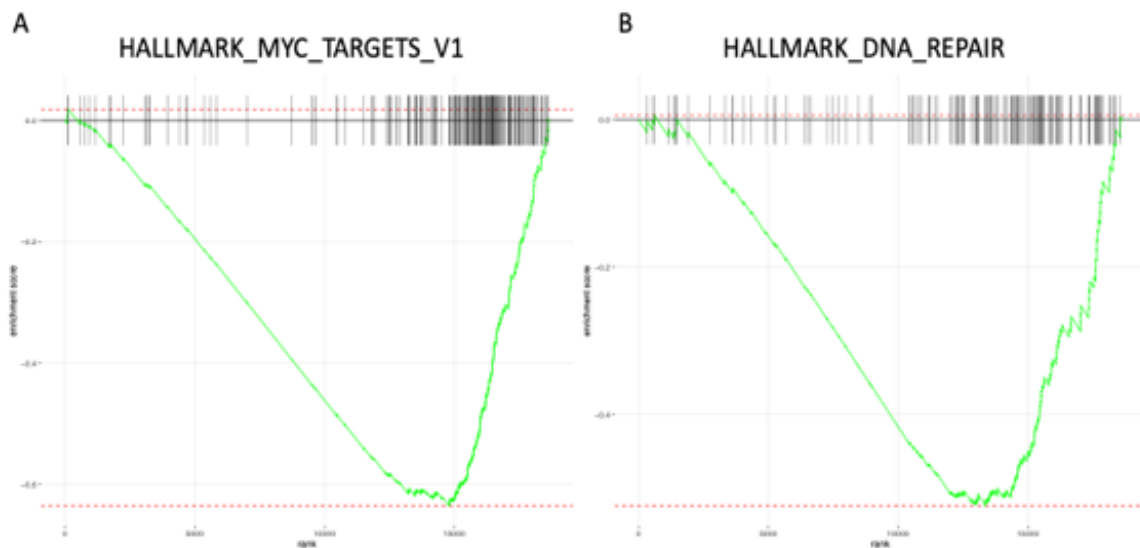


Figure 4.3: Enrichment score plots of key affected pathways. HALLMARK pathway analysis of RNA-seq data reveals negative enrichment for myc and DNA repair -related pathways . For each plot: Y axis: Enrichment score, X axis: Ranked gene list.

Within the oncogenic pathways analysis, the BRCA1- and ATM-related gene sets show genes upregulated upon knockdown of either of the two genes (Figure S4.2). These pathways were positively enriched within the GSEA analysis. This post-treatment enrichment is of particular interest given the involvement of ATM with STING signaling. This is consistent with findings in our *in vitro* studies in AML cell lines and primary samples detailed in previous studies¹²¹ and in Chapter 2 of this thesis. Other significant changes observed in the oncogenic pathway analysis included JAK- and IL-2-related gene sets. This was of particular interest to us given the immune signaling that we reported in our *in vitro* studies in Chapter 2.

4.2.4. Pharmacodynamic effects

We previously reported that treatment of AML cell lines and primary patient samples with the decitabine/talazoparib drug combination *in vitro* leads to HRD that may underlie sensitization to PARPis. HR activity was measured in PBMNCs from a total of 12 patients in Cohorts 1, 3, 4 5, 6 and 7 on Days 1, 5 and 8 (Figure 4.4), using the extrachromosomal assay that we described in Chapter 2. Pre-treatment (Day 1) HR activity was variable. A clear progressive decrease in HR activity from Day 1 to Day 5 to Day 8 was seen in cells of Patient 034 and Patient 042, both of whom achieved CRi, and also in cells of Patient 013 in Cohort 3, who did not respond to treatment, but not in cells of 7 other patients, one of whom achieved HI and 6 of whom did not respond to treatment.

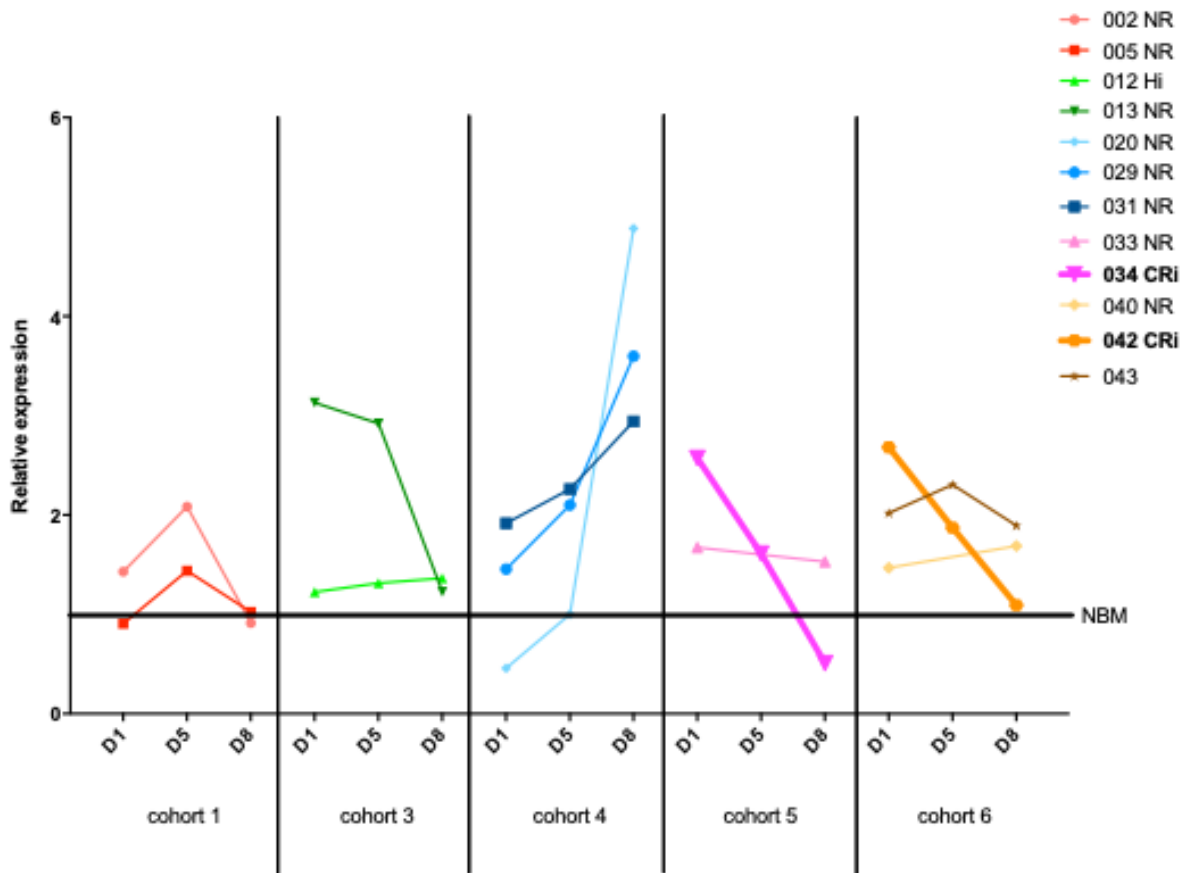


Figure 4.4: Combination treatment generates HRD in patients that show clinical response.

Relative HR activity measured by *in vitro* plasmid based homologous recombination activity assay in patient samples before treatment begin, and on day 5 and day 8 and normalized to HR activity in normal BMMCs.

The HR repair factor RAD51 forms foci in response to DNA damage and RAD51 foci are an established surrogate marker for measuring HR activity in mammalian cells²³⁷. We measured changes in RAD51 and γ H2AX foci in PBMCs of 14 patients using immunostaining for RAD51, as we previously reported¹²¹. While baseline levels of RAD51 varied between

patient samples measured on Day 1, a decrease in RAD51 foci was seen in most patient samples post treatment (Day 5 and Day 8) (Figure 4.5A).

DSBs are an important measure of cytotoxic DNA damage in the cell and levels of γ H2AX foci, measured by immunostaining, are an established marker for DSBs^{238,239}. We quantitated γ H2AX foci in PBMCs from AML patients pretreatment at on Days 5 and Day 8 post treatment, as previously reported¹²¹. While levels of γ H2AX foci varied in Day1 pretreatment samples, an increase in γ H2AX foci with treatment was seen in most, but not all, patients studied (Figure 4.5B). Patients 034 and 043, who achieved CRi, exhibited increases in the number of γ H2AX foci post treatment.

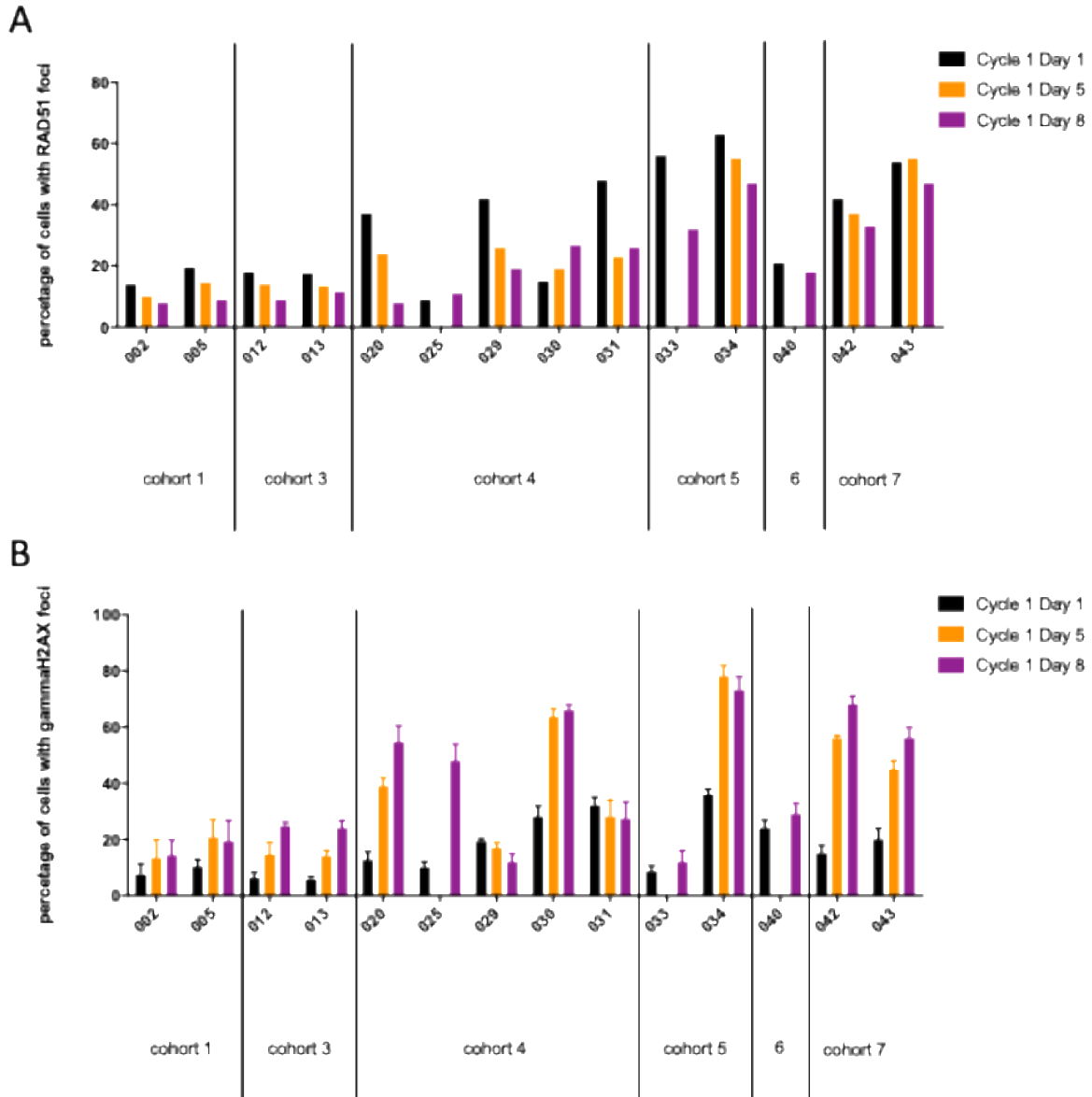


Figure 4.5: Combination treatment downregulates Rad51 foci formation. PBMCs were stained for Rad51 to look at HR initiation and γ H2AX to study the extent of DNA damage before treatment begin, and on day 5 and day 8. (A) Quantification of IF staining for Rad51 foci. (B) Quantification of IF staining for γ H2AX foci. Data represent the mean \pm SEM * $p < 0.05$ (n=3).

As our preclinical data showing increased immune signaling with DAC-TAL treatment (Chapter 2), we examined immune gene expression levels in patient samples after 8 days of treatment, normalized to the pre-treatment sample collected on Day 1 (Figure 4.6). Samples from earlier cohorts (1 and 3) had little to no change in immune gene expression. While immune gene expression changes were variable within and across patient samples in later cohorts, modest increases in immune gene expression were observed in samples from patients with no response to therapy. In contrast, IFI44 was exclusively increased more than 4-fold in the cells of Patient #034 who achieved a CRi.

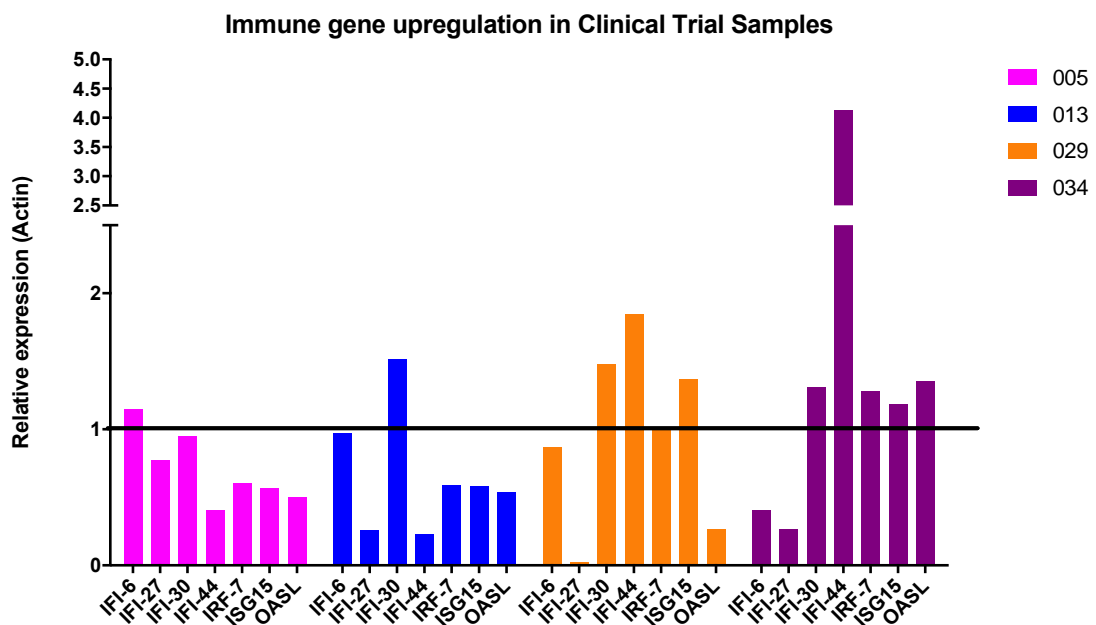


Figure 4.6 Immune gene upregulation in clinical trial patient samples. Relative RNA expression for a subset of IFN $\alpha\beta$ pathway genes after 8 days of treatment in 4 patients from 4 different Cohorts (Patient 005 from Cohort 1, Patient 013 from Cohort 3, Patient 029 from Cohort 4, and Patient 034 from Cohort 5).

Given the important role STING plays in the response to therapy described in Chapter 2, we decided to evaluate STING gene expression changes in clinical trial patient samples collected pre-treatment and at the end of cycle 1 (Figure 4. 7). Ten of the 25 patients had samples collected at these time points and these were processed for RNAseq analysis. Interestingly, STING expression decreased significantly post-treatment in patients 034 and 042, who achieved CRi, and Patient 012, who demonstrated clinical HI. Patients who did not respond to treatment showed no changes in STING expression.

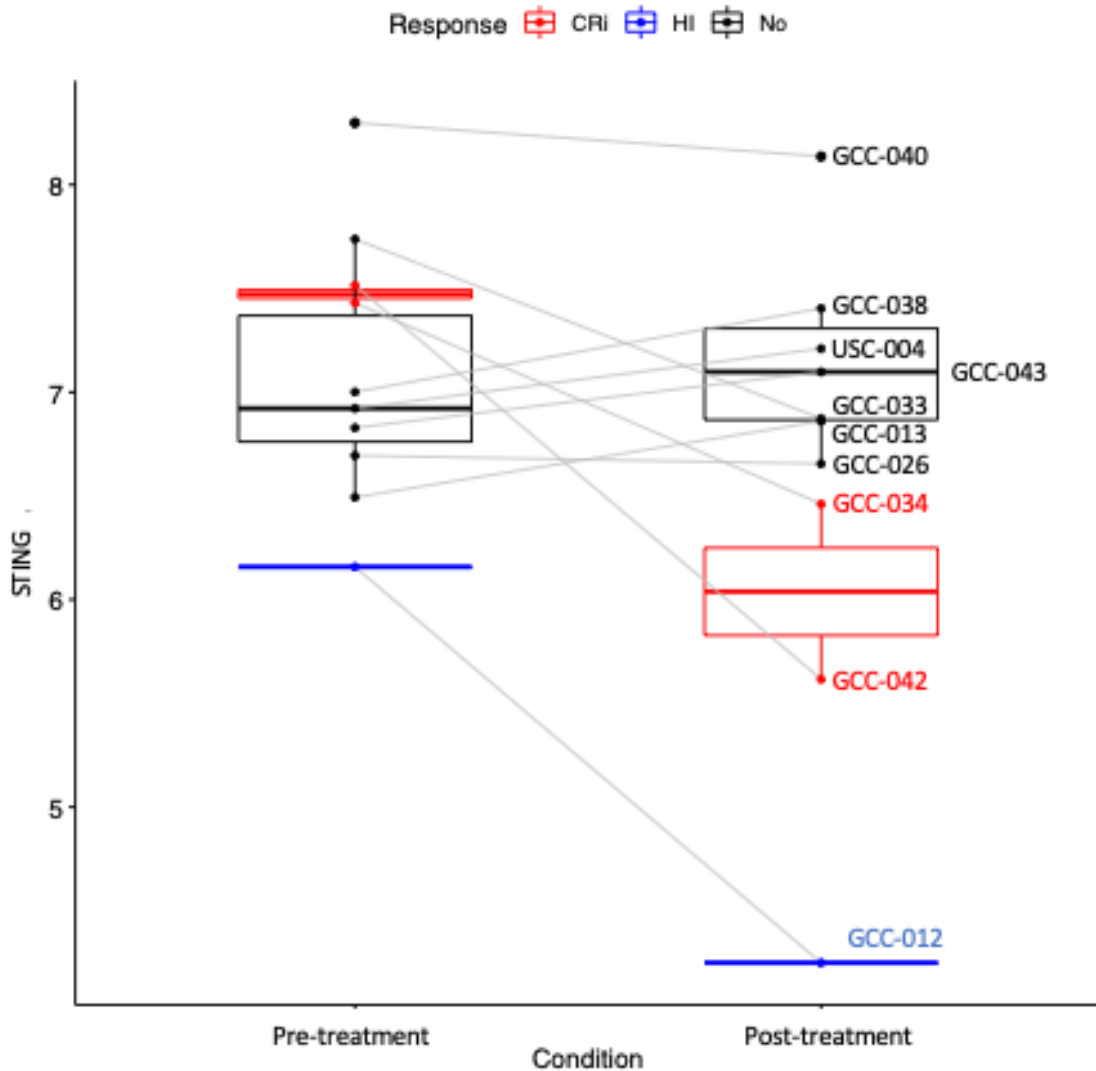


Figure 4.7: STING expression pre- vs post-treatment grouped by response. STING gene expression colored according response: complete response (red), Hi response (blue), or no response (black). Lines connect pre- and post- treatment sample pairs for each patient.

4.3. Discussion

This study is the first to investigate the combination of a DNMTi with a PARPi in AML in the clinical setting, based on preclinical studies¹²¹. Overall, both decitabine and talazoparib were well tolerated and doses were successfully escalated from Cohort 1 to Cohort 7. Given that MTD

had not been reached at dose level 6, and additional cohort was added and the recommended dose of the regimen was decitabine, 20 mg/m² daily for 10 days and talazoparib, 1 mg daily for 28 days.

Clinical activity of the decitabine/talazoparib combination was seen in 5 of the 25 patients treated on the clinical trial. Importantly, 22 of 25 patients had been previously treated with decitabine or azacitidine, including 13 who had previously received decitabine treatment. Two out of the 3 patients who were DNMTi-naïve showed clinical responses; the Cohort 3 patient achieved HI while the Cohort 7 patient achieved CRi. There is a high likelihood that the patients who had received prior DNMTi treatment were DNMTi-resistant. This suggests that this regimen warrants further clinical investigation in DNMTi-naïve patients. Additionally, given our preclinical data showing that the decitabine/talazoparib combination may be particularly effective in AML patients with TP53 mutations (Chapter 2), and that Patient 015, who had prolonged survival on treatment, had a TP53 mutation, clinical investigation of patients with TP53 mutations would potentially personalize this therapy.

Baseline HR activity as well as RAD51 and γ H2AX foci were variable. While HR activity only decreased in 3 out of 14 patient samples examined, two of them were from patients who achieved CRi, and RAD51 foci decreased in nearly all patients on Days 5 and 8 of treatment. Increases in DNA damage, measured by γ H2AX foci formation, were observed in 10 of the 14 patient samples tested and increases in foci formation tracked with dose escalation. Further studies are needed to define the potential role of these parameters as predictors of response.

RNA-seq of the patient samples revealed changes in key DNA repair and immune pathway genes post-treatment and correlate with our preclinical data. Whole exome sequencing analysis was also performed on these trial samples and future directions include pairing these data with the RNAseq data to better capture the full molecular picture for what may define objective response

and survival outcomes in these patients. Furthermore, decreases in STING expression levels were observed in RNA-seq samples of patients who had clinical responses. This was surprising, as we had seen increases in STING activity post combination treatment in in vitro and in vivo AML models. One explanation may be the initial effects of the decitabine/talazoparib combination treatment on the percentage of blasts in the peripheral blood and bone marrow, where initial responses to the treatment can drastically diminish the blast counts^{12,240}. Thus, measurement of STING levels on Day 5 or 8 of treatment may in fact measure STING levels in normal cells rather than AML cells. Indeed, TCGA analysis using the Gene Expression Profiling Interactive Analysis (GEPIA) web interface showed that STING expression is notably elevated in AML cells, compared to normal blood cells, as well as other cancers and normal tissues (Figure 4.8). This is additional evidence that our STING expression data may reflect levels in normal cells, rather than AML cells. Thus, given this information, and given reports that percentages of peripheral blood blasts are generally drastically decreased in AML patients responding to DNMTi therapy^{12,240}, we hypothesize that the decrease in STING expression observed in the RNA-seq samples correlates with treatment response because the amount of blast cells would be significantly lower in responders, essentially measuring STING expression in normal cells. Deconvolution studies of our pre- and post-treatment samples are underway to investigate this.

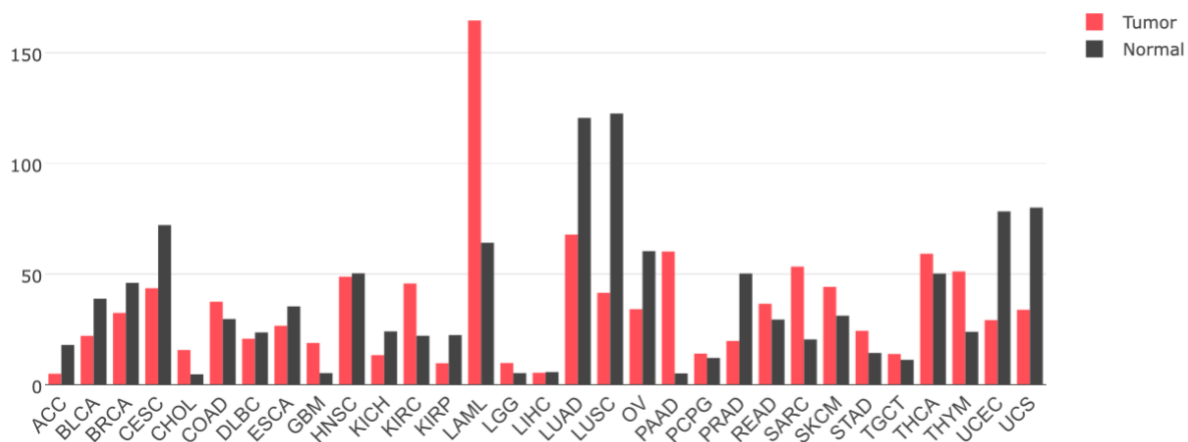


Figure 4.8: STING expression is notably elevated in AML. STING gene expression from TCGA samples of multiple cancers (red) and their normal tissue (black) counterparts. Figure produced using the GEPIA web interface. <http://gepia.cancer-pku.cn/index.html>

STING agonists are currently being tested alone or in combination with a range of other therapeutic agents in clinical trials to elicit immunostimulatory effects in various solid tumors²⁴¹. Notably, there are as yet no clinical trials of STING agonists in AML. Therefore, activating STING via agonists or decitabine/talazoparib treatment could be an attractive mechanism to activate IFN signaling and generate anti-leukemia immune responses¹⁹⁵. Alternatively, decitabine in combination with STING agonists should activate ERVs to further drive these anti-leukemia responses.

Interferon induced protein 44 (IFI44) gene expression was found to be significantly increased in post-treatment cells of one patient who achieved CRi. Interferon inducible proteins (IFIs) have been reported to play a significant role in the immune response to autoimmune disease²⁴², but its roles in cancers are unclear. In head and neck cancers, IFI44 is positively correlated with the infiltration of CD4⁺ cells and macrophages as well as neutrophils²⁴³. In AML,

compared to normal blood, expression of IFI44 in pan-cancer TCGA data is significantly elevated (Figure 4.9). Taken together, these data suggest that IFI44 is abnormally expressed in samples from AML patient who achieved CRi post decitabine/talazoparib treatment. These data may indicate the potential impact of IFI44 on immune infiltration in the leukemia microenvironment. Expansion of the IFI panel in patient samples should identify additional IFIs that correlate with response. Studies in AML immune-competent mice should determine the functional significance of these findings.

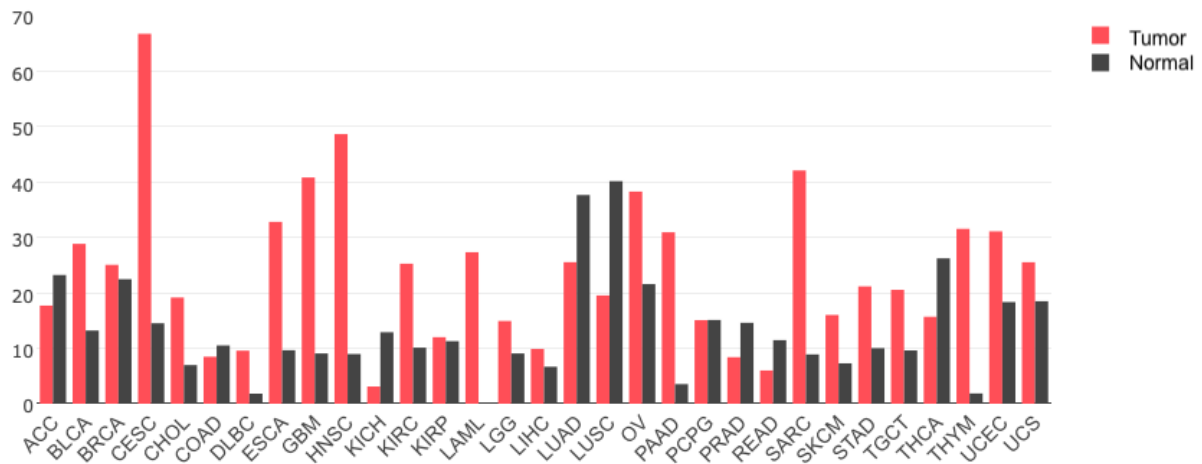


Figure 4.9: IFI44 expression is notably elevated in AML. IFI44 gene expression from TCGA samples of multiple cancers (red) and their normal tissue (black) counterparts. Figure produced using the GEPIA web interface. <http://gepia.cancer-pku.cn/index.html>

4.4. Methods

4.4.1. Patient population

Eligible patients were age ≥ 18 years with AML diagnosed based on 2008 WHO criteria²⁴⁴, occurring *de novo* or following a prior hematologic disorder, including MDS, CMML or Philadelphia chromosome-negative myeloproliferative neoplasm, and/or therapy-

related, relapsed after, or refractory to, first-line therapy, with or without subsequent additional therapy, and currently considered unfit for, or unlikely to respond to, cytotoxic chemotherapy. Prior autologous stem cell transplantation (SCT) was allowed if patients were ≥ 4 weeks from stem cell infusion, and prior allogeneic SCT was allowed if patients were ≥ 60 days from stem cell infusion, had no evidence of graft versus host disease (GVHD) $>$ Grade 1, and were ≥ 2 weeks off all immunosuppressive therapy. Previous cytotoxic chemotherapy had to have been completed at least 3 weeks and radiotherapy at least 2 weeks prior to Day 1 of study treatment and all adverse events recovered to $<$ Grade 1. Prior DNMTi therapy for AML or for a prior hematologic disorder was allowed, with last dose at least 3 weeks prior to Day 1 of study treatment. Other requirements included ECOG performance status ≤ 2 , AST(SGOT)/ALT(SGPT) $\leq 2.5 \times$ institutional upper limit of normal (ULN), total bilirubin below ULN unless thought due to hemolysis or to Gilbert's syndrome, and serum creatinine below ULN or creatinine clearance ≥ 60 mL/min. Exclusion criteria included acute promyelocytic leukemia, known central nervous system leukemia, uncontrolled intercurrent illness or infection, known HIV infection and prior talazoparib treatment. Hyperleukocytosis with $>50,000$ blasts/ μ L was an exclusion; hydroxyurea was permitted for blast count control, but had to be stopped at least 24 hours prior to starting study treatment. Patients were withdrawn from the study if $> 50,000$ blasts/ μ L occurred or recurred >14 days after starting study treatment.

4.4.2. Pre-treatment studies

Bone marrow (BM) aspirate and biopsy were performed within 14 days prior to start of protocol therapy, with cytogenetic analysis performed in 24 of 25 patients and analysis of myeloid mutations in 22 patients as standard-of-care studies.

4.4.3. Treatment

Decitabine was given in the established regimen of IV daily dosing for 5 or 10 days every 28 days. Talazoparib was initiated orally daily on a continuous basis, beginning on Day 1 of Cycle 1. On days when both decitabine and talazoparib were given, decitabine was given after talazoparib. Talazoparib was administered regardless of food intake.

Treatment continued on an ongoing basis until disease progression, intercurrent illness preventing further administration of treatment, unacceptable adverse event(s) or patient or physician decision to stop treatment.

4.4.4. Dose escalation

The dose escalation schema for both drugs is shown in Table 1; the dose combinations tested are in bold. Doses were escalated based on tolerability using a 3+3 design. Dose escalation decision rules are shown in Table 2. Once the maximum tolerated dose (MTD) for decitabine combined with 0.25 mg talazoparib was established, the dose of talazoparib was escalated with the dose of decitabine kept fixed at the provisional MTD dose. There is no further stepping up or down of the drugs in the combination. Finally, talazoparib was tested with 10-day decitabine at MTD doses.

4.4.5. Toxicity evaluation

Dose-limiting toxicities were evaluated in Cycle 1. Toxicities were evaluated according to Version 4.0 of the NCI Common Terminology Criteria for Adverse Events (CTCAE). Dose-limiting toxicity consisted of any of the following adverse events with an attribution of possible, probable, or definitely related to the study therapy: 1) Any grade 4 treatment-related non-hematologic toxicity, except for infection, fever, neutropenic fever or bleeding, which are expected in this patient population; 2) Any grade 3 treatment-related non-hematologic toxicity

that does not resolve to \leq grade 2 within 48 hours, except for infection, fever, neutropenic fever or bleeding, which are expected in this patient population; or 3) Myelosuppression was considered a dose-limiting toxicity if ANC $<0.5 \times 10^9/L$ and platelets $<20 \times 10^9/L$ (untransfused) persist on day 43, with bone marrow cellularity of $\leq 5\%$ and no evidence of leukemia in the bone marrow.

The study was monitored by the UGCCC Data and Safety Monitoring and Quality Assurance Committee.

4.4.6. Response assessment

Response definitions were according to the revised *International Working Group (IWG) response criteria for AML*²⁴⁵.

BM aspirate and biopsy were performed on day 25-29 of cycle 1, and on day 25-29 of each subsequent treatment cycle unless circulating blasts persisted in the peripheral blood (PB), until documentation of CR or CRi. Bone marrow aspirate and biopsy were also performed as needed to evaluate lack of count recovery (neutrophils $<1000/\mu L$ and/or platelets $<50,000/\mu$) by day 43 in the absence of blood blasts.

Duration of response was measured from the time criteria for CR or CRi were met until the first date that recurrent or progressive disease was objectively documented. Progression-free survival (PFS) was defined as the time between study entry and the first date that recurrent or progressive disease was objectively documented, or date of death from any cause. Overall survival was measured from the time of enrollment to the time of death.

4.4.7. Management of hematologic toxicity

Timing of cycle initiation and dose levels of decitabine and talazoparib starting with Cycle 2 were guided by neutrophil/platelet counts after the prior cycle and PB and/or BM blast

percentage. Table 2 shows dose modifications and delays based on Day 28 or later PB counts starting with Cycle 2.

The treating physician could also delay study drug treatment (decitabine and talazoparib) on Day 29 of any cycle regardless of neutrophil/platelet counts and/or leukemic blasts if deemed in the patient's best interest. Treatment was then resumed when it was deemed in the patient's best interest to do so. Reasons for delaying and for restarting were documented in the medical record.

4.4.8. Sample processing

PB samples were obtained for pharmacodynamic studies during Cycle 1 on Day 1 before treatment, then Day 5, one hour after completion of decitabine administration, Day 8, any time, and Day 29, before next treatment. For patients receiving 10-day decitabine, sampling was on Day 1 before treatment, and Days 5, 8 and 10, one hour after completion of decitabine administration. BM samples were collected at screening and on Day 29 of Cycle 1, before treatment.

Mononuclear cells (MNC) were isolated from AML samples by density centrifugation over Ficoll Hypaque (Sigma). Differential cell counts were performed after Wright-Giemsa staining and recorded. MNCs were centrifuged at 1500 rpm for 5 minutes and cell pellets were flash-frozen in liquid nitrogen for RT-PCR, western blotting and PARP trapping analyses. MNCs were also viably frozen in IMDM (Invitrogen) with 10% FBS and 5% DMSO for immunofluorescence assays.

4.4.9. RNA extraction and quantitative PCR

Total RNA was isolated using the NucleoSpin RNA Plus kit (Macherey-Nagel) according to manufacturer protocol. cDNA was synthesized by converting 1-2ug of RNA using

High Capacity cDNA Reverse Transcription kit (Applied Biosystems). Quantitative real-time PCR was performed using Power Sybr Green PCR Master Mix (Applied Biosystems) in a CFX384 Touch Real-Time PCR system (BioRad). The sequences of primers used are listed in Supplementary Materials and Methods.

4.4.10. Immunofluorescence Staining

Viably frozen AML MNCs were thawed and cytospun onto glass slides for 5 min at 200 rpm in PBS on a Shandon Cytospin 4. Cells were fixed for 10 min in 4% paraformaldehyde, washed 3 times in DPBS, permeabilized for 10 min in permeabilization solution (50 mM NaCl, 3 mM MgCl₂, 10 mM HEPES, 200 mM Sucrose and 0.5% Triton X-100 in PBS 1X), washed 3 times in DPBS + 1% BSA, then blocked overnight in 10% FBS. After incubation with mouse monoclonal anti- γ H2A.x (1:100, Upstate) or rabbit polyclonal anti-RAD51 (1:100, Santa Cruz Biotechnologies, Dallas, TX) or isotype controls for one hour at 37°C in DPBS-BSA, cells were washed and then incubated with Dylight 594-anti-mouse or Dylight 488-anti-rabbit (1:200, KPL, Gaithersburg, MD) antibodies for one hour at 37°C prior to counterstaining with 4',6 diamidino-2-phenylindole, dihydrochloride (DAPI, 0.3 μ g/ml, Promega, Madison, WI) in mounting medium (Vectashield, Vector Laboratories, Burlingame, CA).

Images were examined and acquired using a Nikon Eclipse 80i fluorescence microscope (100 \times /1.4 oil, Melville, NY). For quantitation of foci, images from at least 50 cells/slide were captured using a CCD camera and the imaging software NIS Elements (BR 3.00, Nikon). γ H2AX and RAD51 foci contained within these imaged cells were counted and the data were expressed as numbers of foci per cell. Immunostaining was compared on MNCs from AML PB samples obtained on Day 1 pre-treatment and on Day 5 following treatment. Results were reported as mean number of foci/cell in each sample. The Student's t-test was

used to determine differences between pre-treatment and post-treatment samples in individual participants. $p \leq 0.05$ was considered significant.

4.4.11. HR repair analysis

Nuclear extracts were prepared using the Cell Lytic NuCLEAR Extraction Kit (Sigma-Aldrich). Nuclear extracts were dialysed for two hours using the Plus One Mini Dialysis Kit 1kDa (GE Healthcare) in dialysis solution (20 mM HEPES pH9, 100 mM KCl, 0.2 mM EDTA, 20% glycerol, 0.5 mM DTT, 0.1 mM PMSF). Protein content was quantified by Nanodrop and diluted to 0.5 $\mu\text{g}/\mu\text{l}$ in DNase/RNase-free water. Diluted nuclear extracts were incubated with 5 μl each of dl-1 and dl-2 plasmid (Homologous Recombination Assay Kit, Norgen Biotek) in reaction buffer for 2 hours at 30 °C. Plasmid DNA was recovered with the QIAamp DNA mini kit (Qiagen), and the relative quantity of recombined product was determined with the quantitative real-time PCR CFX384 Real Time System (BioRad) using PCR primers spanning the repair site, normalized against amplification of a distant site (primers supplied by Norgen Biotek). PCR product band density of treatment samples (C1D5 and C1D8) was estimated relative to that of C1D1 samples (pretreatment) using Bio-Rad's Quantity One Software. Log transformed fold changes were compared between groups. Samples were normalized to C1D1 (set at 1) and expressed as fold change in HR activity.

4.4.12. Construction and sequencing of directional total RNA-seq libraries

Libraries were prepared by the Van Andel Genomics Core from 500 ng of total RNA using the KAPA RNA HyperPrep Kit with RiboseErase (v1.16) (Kapa Biosystems, Wilmington, MA USA) following manufacturer instructions. RNA was sheared to 300-400 bp. Prior to PCR amplification, cDNA fragments were ligated to IDT for Illumina TruSeq UD Indexed adapters (Illumina Inc, San Diego CA, USA). Quality and quantity of the finished

libraries were assessed using a combination of Agilent DNA High Sensitivity chip (Agilent Technologies, Inc.), QuantiFluor® dsDNA System (Promega Corp., Madison, WI, USA), and Kapa Illumina Library Quantification qPCR assays (Kapa Biosystems). Individually indexed libraries were pooled and 100 bp paired end sequencing was performed on an Illumina NovaSeq6000 sequencer using an S4, 200 bp sequencing kit (Illumina Inc., San Diego, CA, USA) to an average depth of 40-50M reads per sample. Base calling was done by Illumina RTA3 and output of NCS was demultiplexed and converted to FastQ format with Illumina Bcl2fastq v1.9.0.

4.4.13. Statistical analysis

Unless otherwise defined, all data are presented as mean \pm SEM. Statistical analysis for biological assays and mouse studies was performed using Graphpad Prism software to calculate 2-tailed unpaired t test or 1-way or 2-way ANOVA as appropriate.

4.4.14. Data availability

Raw and processed data files related to RNA-seq will be made available through the GEO database repository during publication of the manuscript.

CHAPTER 5: Perspectives and Future Directions

While DNMTis are commonly used for patients who are unfit for the intensive chemotherapy and as a second-line treatment for relapsed/refractory AML, responses are not durable, and novel treatments are needed to improve patient outcomes. We have previously shown that combining DNMTi and PARPi in vitro and in vivo triggers cytotoxic tumor cell DNA damage and cell death¹²¹. We subsequently reported that DNMTis induce a BRCAness phenotype in BRCA-proficient NSCLC and sensitize to PARPi in combination with IR therapy¹²⁸. We next reported that the DNMTi+PARPi combination induces a broad IFN/inflammasome activation that is mechanistically linked to HRD in TNBC and OC cells¹²⁹. We show here that in AML DNMTi+PARPi combination treatment induces an IFN/inflammasome response leading to HRD that is unique to, and dependent on, TP53 status (Chapter 2). Moreover, we validated this immune signaling response with DNMTi+PARPi treatment in an immune competent model of AML (Chapter 3). Finally, based on our preclinical findings in AML, we developed a Phase 1 clinical trial to test tolerability of DNMTi plus PARPi therapy for relapsed/refractory AML (Chapter 4). Thus, findings from our lab now provide compelling evidence for why the combination of a DNMTi and PARPi might be an efficacious therapeutic approach to activating anti-tumor immune signaling in AML.

Previous reports have shown that low doses of DNMTis can transcriptionally activate epigenetically silenced repeat elements, including ERVs, resulting in a cytoplasmic dsRNA response known as viral mimicry, leading to IFN signaling^{81,156,157}. Here we found that mutation or abrogation of tumor suppressor TP53 plays an important role in how DNMTis may activate

transcription of these silenced repeat elements. WT TP53 binds repeat elements and maintains silencing of repeat elements in the genome^{163,173-175}. In contrast, abrogation of TP53 can relieve this genome guardianship, allowing for DNMTi activation of these repeat elements¹⁶³. We show that TP53 mutant AML cells are significantly more sensitive to transcriptional activation of ERVs by DNMTi treatment, leading to strong activation of IFN signaling. This concept may be predicated on our finding that TP53 mutant AMLs have lower ERV basal levels. Greve et. al recently showed that DNMTi treatment results in de-repression of ERV3-1 and global reactivation of transposable elements²⁴⁶. Further studies are necessary to understand how TP53 mutation status affects the DNMTi treatment-induced hypomethylation and reactivation of ERVs.

While PARPis are known to induce synthetic lethality in BRCA-mutant TNBC and OC cells^{135,176}, they can also increase cytosolic dsDNA that activates IFN signaling^{129,165,177}. We show here that in AML with TP53 mutation DNMTi treatment alone can potently drive IFN/inflammasome signaling that is mechanistically linked to the induction of a BRCAness phenotype. In contrast, PARPi treatment alone contributes minimally to immune signaling or HRD in these cells, possibly due to the fact that increased PARP1 levels are seen in many therapy-resistant cancers, connoting increased DNA repair and genomic instability^{116,178-180}. Accordingly, we found that PARP1 levels are significantly elevated in TP53 mutant AMLs, which are known to have increases in genomic instability, suggesting TP53 mutations as an important biomarker to be considered in PARPi therapy response, and PARP expression levels in activation of immune responses with cancer therapy. Other mutations such as those in TET2 and DNMT3A have recently been shown to predict sensitivity to PARPis²⁴⁷ and could be useful biomarkers for patient treatment stratification. Furthermore, due to their effects on immune stimulation, particularly as it relates to the activation of the STING pathway²⁴⁸, PARPis could be advantageous in reducing genomic

instability, which is particularly associated with TP53 mutations in AML. Further studies are necessary to elucidate how PARPi affect genomic instability in TP53 mutant AML.

STING activation is critical for activating anti-cancer immune responses in solid tumors, but less is known about its role in hematologic malignancies, including AML^{177,183,184}. Notably, STING expression is low in many tumors, compared to normal tissues, and research to activate STING-dependent immune signaling is actively being pursued¹⁸¹⁻¹⁸⁴. Several studies have linked STING activation to the actions of PARPi and studies from our lab expand this understanding to a new mechanistic context for the regulation of “BRCAness” in BRCA-proficient settings^{129,249-251}. Accordingly, we recently also reported that DNMTi treatment of TNBC and OC can transcriptionally activate STING¹²⁹. We now show that compared with WT TP53, AML cells with TP53 mutations have higher STING activity at baseline and following DNMTi treatment. Moreover, WT AML cells require DNMTi to be combined PARPi drugs to increase STING activity, but this activity does not reach levels seen in TP53 mutants. Therefore, while induction of IFN/inflammasome signaling and HRD in both TP53 mutant and WT cells is STING-dependent, TP53 mutant AMLs appear particularly poised for STING activation using novel STING activation strategies. In fact, STING agonists are now being tested in clinical trials for various solid tumors, alone or in combination with a range of other therapeutic regimens, to elicit immunostimulatory effects²⁴¹. However, given that there currently are no clinical trials of STING agonists in AML, activating STING via agonists or DNMTi+PARPi treatment could be an attractive approach to activating interferon signaling and generating anti-leukemia immune responses.

While immunotherapy has revolutionized cancer treatment, progress in the application of immunotherapy in AML has been slower compared with solid tumors^{252,253}. Only gemtuzumab

ozogamicin, an anti-CD33 antibody-drug conjugate, has currently been approved as targeted therapy for CD33-positive AML patients²⁵⁴. Trials of other immune therapies, including those based on PD-1 or CTLA-4 inhibition, have yielded modest clinical efficacy²⁵⁵, underscoring the need to enhance these therapies with other agents. DNMTi treatment has also been shown to increase expression of the immune checkpoint PDL1^{133,185,186}. Therefore, x TP53 mutations may define a group of AML patients in whom DNMTis can be used to activate immune signaling and to prime for combination with immune checkpoint therapy currently in the clinic. In fact, recent reports suggest encouraging early results for combining PD-1/PD-L1 checkpoint inhibitors or anti-CTLA4 with DNMTis in clinical trials^{134,187,256}. Final results from these trials should increase our understanding of immune responses in TP53 mutant AML and other genetically distinct AML groups treated with DNMTis. Given the immune enhancing effects of our combination treatment, future considerations should include evaluating how DNMTi+PARPi combination treatment may enhance response to checkpoint inhibition.

TP53 is a key tumor suppressor whose main function is to preserve genetic integrity by preventing proliferation of damaged cells, a function that has led to its famous title of “guardian of the genome”^{257,258}. It is mutated in more than half of all human cancers, making it the most frequently mutated gene in cancer and an interesting therapeutic target^{50,258,259}. TP53-targeting therapeutic strategies revolve around attempts to restore its WT conformation and transcriptional activity, targeting it for degradation, and inducing synthetic lethality^{258,260,261}. Small molecule compounds, synthetic small peptides, CRISPR/Cas9-mediated genome editing, small interference RNAs (RNAi) as well as immunotherapies have been explored in attempts to achieve this therapeutic goal, but all of these approaches have various intrinsic problems that warrant further investigation and optimization before clinical application can be considered²⁵⁸. Our results,

described in this body of work, show that TP53 mutant AMLs appear particularly poised for activation of IFN/inflammasome signaling, and that this activation can be achieved using DNMTi+PARPi combination treatment. This forms a basis for further combinatorial approaches in the treatment of AML, and may also be applicable to other cancers with TP53 mutations, potentially personalizing this therapy.

Appendix

Appendix Table S2.1: Cytogenetic and molecular features AML primary samples treated with DNMTi+PARPi in vitro

Sample #	Age	Sex	WBC	% blood blasts	% marrow blasts	Karyotype	Category	Mutations	TP53 Status
156	41	F	376.8	92	N/A	46,XX	Normal/ Interm	FLT3-ITD FLT3 TKD NPM1 IDH1	WT
161	59	M	96.3	5	30	47,XY,+8	Interm	SRSF2 SETBP1 TET2 x 2 EZH2	WT
171	64	F	23.7	47	N/A	44- 45,XX,add(1)(p36.1), -5, add(12)(p13), der(14)t(1;14)(p22;p1 3),-16,-17,-22, +1- 3mar	Complex	TP53 84% TET2 IDH1	Mutant
184	51	M	80	86	85	46,XY,t(2;14)(q23;q3 2)	Interm	FLT3-ITD RNX1 x 2 SF3B1	WT
190	67	M	190.6	63	N/A	46,XY,add(11)(p11.2 ,add(17)(p11.2)	Interm	SRSF2 RUNX1 TET2	WT
457	69	F	1.2	0	44	46,XX,- 2[15],der(5)t(?;?;5)(q23;?;q15)[15], del(7)(q21)[14],add(9)p23[12], del(17)(p11.2)[15],- 20[4],+1-2mar	Complex	TP53 42.8%	Mutant

Appendix Table S2.2: Primers used for qRT-PCR

Name	Source	Identifier	Sequence
actin	Qiagen	QT00095431	
GAPDH	IDT		(f) 5'-GTCTCCTCTGACTTCAACAGCG-3'
GAPDH	IDT		(r) 5'-ACCACCCTGTTGCTGTAGCCAA-3'
ERV9	IDT		(f) 5'-TCTTGGAGTCCTCACTCAAACCTC-3'
ERV9	IDT		(r) 5'-ACTGCTGCAACTACCCTTAAACA-3'
ERV-K1	IDT		(f) 5'-ATCCTATGGCACCACCTAGTA-3'
ERV-K1	IDT		(r) 5'-GCCTCAGTATCTCCTTCCTTTC-3'
ERVV2	IDT		(f) 5'-CTTCTTTCTGAGCTCCTGTCTC-3'
ERVV2	IDT		(r) 5'-GTCCTCTGGTTCTTGGTCTTC-3'
ERVMER34-1	IDT		(f) 5'-CCATGGAAGCTCAAGGTCTATC-3'
ERVMER34-1	IDT		(r) 5'-GAAGGGTCCACTGCCATTT-3'
ERVW1	IDT		(f) 5'-CAAGTCCCTTCCCTCTAATTCC-3'
ERVW1	IDT		(r) 5'-TCCACTCCAGCCACTTTAAC-3'
ERV-FRD 1	IDT		(f) 5'-AGCCAGCTCTCAAAGGAAATAG-3'
ERV-FRD 1	IDT		(r) 5'-GAAGGACTACGGCTGCTAAAG-3'
ERVW2	IDT		(f) 5'-CCACTGTCTGTTGGACTTACTT-3'
ERVW2	IDT		(r) 5'-TGGGAGATTGCTTCCTTTACTT-3'
ERV-H1	IDT		(f) 5'-GCCCATTTCTCTCTCCATATC-3'
ERV-H1	IDT		(r) 5'-CCTGACATTCCTGCCTTCTTA-3'
ERVFXA34	IDT		(f) 5'-CAGGAAACTAACTTTCAGCCAGA-3'
ERVFXA34	IDT		(r) 5'-TAAAGAGGGCATGGAGTAATTGA-3'
ERV-Fc1	IDT		(f) 5'-TACACCCTTACTCCCGTCTT-3'
ERV-Fc1	IDT		(r) 5'-GCCTAACATTCCGACCTCATAC-3'
ERV-Fc2	IDT		(f) 5'-CTGGAAGCTACACACTCCATAC-3'
ERV-Fc2	IDT		(r) 5'-TGCCAAGAGGTGGGTTATTC-3'
ERV-Fb1	IDT		(f) 5'-ATATCCCTCACCACGATCCTAATA-3'
ERV-Fb1	IDT		(r) 5'-CCCTCTGTAGTGCAAAGACTGATA-3'
ERV-K8	IDT		(f) 5'-CCCATCAATCCACCAAGTCTTA-3'
ERV-K8	IDT		(r) 5'-CCTATTTCTTCGGACCTGTTCTT-3'
ERV-K10	IDT		(f) 5'-GTCCCAAGTGTTTCAGGGAATA-3'
ERV-K10	IDT		(r) 5'-GAAGCAGAGAGACTGCTTGTATAG-3'
ATM	Qiagen	QT00061593	
ATR	Qiagen	QT01844150	
BRCA1	Qiagen	QT00039305	
BRCA2	Qiagen	QT00008449	

Appendix Table S2.2 continued

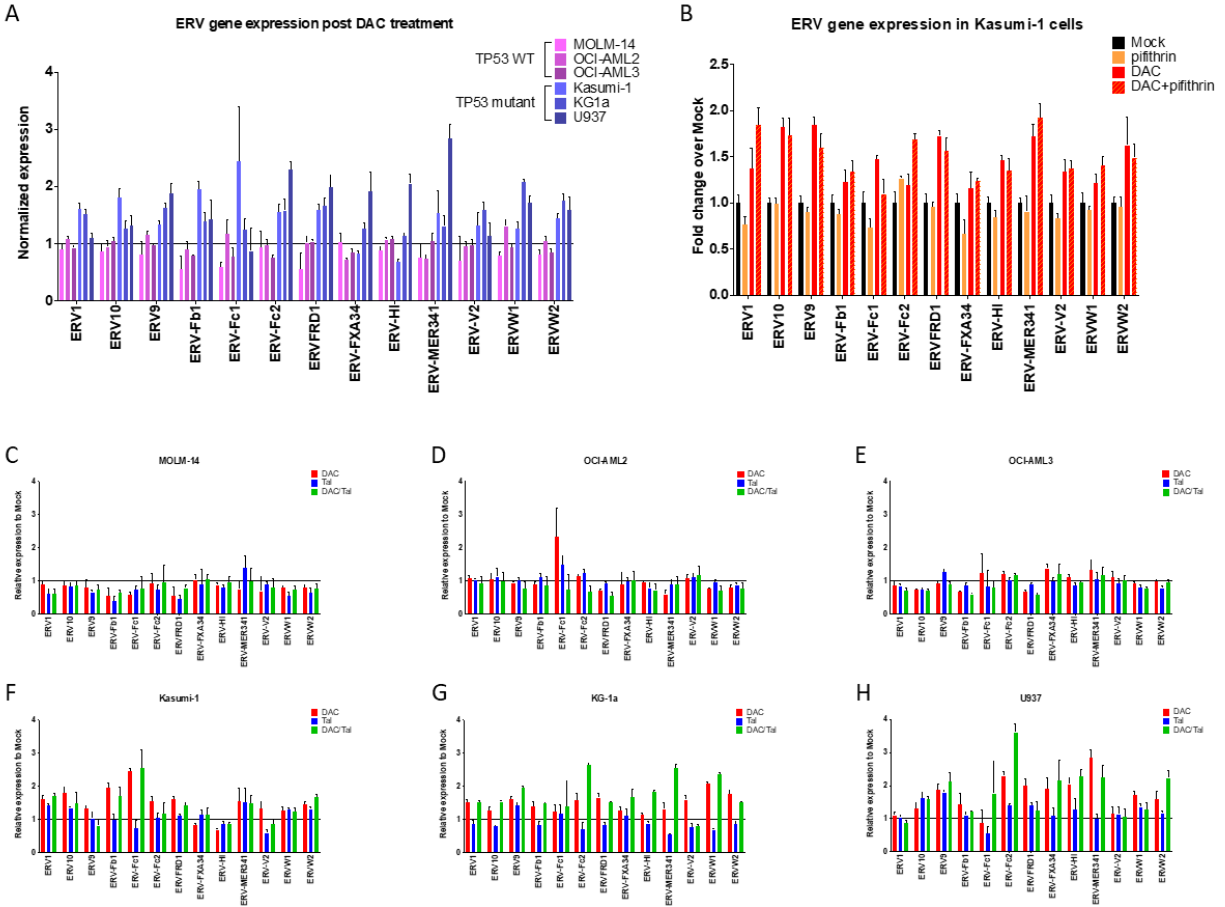
BRIP1/FANCI	Qiagen	QT00086548	
c17orf70	Qiagen	QT01026207	
c19orf19	Qiagen	QT00036918	
CHK1	Qiagen	QT00006734	
CtIP	Qiagen	QT00090713	
FANCA	Qiagen	QT00033404	
FANCB	Qiagen	QT000468	
FANCC	IDT		(f) 5'-TGGAGGCTCTCCTCATCTGT
FANCC	IDT		(r) 5'-GCATTTCGATCCTTCTCAGACA
FANCD2	Qiagen	QT01000433	Hs_FANCD2_VA.1_SG QT01000433
FANCE	IDT		(f) 5'-ATGAGAAGGAGAGACCCGAA-3'
FANCE	IDT		(r) 5'-GAAGTCAAGGAGAGGATCCG-3'
FANCF	Qiagen	QT00241136	Hs_FANCF_1_SG QT00241136
FANCG	Qiagen	QT00064967	Hs_FANCG_1_SG QT00064967
FANCI	Qiagen	QT000468	Hs_FANCI_1_SG QT000468
FANCL	Qiagen	QT00062454	Hs_FANCL_1_SG QT00062454
FANCM	Qiagen	QT00231189	Hs_FANCM_1_SG QT00231189
MRE11	Qiagen	QT00037926	Hs_MRE11A_1_SG QT00037926
PALB2	Qiagen	QT00068523	Hs_PALB2_1_SG QT00068523
RAD50	Qiagen	QT00037170	Hs_RAD50_1_SG QT00037170
RAD51	Qiagen	QT00072688	Hs_RAD51_1_SG QT00072688
RAD52	Qiagen	QT00098329	Hs_RAD52_1_SG QT00098329
RPA	Qiagen	QT00071645	Hs_RPAIN_1_SG QT00071645
53BP1	Qiagen	QT00050785	
ATF3	Qiagen	QT00997164	
B2M	Qiagen	QT00088935	HS_B2M_1_SG QT00088935
CCL5	Qiagen	QT00090083	HS_CCL5_1_SG QT00090083
EGR1	Qiagen	QT00218505	
GADD45A	IDT		(f) 5'-GCCTGTGAGTGAGTGCAGAA-3'
GADD45A	IDT		(r) 5'-ATCTCTGTTCGTCGTCCTCGT-3'
HES1	Qiagen	QT00039648	
ID2	Qiagen	QT00210637	
IFI27	IDT		(f) 5'-ATCAGCAGTGACCAGTGTGG-3'
IFI27	IDT		(r) 5'-TGGCCACAACCTCCTCCAATC-3'
IFI30	IDT		(f) 5'-TGGGAGCTGGACCCTGTAAA-3'
IFI30	IDT		(r) 5'-CCTCCCTTAGATTCCCTATTTGCT-3'
IFI44	IDT		(f) 5'-TGGGAGCTGGACCCTGTAAA-3'
IFI44	IDT		(r) 5'-CCTCCCTTAGATTCCCTATTTGCT-3'
IFI6	IDT		(f) 5'-CAAGGTCTAGTGACGGAGCC-3'

Appendix Table S2.2 continued

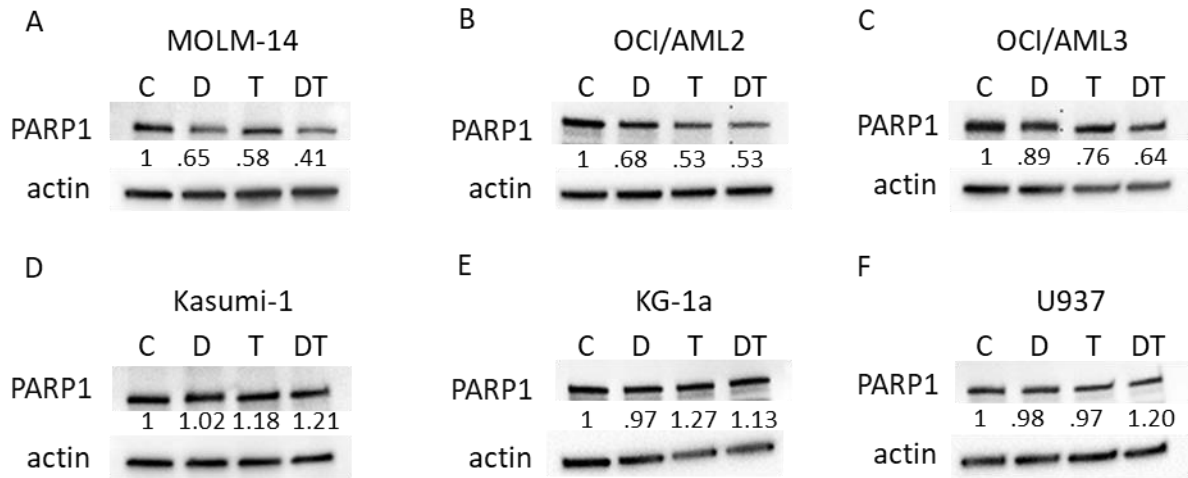
IFI6	IDT		(r) 5'-TTTCTTACCTGCCTCCACCC-3'
IFNb1	IDT		(f) 5'-CTTGGATTCTTACAAAGAAGCAGC-3'
IFNb1	IDT		(r) 5'-TCCTCCTTCTGGAAGTCTGCA-3'
IL23A	Qiagen	QT00204078	
IL7R	Qiagen	QT00053634	
IRF3	IDT		(f) 5'-TCTGCCCTCAACCGCAAAGAAG-3'
IRF3	IDT		(r) 5'-TACTGCCTCCACCATTGGTGTC-3'
IRF7	IDT		(f) 5'-CCACGCTATAACCATCTACCTGG-3'
IRF7	IDT		(r) 5'-GCTGCTATCCAGGGAAGACACA-3'
IRF9	Qiagen	QT00001113	
ISG15	IDT		(f) 5'-CAGCCATGGGCTGGGAC-3'
ISG15	IDT		(r) 5'-CTTCAGCTCTGACACCGACA-3'
OASL	IDT		(f) 5'-TCGTGAAACATCGGCCAACT-3'
OASL	IDT		(r) 5'-ACCTGGCTTTCACATACTGCT-3'
RHOB	Qiagen	QT00227409	
SERPINB8	Qiagen	QT01005956	
TRIB1	Qiagen	QT00066262	
TMEM173	Qiagen	QT00055440	
TNF	Qiagen	QT00029162	

Appendix Table S2.3: TCGA TP53 mutated AML samples identified using Vadakekolathu et al 2020

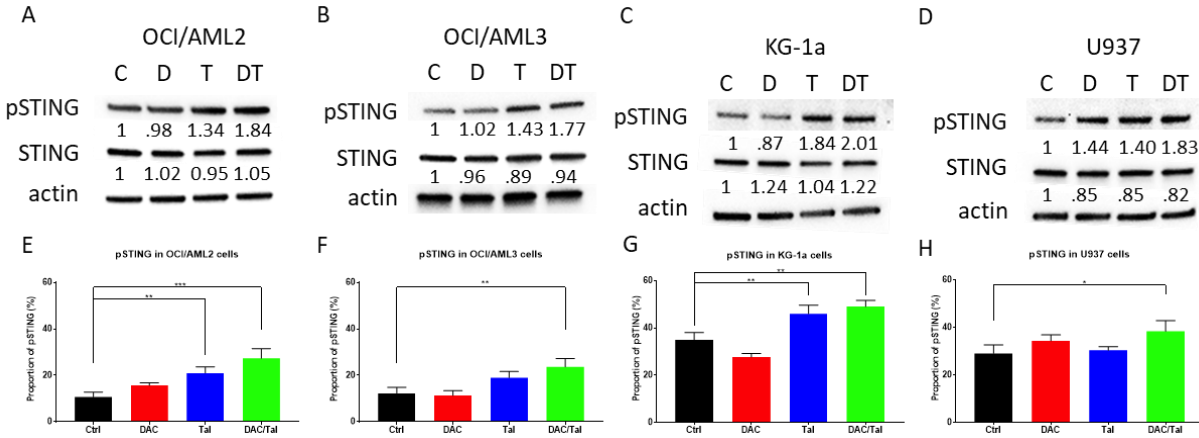
Mutated Samples
TCGA-AB-2943-03
TCGA-AB-2935-03
TCGA-AB-2813-03
TCGA-AB-2938-03
TCGA-AB-2908-03
TCGA-AB-2885-03
TCGA-AB-2829-03
TCGA-AB-2904-03
TCGA-AB-2952-03
TCGA-AB-2941-03
TCGA-AB-2878-03
TCGA-AB-2820-03
TCGA-AB-2860-03
TCGA-AB-2838-03
TCGA-AB-2868-03
TCGA-AB-2857-03



Appendix Figure S2.1: DNMTi treatment increases ERV gene expression in TP53 mutant AML. (A) Relative RNA expression for a subset of ERV genes after mock or 10 nM DAC treatment in MOLM-14, OCI-AML2, OCI-AML3, Kasumi-1, KG-1a, and U937 cell lines (72hrs, n = 3). (B) Relative RNA expression for a subset of ERV genes after mock or 10 nM DAC treatment ± 50 uM pifithrin in MOLM-14 cells (72hrs, n = 3). (C-H) Relative RNA expression for a subset of ERV genes after mock, 10 nM DAC, 5 nM Tal, or DAC/Tal combination: 10 nM DAC + 5 nM Tal treatment in MOLM-14 (C), OCI-AML2 (D), OCI-AML3 (E), Kasumi-1 (F), KG-1a (G), and U937 (H) cell lines (72hrs, n = 3).



Appendix Figure S2.2: PARP1 protein levels decrease after DNMTi+PARPi combination treatment. (A-F) Immunoblot for PARP1 after mock, 10 nM DAC, 5 nM Tal, or DAC/Tal combination: 10 nM DAC + 5 nM Tal treatment in MOLM-14 (A), OCI-AML2 (B), OCI-AML3 (C), Kasumi-1 (D), KG-1a (E), and U937 (F) cell lines with β -actin used as a loading control (72hrs, n = 3).



Appendix Figure S2.3: STING activity is increased in TP53 mutant AML after

DNMTi+PARPi combination treatment. (A-B) Immunoblot for pSTING and STING in TP53

WT OCI/AML2 (A) and OCI/AML3 (B) cells after mock, 10 nM DAC, 5 nM Tal, or DAC/Tal combination: 10 nM DAC + 5 nM Tal treatment with vinculin used as a loading control,

quantified values below each respective protein (72hrs, n = 3). (C-D) Quantification of

proportion of pSTING in TP53 WT OCI/AML2 (C) and OCI/AML3 (D) cells after mock, 10 nM DAC, 5 nM Tal, or DAC/Tal combination: 10 nM DAC + 5 nM Tal treatment (72hrs, n = 3). (E-

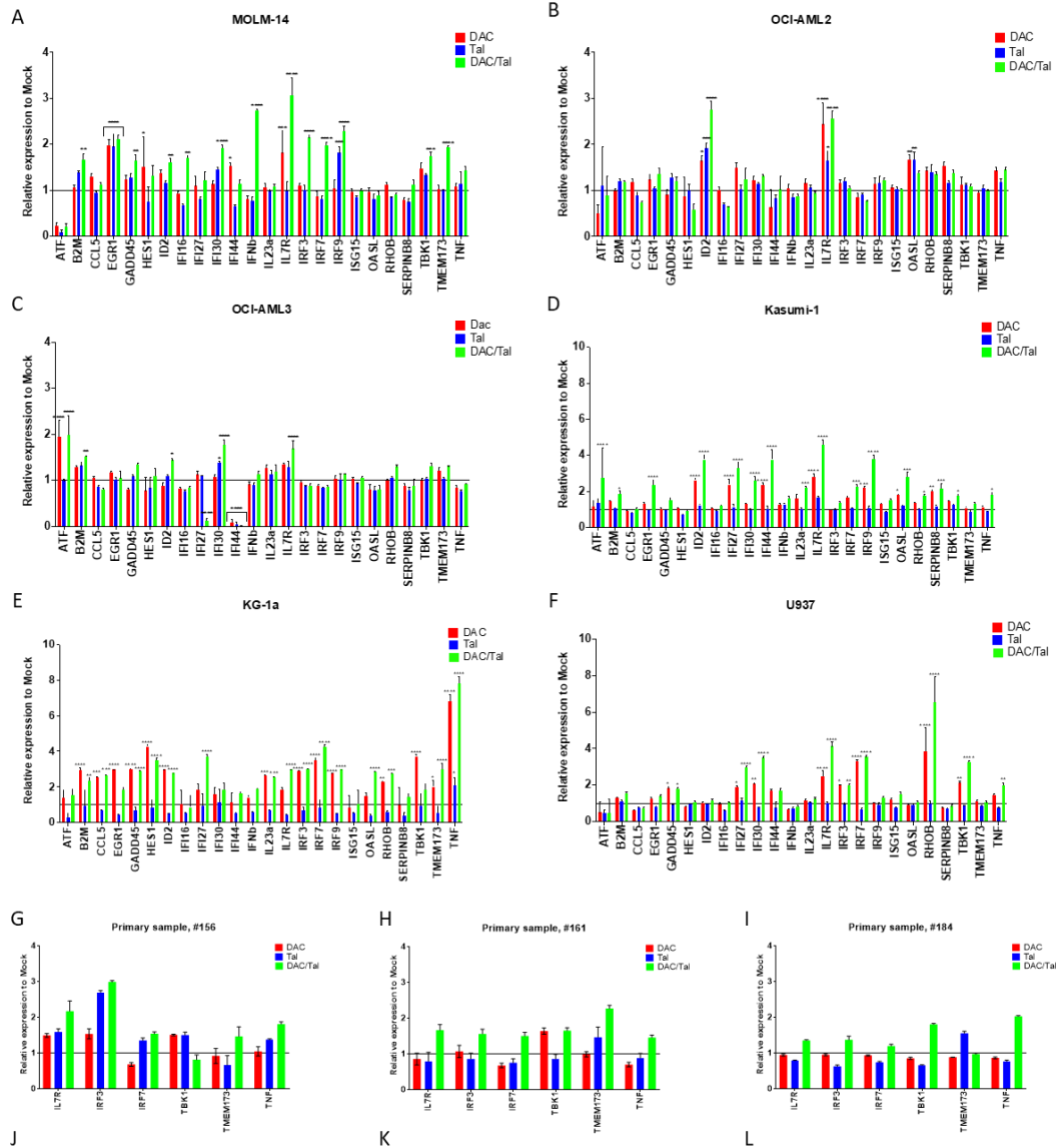
F) Immunoblot for pSTING and STING in TP53 mutant KG-1a (E) and U937 (F) cells after

mock, 10 nM DAC, 5 nM Tal, or DAC/Tal combination: 10 nM DAC + 5 nM Tal treatment with vinculin used as a loading control, quantified values below each respective protein (72hrs, n = 3).

(G-H) Quantification of proportion of pSTING in TP53 mutant KG-1a (G) and U937 (H) cells

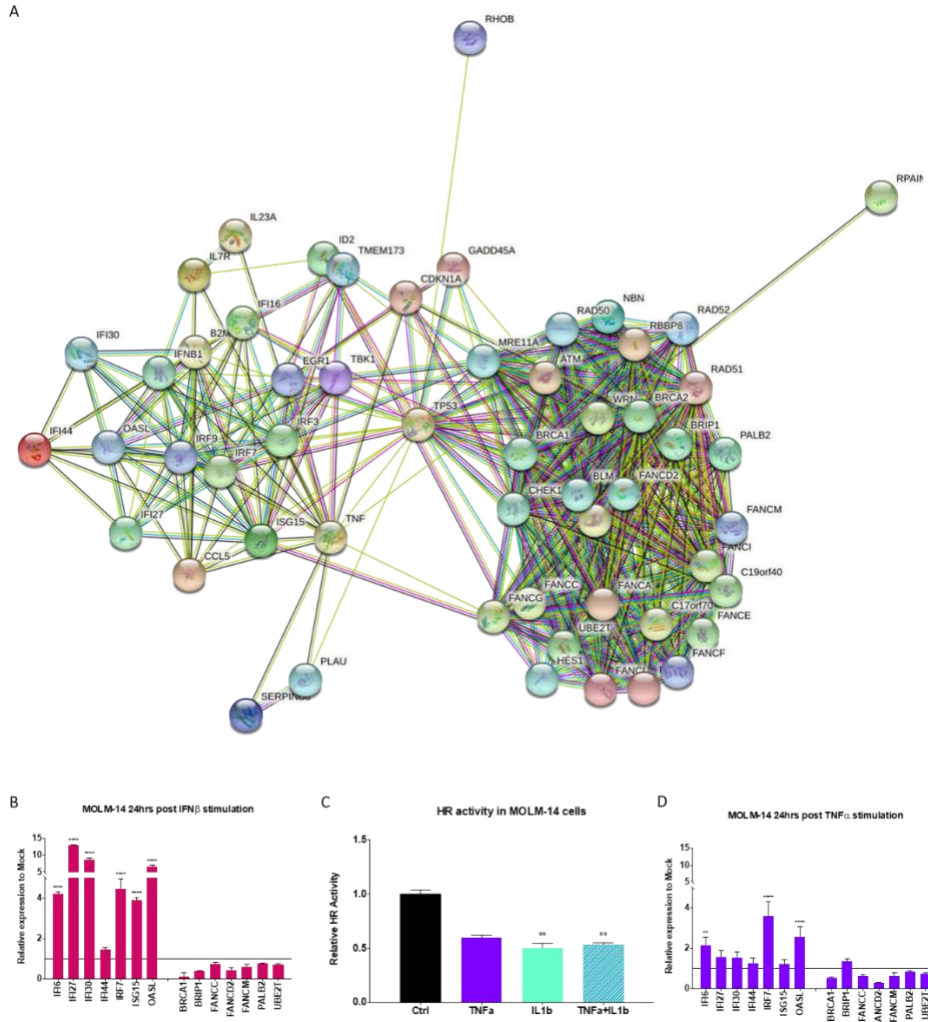
after mock, 10 nM DAC, 5 nM Tal, or DAC/Tal combination: 10 nM DAC + 5 nM Tal treatment (72hrs, n = 3). All data are presented as mean \pm SEM with statistical significance derived from

two-tailed unpaired Student's t test (or ANOVA),

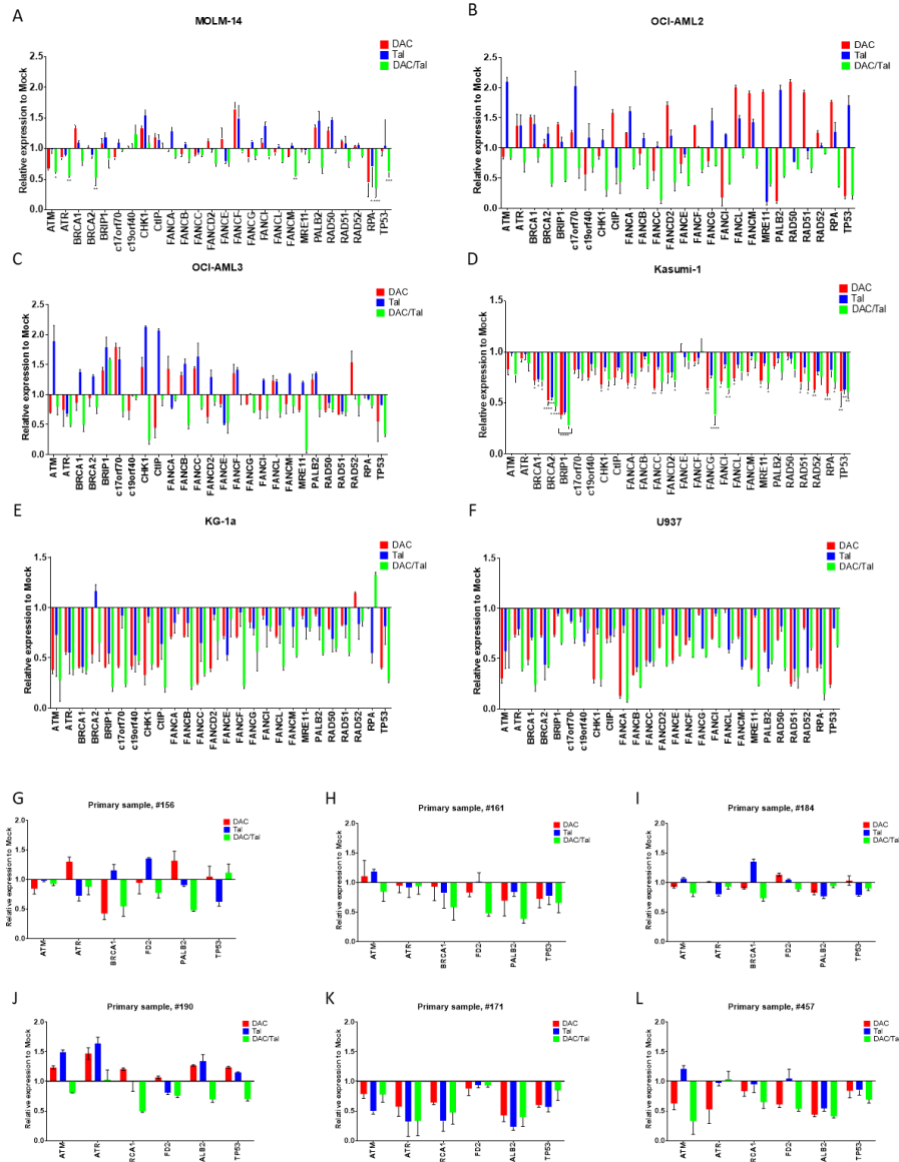


Appendix Figure S2.4: DNMTi treatment increases IFN signaling in TP53 mutant AML.

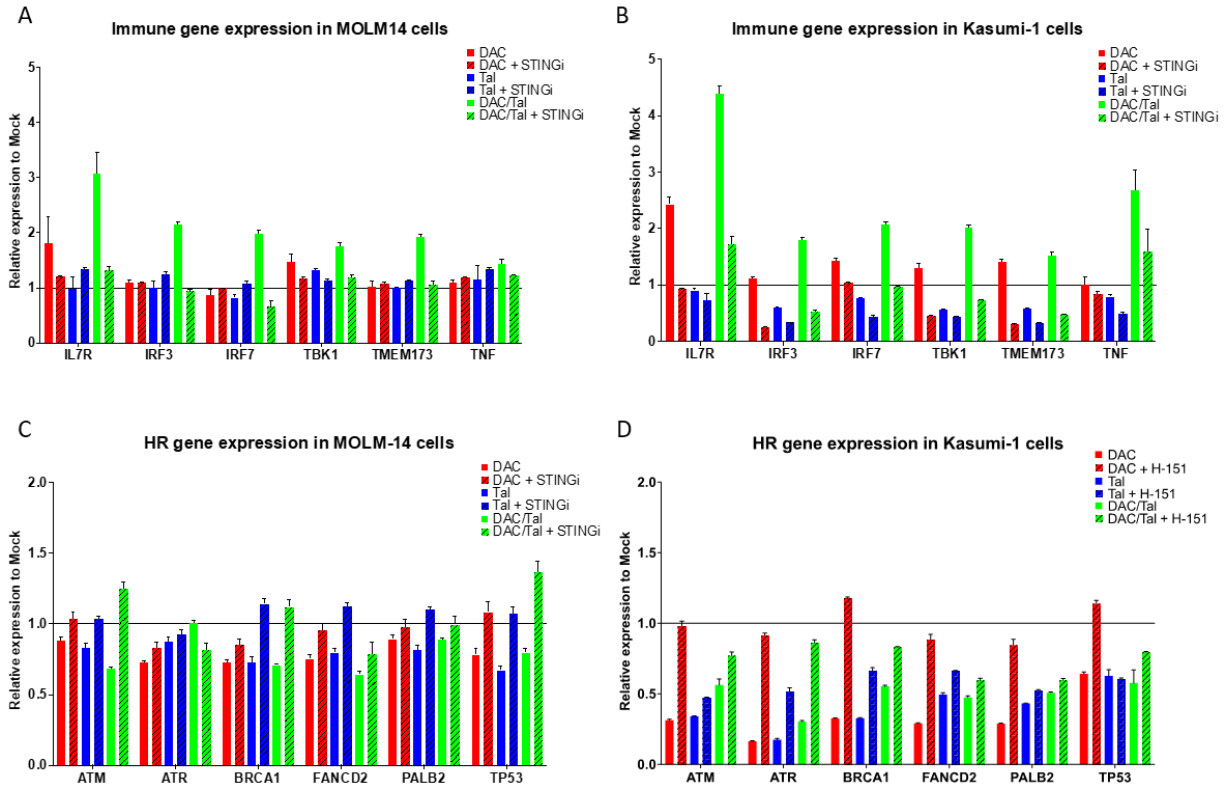
(A-L) Relative RNA expression for a subset of Immune genes after mock, 10 nM DAC, 5 nM Tal, or DAC/Tal combination: 10 nM DAC + 5 nM Tal treatment in TP53 WT MOLM-14 (A), OCI-AML2 (B), and OCI-AML3 (C) cell lines, TP53 mutant Kasumi-1 (D), KG-1a (E), and U937 (F) cell lines and TP53 WT (G-J) and mutant (K-L) primary samples (72hrs, n = 3). All data are presented as mean \pm SEM with statistical significance derived from two-tailed unpaired Student's t test (or ANOVA).



Appendix Figure S2.5: Immune and DNA repair pathways are linked. (A) STRING protein–protein interaction map of homologous recombination and IFN genes of interest. See Fig. S5A for an expanded version (B) Relative RNA expression for a subset of immune and HR genes 24hrs after 100 ng/mL IFN β treatment in in MOLM-14 cells (n = 3). (C) Relative HR activity analysis 24h after 50 ng/mL TNF α , 1 ng/mL IL1- β , or 50 ng/mL TNF α + 1 ng/mL IL1- β treatment in in MOLM-14 cells (n = 3). (D) Relative RNA expression for a subset of immune and HR genes 24hrs after 50 ng/mL TNF α treatment in in MOLM-14 cells (n = 3). All data are presented as mean \pm SEM with statistical significance derived from two-tailed unpaired Student’s t test (or ANOVA).

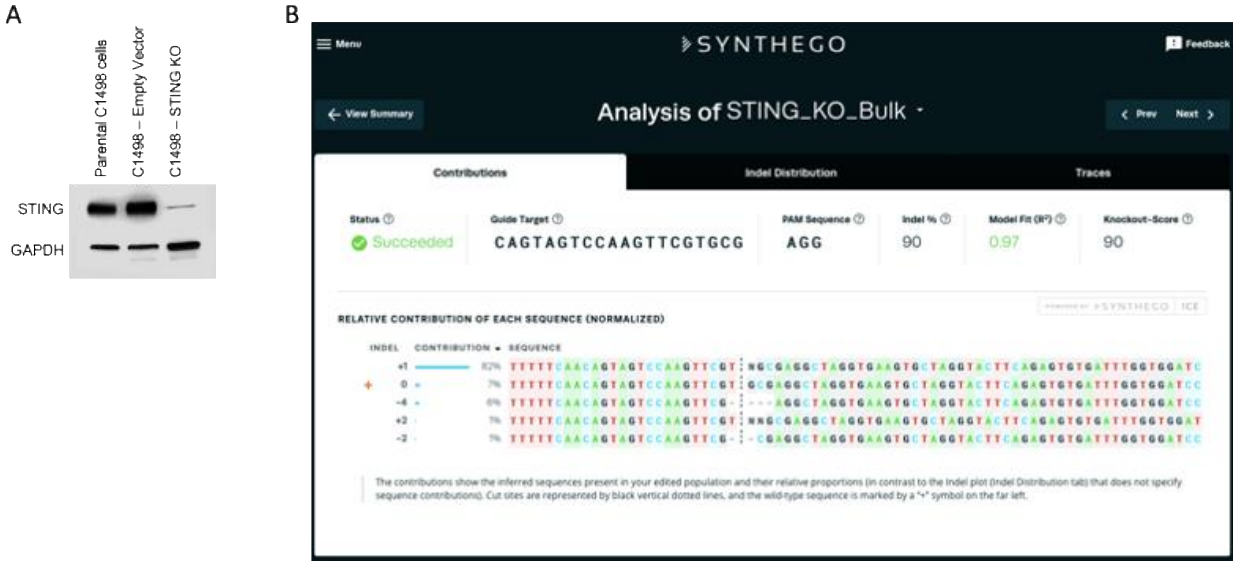


Appendix Figure S2.6: DNMTi treatment decreases HR gene expression levels in TP53 mutant AML. (A-L) Relative RNA expression for a subset of HR genes after mock, 10 nM DAC, 5 nM Tal, or DAC/Tal combination: 10 nM DAC + 5 nM Tal treatment in TP53 WT MOLM-14 (A), OCI-AML2 (B), and OCI-AML3 (C) cell lines, TP53 mutant Kasumi-1 (D), KG-1a (E), and U937 (F) cell lines and TP53 WT (G-J) and mutant (K-L) primary samples (72hrs, n = 3). All data are presented as mean \pm SEM with statistical significance derived from two-tailed unpaired Student's t test (or ANOVA).



Appendix Figure S2.7: STING inhibition abrogates IFN signaling and rescues HR activity.

(A-B) Relative RNA expression for a subset of immune genes after mock, 10 nM DAC, 5 nM Tal, or DAC/Tal combination: 10 nM DAC + 5 nM Tal treatment \pm 500 nM STINGi for all conditions in MOLM-14 (A) and Kasumi-1 (B) cell lines (72hrs, n = 3). (C-D) Relative RNA expression for a subset of HR genes after mock, 10 nM DAC, 5 nM Tal, or DAC/Tal combination: 10 nM DAC + 5 nM Tal treatment \pm 500 nM STINGi for all conditions in MOLM-14 (C) and Kasumi-1 (D) cell lines (72hrs, n = 3).



Appendix Figure S3.1: Confirmation of STING CRISPR-Cas9 KO. KO confirmation was performed by (A) western blot analysis and by (B) sanger sequencing through Genewiz, and analysis using the Synthego online platform.

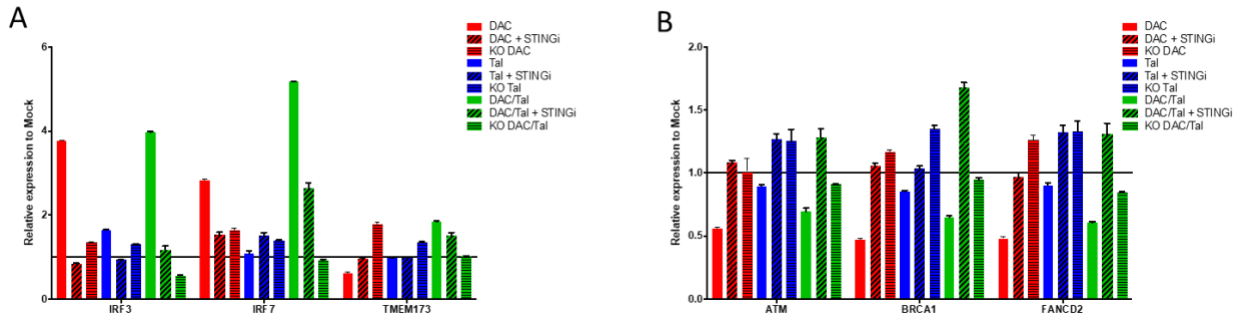
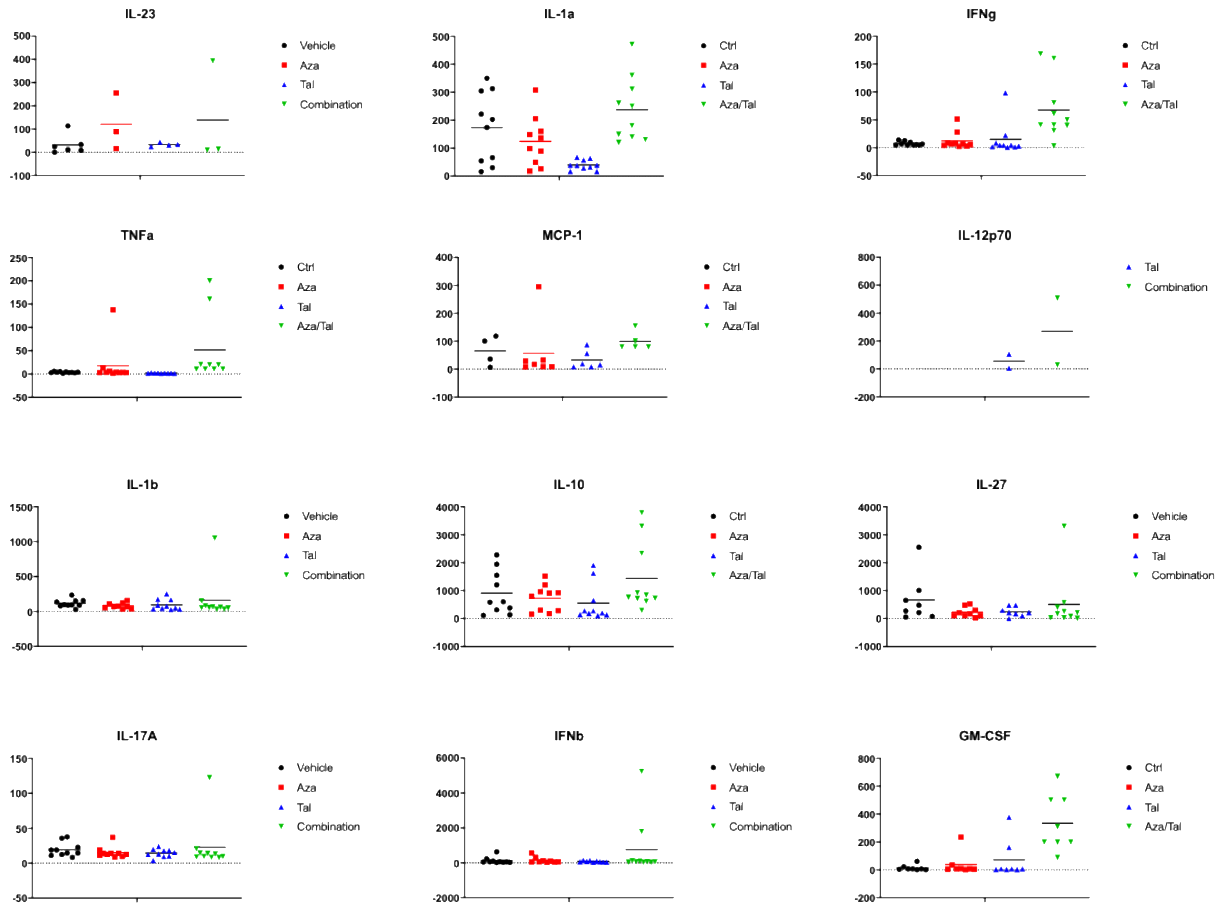
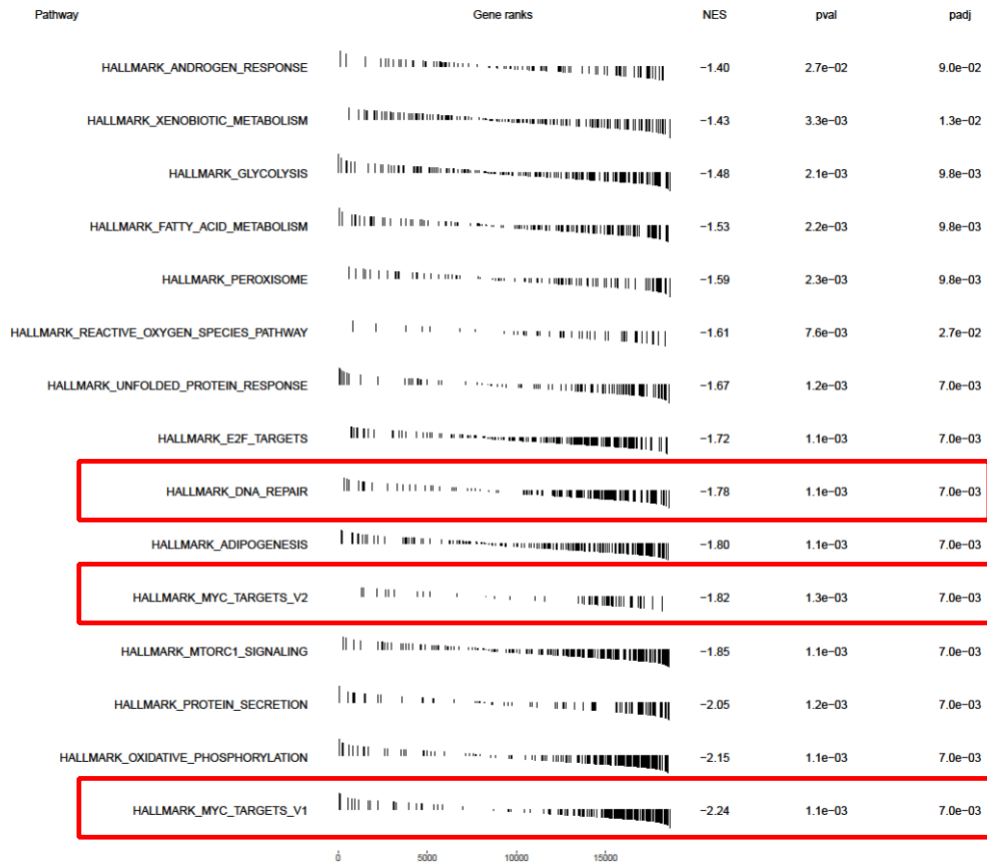


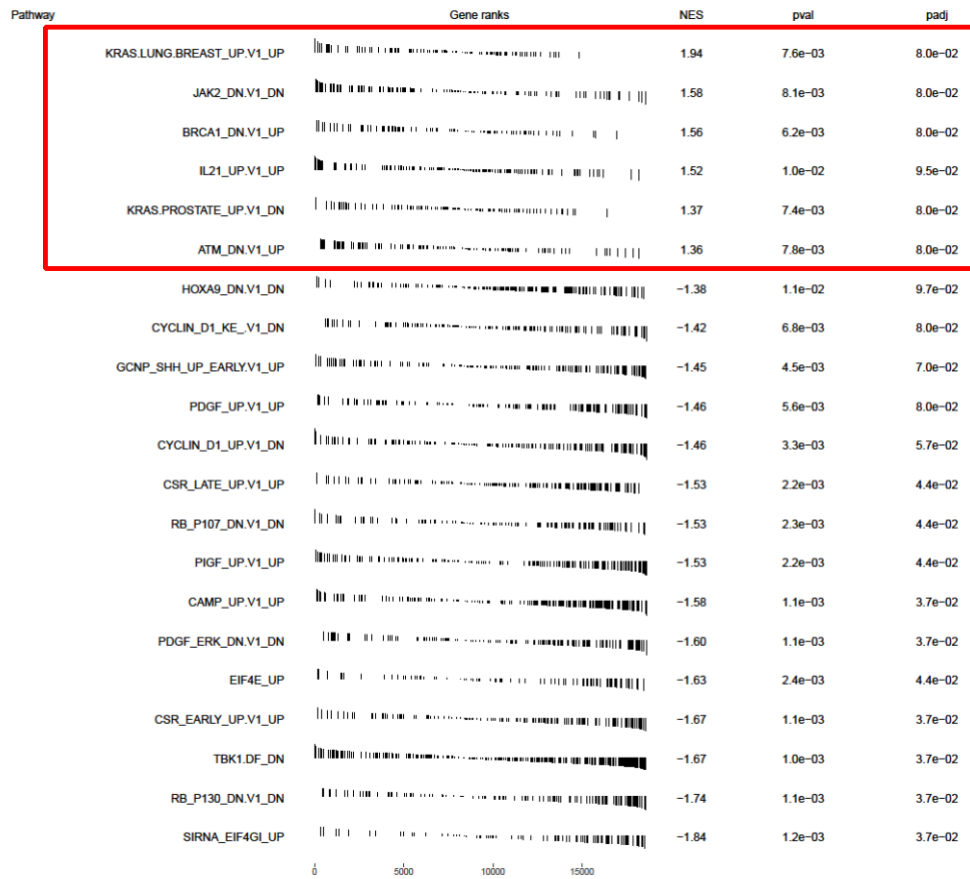
Figure S3.2: STING inhibition abrogates IFN signaling. (A-B) Relative expression of immune (A) and HR (B) genes after CRISPR KO of STING, or co-treatment with 500nM STINGi in C1498 cells treated with vehicle, 10 nM DAC, 5 nM Tal, or DAC/Tal combination: 10 nM DAC + 5 nM Tal \pm 500 nM STINGi for all conditions (72hrs, n = 3). All data are presented as mean \pm SEM with statistical significance derived from two-tailed unpaired Student's t test (or ANOVA).



Appendix Figure S3.3: DNMTi and PARPi combination therapy enhances immune signaling in serum of tumor-bearing mice. Cytokine expression measured via flow cytometry using serum extracted from mice after 14 days of treatment.



Appendix Figure S4.1: Hallmark pathway analysis of clinical trial samples. GSEA using the MSigDB Hallmark gene sets showed particularly negative enrichment for myc and DNA repair related pathways. FDR-based padj == 0.1.



Appendix Figure S4.2: Oncogenic pathway analysis of clinical trial samples. GSEA using the MSigDB oncogenic signatures (C6) showed positive enrichment for pathways associated with knockdown of BRCA1 and ATM related gene sets. FDR-based padj == 0.1.

References

1. Sell S. Leukemia: stem cells, maturation arrest, and differentiation therapy. *Stem Cell Rev.* 2005;1(3):197-205.
2. Lim WF, Inoue-Yokoo T, Tan KS, Lai MI, Sugiyama D. Hematopoietic cell differentiation from embryonic and induced pluripotent stem cells. *Stem Cell Res Ther.* 2013;4(3):71.
3. Liepman MK. Chronic leukemias. *Int J Dermatol.* 1982;21(6):350-355.
4. Hodgson K, Ferrer G, Montserrat E, Moreno C. Chronic lymphocytic leukemia and autoimmunity: a systematic review. *Haematologica.* 2011;96(5):752-761.
5. Basso G, Buldini B, De Zen L, Orfao A. New methodologic approaches for immunophenotyping acute leukemias. *Haematologica.* 2001;86(7):675-692.
6. Look AT. Oncogenic transcription factors in the human acute leukemias. *Science.* 1997;278(5340):1059-1064.
7. Showel MM, Levis M. Advances in treating acute myeloid leukemia. *F1000Prime Rep.* 2014;6:96.
8. Harrison CJ. Acute lymphoblastic leukemia. *Clin Lab Med.* 2011;31(4):631-647, ix.
9. Kumar CC. Genetic abnormalities and challenges in the treatment of acute myeloid leukemia. *Genes Cancer.* 2011;2(2):95-107.
10. Slany RK. The molecular biology of mixed lineage leukemia. *Haematologica.* 2009;94(7):984-993.
11. Vadakekolathu J, Minden MD, Hood T, et al. Immune landscapes predict chemotherapy resistance and immunotherapy response in acute myeloid leukemia. *Sci Transl Med.* 2020;12(546).
12. Narayanan D, Weinberg OK. How I investigate acute myeloid leukemia. *Int J Lab Hematol.* 2020;42(1):3-15.
13. De Kouchkovsky I, Abdul-Hay M. 'Acute myeloid leukemia: a comprehensive review and 2016 update'. *Blood Cancer J.* 2016;6(7):e441.
14. Pasquer H, Tostain M, Kaci N, Roux B, Benajiba L. Descriptive and Functional Genomics in Acute Myeloid Leukemia (AML): Paving the Road for a Cure. *Cancers (Basel).* 2021;13(4).
15. Dutta S, Pregartner G, Rucker FG, et al. Functional Classification of TP53 Mutations in Acute Myeloid Leukemia. *Cancers (Basel).* 2020;12(3).
16. Dohner H, Weisdorf DJ, Bloomfield CD. Acute Myeloid Leukemia. *N Engl J Med.* 2015;373(12):1136-1152.
17. Bennett JM, Catovsky D, Daniel MT, et al. Proposals for the classification of the acute leukaemias. French-American-British (FAB) co-operative group. *Br J Haematol.* 1976;33(4):451-458.

18. Tenen DG. Disruption of differentiation in human cancer: AML shows the way. *Nat Rev Cancer*. 2003;3(2):89-101.
19. Bennett JM, Catovsky D, Daniel MT, et al. Proposed revised criteria for the classification of acute myeloid leukemia. A report of the French-American-British Cooperative Group. *Ann Intern Med*. 1985;103(4):620-625.
20. Hasserjian RP. Acute myeloid leukemia: advances in diagnosis and classification. *Int J Lab Hematol*. 2013;35(3):358-366.
21. Vardiman JW, Thiele J, Arber DA, et al. The 2008 revision of the World Health Organization (WHO) classification of myeloid neoplasms and acute leukemia: rationale and important changes. *Blood*. 2009;114(5):937-951.
22. Vardiman JW, Harris NL, Brunning RD. The World Health Organization (WHO) classification of the myeloid neoplasms. *Blood*. 2002;100(7):2292-2302.
23. Hwang SM. Classification of acute myeloid leukemia. *Blood Res*. 2020;55(S1):S1-S4.
24. Dohner H, Dolnik A, Tang L, et al. Cytogenetics and gene mutations influence survival in older patients with acute myeloid leukemia treated with azacitidine or conventional care. *Leukemia*. 2018;32(12):2546-2557.
25. Dohner H, Estey E, Grimwade D, et al. Diagnosis and management of AML in adults: 2017 ELN recommendations from an international expert panel. *Blood*. 2017;129(4):424-447.
26. Dash A, Gilliland DG. Molecular genetics of acute myeloid leukaemia. *Best Pract Res Clin Haematol*. 2001;14(1):49-64.
27. Kelly LM, Gilliland DG. Genetics of myeloid leukemias. *Annu Rev Genomics Hum Genet*. 2002;3:179-198.
28. Licht JD. AML1 and the AML1-ETO fusion protein in the pathogenesis of t(8;21) AML. *Oncogene*. 2001;20(40):5660-5679.
29. Al-Harbi S, Aljurf M, Mohty M, Almohareb F, Ahmed SOA. An update on the molecular pathogenesis and potential therapeutic targeting of AML with t(8;21)(q22;q22.1);RUNX1-RUNX1T1. *Blood Adv*. 2020;4(1):229-238.
30. Gustafson SA, Lin P, Chen SS, et al. Therapy-related acute myeloid leukemia with t(8;21) (q22;q22) shares many features with de novo acute myeloid leukemia with t(8;21)(q22;q22) but does not have a favorable outcome. *Am J Clin Pathol*. 2009;131(5):647-655.
31. Wang W, Tang G, Cortes JE, et al. Chromosomal rearrangement involving 11q23 locus in chronic myelogenous leukemia: a rare phenomenon frequently associated with disease progression and poor prognosis. *J Hematol Oncol*. 2015;8:32.
32. Zuo W, Wang SA, DiNardo C, et al. Acute leukaemia and myelodysplastic syndromes with chromosomal rearrangement involving 11q23 locus, but not MLL gene. *J Clin Pathol*. 2017;70(3):244-249.

33. Britten O, Ragusa D, Tosi S, Kamel YM. MLL-Rearranged Acute Leukemia with t(4;11)(q21;q23)-Current Treatment Options. Is There a Role for CAR-T Cell Therapy? *Cells*. 2019;8(11).
34. Cox MC, Panetta P, Lo-Coco F, et al. Chromosomal aberration of the 11q23 locus in acute leukemia and frequency of MLL gene translocation: results in 378 adult patients. *Am J Clin Pathol*. 2004;122(2):298-306.
35. Strissel PL, Strick R, Tomek RJ, Roe BA, Rowley JD, Zeleznik-Le NJ. DNA structural properties of AF9 are similar to MLL and could act as recombination hot spots resulting in MLL/AF9 translocations and leukemogenesis. *Hum Mol Genet*. 2000;9(11):1671-1679.
36. Balgobind BV, Zwaan CM, Pieters R, Van den Heuvel-Eibrink MM. The heterogeneity of pediatric MLL-rearranged acute myeloid leukemia. *Leukemia*. 2011;25(8):1239-1248.
37. Yoon JH, Kim HJ, Shin SH, et al. Stratification of de novo adult acute myelogenous leukemia with adverse-risk karyotype: can we overcome the worse prognosis of adverse-risk group acute myelogenous leukemia with hematopoietic stem cell transplantation? *Biol Blood Marrow Transplant*. 2014;20(1):80-88.
38. Mrozek K, Eisfeld AK, Kohlschmidt J, et al. Complex karyotype in de novo acute myeloid leukemia: typical and atypical subtypes differ molecularly and clinically. *Leukemia*. 2019;33(7):1620-1634.
39. Guryanova OA, Shank K, Spitzer B, et al. DNMT3A mutations promote anthracycline resistance in acute myeloid leukemia via impaired nucleosome remodeling. *Nat Med*. 2016.
40. Xu W, Yang H, Liu Y, et al. Oncometabolite 2-hydroxyglutarate is a competitive inhibitor of alpha-ketoglutarate-dependent dioxygenases. *Cancer Cell*. 2011;19(1):17-30.
41. Mazor T, Chesnelong C, Pankov A, et al. Clonal expansion and epigenetic reprogramming following deletion or amplification of mutant IDH1. *Proc Natl Acad Sci U S A*. 2017;114(40):10743-10748.
42. Figueroa ME, Abdel-Wahab O, Lu C, et al. Leukemic IDH1 and IDH2 mutations result in a hypermethylation phenotype, disrupt TET2 function, and impair hematopoietic differentiation. *Cancer Cell*. 2010;18(6):553-567.
43. Yanada M, Matsuo K, Suzuki T, Kiyoi H, Naoe T. Prognostic significance of FLT3 internal tandem duplication and tyrosine kinase domain mutations for acute myeloid leukemia: a meta-analysis. *Leukemia*. 2005;19(8):1345-1349.
44. Nakao M, Yokota S, Iwai T, et al. Internal tandem duplication of the flt3 gene found in acute myeloid leukemia. *Leukemia*. 1996;10(12):1911-1918.
45. Yamamoto Y, Kiyoi H, Nakano Y, et al. Activating mutation of D835 within the activation loop of FLT3 in human hematologic malignancies. *Blood*. 2001;97(8):2434-2439.
46. Barbosa K, Li S, Adams PD, Deshpande AJ. The role of TP53 in acute myeloid leukemia: Challenges and opportunities. *Genes Chromosomes Cancer*. 2019;58(12):875-888.

47. Hunter AM, Sallman DA. Current status and new treatment approaches in TP53 mutated AML. *Best Pract Res Clin Haematol.* 2019;32(2):134-144.
48. Stengel A, Kern W, Haferlach T, Meggendorfer M, Fasan A, Haferlach C. The impact of TP53 mutations and TP53 deletions on survival varies between AML, ALL, MDS and CLL: an analysis of 3307 cases. *Leukemia.* 2017;31(3):705-711.
49. Sallman DA, Komrokji R, Vaupel C, et al. Impact of TP53 mutation variant allele frequency on phenotype and outcomes in myelodysplastic syndromes. *Leukemia.* 2016;30(3):666-673.
50. Molica M, Mazzone C, Niscola P, de Fabritiis P. TP53 Mutations in Acute Myeloid Leukemia: Still a Daunting Challenge? *Front Oncol.* 2020;10:610820.
51. Loizou E, Banito A, Livshits G, et al. A Gain-of-Function p53-Mutant Oncogene Promotes Cell Fate Plasticity and Myeloid Leukemia through the Pluripotency Factor FOXH1. *Cancer Discov.* 2019;9(7):962-979.
52. Brosh R, Rotter V. When mutants gain new powers: news from the mutant p53 field. *Nat Rev Cancer.* 2009;9(10):701-713.
53. Boettcher S, Miller PG, Sharma R, et al. A dominant-negative effect drives selection of TP53 missense mutations in myeloid malignancies. *Science.* 2019;365(6453):599-604.
54. Kotler E, Shani O, Goldfeld G, et al. A Systematic p53 Mutation Library Links Differential Functional Impact to Cancer Mutation Pattern and Evolutionary Conservation. *Mol Cell.* 2018;71(5):873.
55. Bouaoun L, Sonkin D, Ardin M, et al. TP53 Variations in Human Cancers: New Lessons from the IARC TP53 Database and Genomics Data. *Hum Mutat.* 2016;37(9):865-876.
56. Olivier M, Hollstein M, Hainaut P. TP53 mutations in human cancers: origins, consequences, and clinical use. *Cold Spring Harb Perspect Biol.* 2010;2(1):a001008.
57. Schilling T, Kairat A, Melino G, et al. Interference with the p53 family network contributes to the gain of oncogenic function of mutant p53 in hepatocellular carcinoma. *Biochem Biophys Res Commun.* 2010;394(3):817-823.
58. Rucker FG, Schlenk RF, Bullinger L, et al. TP53 alterations in acute myeloid leukemia with complex karyotype correlate with specific copy number alterations, monosomal karyotype, and dismal outcome. *Blood.* 2012;119(9):2114-2121.
59. Kelly TK, De Carvalho DD, Jones PA. Epigenetic modifications as therapeutic targets. *Nature biotechnology.* 2010;28(10):1069-1078.
60. Stein GS, Messier TL, Gordon JA, et al. Oncogenic epigenetic control. *Aging (Albany NY).* 2016;8(4):565-566.
61. Stein GS, Stein JL, Van Wijnen AJ, et al. Transcription factor-mediated epigenetic regulation of cell growth and phenotype for biological control and cancer. *Adv Enzyme Regul.* 2010;50(1):160-167.
62. Jones PA, Baylin SB. The epigenomics of cancer. *Cell.* 2007;128(4):683-692.
63. Conway O'Brien E, Prideaux S, Chevassut T. The epigenetic landscape of acute myeloid leukemia. *Adv Hematol.* 2014;2014:103175.

64. Delcuve GP, Rastegar M, Davie JR. Epigenetic control. *Journal of cellular physiology*. 2009;219(2):243-250.
65. Suvà ML, Riggi N, Bernstein BE. Epigenetic reprogramming in cancer. *Science*. 2013;339(6127):1567-1570.
66. Issa JP, Baylin SB, Herman JG. DNA methylation changes in hematologic malignancies: biologic and clinical implications. *Leukemia*. 1997;11 Suppl 1:S7-11.
67. Baylin SB, Jones PA. A decade of exploring the cancer epigenome—biological and translational implications. *Nature Reviews Cancer*. 2011;11(10):726-734.
68. Wouters BJ, Delwel R. Epigenetics and approaches to targeted epigenetic therapy in acute myeloid leukemia. *Blood*. 2016;127(1):42-52.
69. Munoz P, Iliou MS, Esteller M. Epigenetic alterations involved in cancer stem cell reprogramming. *Mol Oncol*. 2012;6(6):620-636.
70. Gottlicher M, Minucci S, Zhu P, et al. Valproic acid defines a novel class of HDAC inhibitors inducing differentiation of transformed cells. *EMBO J*. 2001;20(24):6969-6978.
71. He L, He X, Lim LP, et al. A microRNA component of the p53 tumour suppressor network. *Nature*. 2007;447(7148):1130-1134.
72. Li KK, Luo L-F, Shen Y, Xu J, Chen Z, Chen S-J. DNA methyltransferases in hematologic malignancies. Paper presented at: Seminars in hematology2013.
73. Yang H, Bueso-Ramos C, DiNardo C, et al. Expression of PD-L1, PD-L2, PD-1 and CTLA4 in myelodysplastic syndromes is enhanced by treatment with hypomethylating agents. *Leukemia*. 2014;28(6):1280-1288.
74. Anguille S, Lion E, Willemen Y, Van Tendeloo VF, Berneman ZN, Smits EL. Interferon-alpha in acute myeloid leukemia: an old drug revisited. *Leukemia*. 2011;25(5):739-748.
75. Radpour R, Stucki M, Riether C, Ochsenbein AF. Epigenetic Silencing of Immune-Checkpoint Receptors in Bone Marrow- Infiltrating T Cells in Acute Myeloid Leukemia. *Front Oncol*. 2021;11:663406.
76. Taghiloo S, Asgarian-Omran H. Immune evasion mechanisms in acute myeloid leukemia: A focus on immune checkpoint pathways. *Crit Rev Oncol Hematol*. 2021;157:103164.
77. Teague RM, Kline J. Immune evasion in acute myeloid leukemia: current concepts and future directions. *J Immunother Cancer*. 2013;1(13).
78. Curran E, Corrales L, Kline J. Targeting the innate immune system as immunotherapy for acute myeloid leukemia. *Front Oncol*. 2015;5:83.
79. Saleh R, Toor SM, Sasidharan Nair V, Elkord E. Role of Epigenetic Modifications in Inhibitory Immune Checkpoints in Cancer Development and Progression. *Front Immunol*. 2020;11:1469.
80. Yoshikawa Y, Kuribayashi K, Minami T, Ohmuraya M, Kijima T. Epigenetic Alterations and Biomarkers for Immune Checkpoint Inhibitors-Current Standards and Future

- Perspectives in Malignant Pleural Mesothelioma Treatment. *Front Oncol.* 2020;10:554570.
81. Chiappinelli KB, Strissel PL, Desrichard A, et al. Inhibiting DNA Methylation Causes an Interferon Response in Cancer via dsRNA Including Endogenous Retroviruses. *Cell.* 2015;162(5):974-986.
 82. Topper MJ, Vaz M, Chiappinelli KB, et al. Epigenetic Therapy Ties MYC Depletion to Reversing Immune Evasion and Treating Lung Cancer. *Cell.* 2017;171(6):1284-1300 e1221.
 83. Topper MJ, Vaz M, Marrone KA, Brahmer JR, Baylin SB. The emerging role of epigenetic therapeutics in immuno-oncology. *Nat Rev Clin Oncol.* 2020;17(2):75-90.
 84. Watts J, Nimer S. Recent advances in the understanding and treatment of acute myeloid leukemia. *F1000Res.* 2018;7.
 85. Liu H. Emerging agents and regimens for AML. *J Hematol Oncol.* 2021;14(1):49.
 86. Kantarjian H, Kadia T, DiNardo C, et al. Acute myeloid leukemia: current progress and future directions. *Blood Cancer J.* 2021;11(2):41.
 87. Tallman MS, Gilliland DG, Rowe JM. Drug therapy for acute myeloid leukemia. *Blood.* 2005;106(4):1154-1163.
 88. Adige S, Lapidus RG, Carter-Cooper BA, et al. Equipotent doses of daunorubicin and idarubicin for AML: a meta-analysis of clinical trials versus in vitro estimation. *Cancer Chemother Pharmacol.* 2019;83(6):1105-1112.
 89. Wiernik PH, Banks PL, Case DC, Jr., et al. Cytarabine plus idarubicin or daunorubicin as induction and consolidation therapy for previously untreated adult patients with acute myeloid leukemia. *Blood.* 1992;79(2):313-319.
 90. Wiernik PH, Case DC, Jr., Periman PO, et al. A multicenter trial of cytarabine plus idarubicin or daunorubicin as induction therapy for adult nonlymphocytic leukemia. *Semin Oncol.* 1989;16(1 Suppl 2):25-29.
 91. Chu MY, Fischer GA. A proposed mechanism of action of 1-beta-D-arabinofuranosyl-cytosine as an inhibitor of the growth of leukemic cells. *Biochem Pharmacol.* 1962;11:423-430.
 92. Gewirtz DA. A critical evaluation of the mechanisms of action proposed for the antitumor effects of the anthracycline antibiotics adriamycin and daunorubicin. *Biochem Pharmacol.* 1999;57(7):727-741.
 93. GROUP TAC. A systematic collaborative overview of randomized trials comparing idarubicin with daunorubicin (or other anthracyclines) as induction therapy for acute myeloid leukaemia. AML Collaborative Group. *Br J Haematol.* 1998;103(1):100-109.
 94. Mangan JK, Luger SM. Salvage therapy for relapsed or refractory acute myeloid leukemia. *Ther Adv Hematol.* 2011;2(2):73-82.
 95. Schlenk RF. Post-remission therapy for acute myeloid leukemia. *Haematologica.* 2014;99(11):1663-1670.

96. Vyas P, Appelbaum FR, Craddock C. Allogeneic hematopoietic cell transplantation for acute myeloid leukemia. *Biol Blood Marrow Transplant*. 2015;21(1):8-15.
97. Dombret H, Gardin C. An update of current treatments for adult acute myeloid leukemia. *Blood*. 2016;127(1):53-61.
98. Middeke JM, Beelen D, Stadler M, et al. Outcome of high-risk acute myeloid leukemia after allogeneic hematopoietic cell transplantation: negative impact of abnl(17p) and -5/5q. *Blood*. 2012;120(12):2521-2528.
99. Brandwein JM, Geddes M, Kassis J, et al. Treatment of older patients with acute myeloid leukemia (AML): a Canadian consensus. *Am J Blood Res*. 2013;3(2):141-164.
100. Diesch J, Zwick A, Garz AK, Palau A, Buschbeck M, Gotze KS. A clinical-molecular update on azanucleoside-based therapy for the treatment of hematologic cancers. *Clin Epigenetics*. 2016;8:71.
101. Daver N, Cortes J, Kantarjian H, Ravandi F. Acute myeloid leukemia: advancing clinical trials and promising therapeutics. *Expert Rev Hematol*. 2016;9(5):433-445.
102. Szer J. The prevalent predicament of relapsed acute myeloid leukemia. *Hematology Am Soc Hematol Educ Program*. 2012;2012:43-48.
103. Yang X, Lay F, Han H, Jones PA. Targeting DNA methylation for epigenetic therapy. *Trends Pharmacol Sci*. 2010;31(11):536-546.
104. Tsai HC, Li H, Van Neste L, et al. Transient low doses of DNA-demethylating agents exert durable antitumor effects on hematological and epithelial tumor cells. *Cancer Cell*. 2012;21(3):430-446.
105. Dombret H, Seymour JF, Butrym A, et al. International phase 3 study of azacitidine vs conventional care regimens in older patients with newly diagnosed AML with >30% blasts. *Blood*. 2015;126(3):291-299.
106. Issa JP. DNA methylation as a therapeutic target in cancer. *Clin Cancer Res*. 2007;13(6):1634-1637.
107. Gravina GL, Festuccia C, Marampon F, et al. Biological rationale for the use of DNA methyltransferase inhibitors as new strategy for modulation of tumor response to chemotherapy and radiation. *Mol Cancer*. 2010;9:305.
108. Hanahan D, Weinberg RA. The hallmarks of cancer. *Cell*. 2000;100(1):57-70.
109. Oronsky B, Oronsky N, Knox S, Fanger G, Scicinski J. Episensitization: therapeutic tumor resensitization by epigenetic agents: a review and reassessment. *Anticancer Agents Med Chem*. 2014;14(8):1121-1127.
110. Oronsky B, Oronsky N, Scicinski J, Fanger G, Lybeck M, Reid T. Rewriting the epigenetic code for tumor resensitization: a review. *Transl Oncol*. 2014;7(5):626-631.
111. Soengas MS, Capodieci P, Polsky D, et al. Inactivation of the apoptosis effector Apaf-1 in malignant melanoma. *Nature*. 2001;409(6817):207-211.
112. Lahtz C, Pfeifer GP. Epigenetic changes of DNA repair genes in cancer. *J Mol Cell Biol*. 2011;3(1):51-58.

113. Sharma S, Kelly TK, Jones PA. Epigenetics in cancer. *Carcinogenesis*. 2010;31(1):27-36.
114. Ummarino S, Hausman C, Di Ruscio A. The PARP Way to Epigenetic Changes. *Genes (Basel)*. 2021;12(3).
115. Wei H, Yu X. Functions of PARylation in DNA Damage Repair Pathways. *Genomics Proteomics Bioinformatics*. 2016;14(3):131-139.
116. Ray Chaudhuri A, Nussenzweig A. The multifaceted roles of PARP1 in DNA repair and chromatin remodelling. *Nat Rev Mol Cell Biol*. 2017;18(10):610-621.
117. Alhmoud JF, Woolley JF, Al Moustafa AE, Malki MI. DNA Damage/Repair Management in Cancers. *Cancers (Basel)*. 2020;12(4).
118. Rassool FV, Tomkinson AE. Targeting abnormal DNA double strand break repair in cancer. *Cell Mol Life Sci*. 2010;67(21):3699-3710.
119. Murai J, Huang SY, Das BB, et al. Trapping of PARP1 and PARP2 by Clinical PARP Inhibitors. *Cancer Res*. 2012;72(21):5588-5599.
120. Wang H, Zhang S, Song L, Qu M, Zou Z. Synergistic lethality between PARP-trapping and alantolactone-induced oxidative DNA damage in homologous recombination-proficient cancer cells. *Oncogene*. 2020;39(14):2905-2920.
121. Muvarak NE, Chowdhury K, Xia L, et al. Enhancing the Cytotoxic Effects of PARP Inhibitors with DNA Demethylating Agents - A Potential Therapy for Cancer. *Cancer Cell*. 2016;30(4):637-650.
122. Helleday T. The underlying mechanism for the PARP and BRCA synthetic lethality: clearing up the misunderstandings. *Mol Oncol*. 2011;5(4):387-393.
123. Li H, Liu ZY, Wu N, Chen YC, Cheng Q, Wang J. PARP inhibitor resistance: the underlying mechanisms and clinical implications. *Mol Cancer*. 2020;19(1):107.
124. Bryant HE, Schultz N, Thomas HD, et al. Specific killing of BRCA2-deficient tumours with inhibitors of poly(ADP-ribose) polymerase. *Nature*. 2005;434(7035):913-917.
125. Li M, Yu X. The role of poly(ADP-ribosylation) in DNA damage response and cancer chemotherapy. *Oncogene*. 2015;34(26):3349-3356.
126. Wang R, Han Y, Zhao Z, et al. Link synthetic lethality to drug sensitivity of cancer cells. *Brief Bioinform*. 2019;20(4):1295-1307.
127. Kim DS, Camacho CV, Kraus WL. Alternate therapeutic pathways for PARP inhibitors and potential mechanisms of resistance. *Exp Mol Med*. 2021;53(1):42-51.
128. Abbotts R, Topper MJ, Biondi C, et al. DNA methyltransferase inhibitors induce a BRCAness phenotype that sensitizes NSCLC to PARP inhibitor and ionizing radiation. *Proc Natl Acad Sci U S A*. 2019.
129. McLaughlin L, Stojanovic L, Kogan A, et al. Pharmacologic Induction of Innate Immune Signaling Directly Drives Homologous Recombination Deficiency. *Proc Natl Acad Sci U S A*. 2020;in press.

130. Thein MS, Ershler WB, Jemal A, Yates JW, Baer MR. Outcome of older patients with acute myeloid leukemia: an analysis of SEER data over 3 decades. *Cancer*. 2013;119(15):2720-2727.
131. Lohse I, Statz-Geary K, Brothers SP, Wahlestedt C. Precision medicine in the treatment stratification of AML patients: challenges and progress. *Oncotarget*. 2018;9(102):37790-37797.
132. Bories P, Prade N, Lagarde S, et al. Impact of TP53 mutations in acute myeloid leukemia patients treated with azacitidine. *PLoS One*. 2020;15(10):e0238795.
133. Emran AA, Chatterjee A, Rodger EJ, et al. Targeting DNA Methylation and EZH2 Activity to Overcome Melanoma Resistance to Immunotherapy. *Trends Immunol*. 2019;40(4):328-344.
134. Chiappinelli KB, Zahnow CA, Ahuja N, Baylin SB. Combining Epigenetic and Immunotherapy to Combat Cancer. *Cancer Res*. 2016;76(7):1683-1689.
135. Faraoni I, Graziani G. Role of BRCA Mutations in Cancer Treatment with Poly(ADP-ribose) Polymerase (PARP) Inhibitors. *Cancers (Basel)*. 2018;10(12).
136. Kogan AA, Lapidus RG, Baer MR, Rassool FV. Exploiting epigenetically mediated changes: Acute myeloid leukemia, leukemia stem cells and the bone marrow microenvironment. *Adv Cancer Res*. 2019;141:213-253.
137. Bullinger L, Dohner K, Dohner H. Genomics of Acute Myeloid Leukemia Diagnosis and Pathways. *J Clin Oncol*. 2017;35(9):934-946.
138. Bowen D, Groves MJ, Burnett AK, et al. TP53 gene mutation is frequent in patients with acute myeloid leukemia and complex karyotype, and is associated with very poor prognosis. *Leukemia*. 2009;23(1):203-206.
139. Haferlach C, Dicker F, Herholz H, Schnittger S, Kern W, Haferlach T. Mutations of the TP53 gene in acute myeloid leukemia are strongly associated with a complex aberrant karyotype. *Leukemia*. 2008;22(8):1539-1541.
140. Tiwari B, Jones AE, Abrams JM. Transposons, p53 and Genome Security. *Trends Genet*. 2018;34(11):846-855.
141. Hoffman RM. Is DNA methylation the new guardian of the genome? *Mol Cytogenet*. 2017;10:11.
142. Carbone M, Reale A, Di Sauro A, et al. PARP-1 interaction with VP1 capsid protein regulates polyomavirus early gene expression. *J Mol Biol*. 2006;363(4):773-785.
143. Zampieri M, Guastafierro T, Calabrese R, et al. ADP-ribose polymers localized on Ctf-Parp1-Dnmt1 complex prevent methylation of Ctf target sites. *Biochem J*. 2012;441(2):645-652.
144. Issa JP, Garcia-Manero G, Giles FJ, et al. Phase 1 study of low-dose prolonged exposure schedules of the hypomethylating agent 5-aza-2'-deoxycytidine (decitabine) in hematopoietic malignancies. *Blood*. 2004;103(5):1635-1640.

145. Kantarjian H, Oki Y, Garcia-Manero G, et al. Results of a randomized study of 3 schedules of low-dose decitabine in higher-risk myelodysplastic syndrome and chronic myelomonocytic leukemia. *Blood*. 2007;109(1):52-57.
146. Baylin SB, Jones PA. A decade of exploring the cancer epigenome - biological and translational implications. *Nat Rev Cancer*. 2011;11(10):726-734.
147. Fennell KA, Bell CC, Dawson MA. Epigenetic therapies in acute myeloid leukemia: where to from here? *Blood*. 2019;134(22):1891-1901.
148. Nieto M, Samper E, Fraga MF, Gonzalez de Buitrago G, Esteller M, Serrano M. The absence of p53 is critical for the induction of apoptosis by 5-aza-2'-deoxycytidine. *Oncogene*. 2004;23(3):735-743.
149. Yi L, Sun Y, Levine A. Selected drugs that inhibit DNA methylation can preferentially kill p53 deficient cells. *Oncotarget*. 2014;5(19):8924-8936.
150. Welch JS, Petti AA, Miller CA, et al. TP53 and Decitabine in Acute Myeloid Leukemia and Myelodysplastic Syndromes. *N Engl J Med*. 2016;375(21):2023-2036.
151. Mateo J, Carreira S, Sandhu S, et al. DNA-Repair Defects and Olaparib in Metastatic Prostate Cancer. *N Engl J Med*. 2015;373(18):1697-1708.
152. D'Andrea AD. Susceptibility pathways in Fanconi's anemia and breast cancer. *N Engl J Med*. 2010;362(20):1909-1919.
153. Weiser TS, Guo ZS, Ohnmacht GA, et al. Sequential 5-Aza-2 deoxycytidine-depsipeptide FR901228 treatment induces apoptosis preferentially in cancer cells and facilitates their recognition by cytolytic T lymphocytes specific for NY-ESO-1. *J Immunother*. 2001;24(2):151-161.
154. Oi S, Natsume A, Ito M, et al. Synergistic induction of NY-ESO-1 antigen expression by a novel histone deacetylase inhibitor, valproic acid, with 5-aza-2'-deoxycytidine in glioma cells. *J Neurooncol*. 2009;92(1):15-22.
155. Moreno-Bost A, Szmania S, Stone K, et al. Epigenetic modulation of MAGE-A3 antigen expression in multiple myeloma following treatment with the demethylation agent 5-azacitidine and the histone deacetylase inhibitor MGCD0103. *Cytotherapy*. 2011;13(5):618-628.
156. Li H, Chiappinelli KB, Guzzetta AA, et al. Immune regulation by low doses of the DNA methyltransferase inhibitor 5-azacitidine in common human epithelial cancers. *Oncotarget*. 2014;5(3):587-598.
157. Wrangle J, Wang W, Koch A, et al. Alterations of immune response of Non-Small Cell Lung Cancer with Azacytidine. *Oncotarget*. 2013;4(11):2067-2079.
158. Alcazer V, Bonaventura P, Depil S. Human Endogenous Retroviruses (HERVs): Shaping the Innate Immune Response in Cancers. *Cancers (Basel)*. 2020;12(3).
159. Deng L, Liang H, Xu M, et al. STING-Dependent Cytosolic DNA Sensing Promotes Radiation-Induced Type I Interferon-Dependent Antitumor Immunity in Immunogenic Tumors. *Immunity*. 2014;41(5):843-852.

160. Ding L, Kim HJ, Wang Q, et al. PARP Inhibition Elicits STING-Dependent Antitumor Immunity in Brca1-Deficient Ovarian Cancer. *Cell Rep.* 2018;25(11):2972-2980 e2975.
161. Paludan SR, Reinert LS, Hornung V. DNA-stimulated cell death: implications for host defence, inflammatory diseases and cancer. *Nat Rev Immunol.* 2019;19(3):141-153.
162. Levine AJ, Berger SL. The interplay between epigenetic changes and the p53 protein in stem cells. *Genes Dev.* 2017;31(12):1195-1201.
163. Leonova KI, Brodsky L, Lipchick B, et al. p53 cooperates with DNA methylation and a suicidal interferon response to maintain epigenetic silencing of repeats and noncoding RNAs. *Proc Natl Acad Sci U S A.* 2013;110(1):E89-98.
164. Kwon J, Bakhoun SF. The Cytosolic DNA-Sensing cGAS-STING Pathway in Cancer. *Cancer Discov.* 2020;10(1):26-39.
165. Kim C, Wang XD, Yu Y. PARP1 inhibitors trigger innate immunity via PARP1 trapping-induced DNA damage response. *Elife.* 2020;9.
166. Sullivan KD, Galbraith MD, Andrysik Z, Espinosa JM. Mechanisms of transcriptional regulation by p53. *Cell Death Differ.* 2018;25(1):133-143.
167. Komarov PG, Komarova EA, Kondratov RV, et al. A chemical inhibitor of p53 that protects mice from the side effects of cancer therapy. *Science.* 1999;285(5434):1733-1737.
168. Cancer Genome Atlas Research N, Weinstein JN, Collisson EA, et al. The Cancer Genome Atlas Pan-Cancer analysis project. *Nat Genet.* 2013;45(10):1113-1120.
169. Szklarczyk D, Gable AL, Lyon D, et al. STRING v11: protein-protein association networks with increased coverage, supporting functional discovery in genome-wide experimental datasets. *Nucleic Acids Res.* 2019;47(D1):D607-D613.
170. Schwartz DM, Kanno Y, Villarino A, Ward M, Gadina M, O'Shea JJ. JAK inhibition as a therapeutic strategy for immune and inflammatory diseases. *Nat Rev Drug Discov.* 2017;17(1):78.
171. Haag SM, Gulen MF, Reymond L, et al. Targeting STING with covalent small-molecule inhibitors. *Nature.* 2018;559(7713):269-273.
172. Ahn J, Barber GN. STING signaling and host defense against microbial infection. *Exp Mol Med.* 2019;51(12):1-10.
173. Sammons MA, Nguyen TT, McDade SS, Fischer M. Tumor suppressor p53: from engaging DNA to target gene regulation. *Nucleic Acids Res.* 2020;48(16):8848-8869.
174. Bao F, LoVerso PR, Fisk JN, Zhurkin VB, Cui F. p53 binding sites in normal and cancer cells are characterized by distinct chromatin context. *Cell Cycle.* 2017;16(21):2073-2085.
175. Harris CR, Dewan A, Zupnick A, et al. p53 responsive elements in human retrotransposons. *Oncogene.* 2009;28(44):3857-3865.
176. Konecny GE, Kristeleit RS. PARP inhibitors for BRCA1/2-mutated and sporadic ovarian cancer: current practice and future directions. *Br J Cancer.* 2016;115(10):1157-1173.

177. Shen J, Zhao W, Ju Z, et al. PARPi Triggers the STING-Dependent Immune Response and Enhances the Therapeutic Efficacy of Immune Checkpoint Blockade Independent of BRCAness. *Cancer Res.* 2019;79(2):311-319.
178. Muvarak N, Kelley S, Robert C, et al. c-MYC Generates Repair Errors via Increased Transcription of Alternative-NHEJ Factors, LIG3 and PARP1, in Tyrosine Kinase-Activated Leukemias. *Mol Cancer Res.* 2015;13(4):699-712.
179. Tobin LA, Robert C, Nagaria P, et al. Targeting abnormal DNA repair in therapy-resistant breast cancers. *Mol Cancer Res.* 2012;10(1):96-107.
180. Rosado MM, Bennici E, Novelli F, Pioli C. Beyond DNA repair, the immunological role of PARP-1 and its siblings. *Immunology.* 2013;139(4):428-437.
181. Flood BA, Higgs EF, Li S, Luke JJ, Gajewski TF. STING pathway agonism as a cancer therapeutic. *Immunol Rev.* 2019;290(1):24-38.
182. Sokolowska O, Nowis D. STING Signaling in Cancer Cells: Important or Not? *Arch Immunol Ther Exp (Warsz).* 2018;66(2):125-132.
183. Wayne J, Brooks T, Landras A, Massey AJ. Targeting DNA damage response pathways to activate the STING innate immune signaling pathway in human cancer cells. *FEBS J.* 2021.
184. Parkes EE, Walker SM, Taggart LE, et al. Activation of STING-Dependent Innate Immune Signaling By S-Phase-Specific DNA Damage in Breast Cancer. *J Natl Cancer Inst.* 2017;109(1).
185. Chatterjee A, Rodger EJ, Ahn A, et al. Marked Global DNA Hypomethylation Is Associated with Constitutive PD-L1 Expression in Melanoma. *iScience.* 2018;4:312-325.
186. Perrier A, Didelot A, Laurent-Puig P, Blons H, Garinet S. Epigenetic Mechanisms of Resistance to Immune Checkpoint Inhibitors. *Biomolecules.* 2020;10(7).
187. Wang M, Liu Y, Cheng Y, Wei Y, Wei X. Immune checkpoint blockade and its combination therapy with small-molecule inhibitors for cancer treatment. *Biochim Biophys Acta Rev Cancer.* 2019;1871(2):199-224.
188. Wang L, Amoozgar Z, Huang J, et al. Decitabine Enhances Lymphocyte Migration and Function and Synergizes with CTLA-4 Blockade in a Murine Ovarian Cancer Model. *Cancer Immunol Res.* 2015;3(9):1030-1041.
189. Colaprico A, Silva TC, Olsen C, et al. TCGAbiolinks: an R/Bioconductor package for integrative analysis of TCGA data. *Nucleic Acids Res.* 2016;44(8):e71.
190. Vadakekolathu J, Lai C, Reeder S, et al. TP53 abnormalities correlate with immune infiltration and associate with response to flotetuzumab immunotherapy in AML. *Blood Adv.* 2020;4(20):5011-5024.
191. von Mering C, Jensen LJ, Snel B, et al. STRING: known and predicted protein-protein associations, integrated and transferred across organisms. *Nucleic Acids Res.* 2005;33(Database issue):D433-437.

192. Panoskaltsis N, Reid CD, Knight SC. Quantification and cytokine production of circulating lymphoid and myeloid cells in acute myelogenous leukaemia. *Leukemia*. 2003;17(4):716-730.
193. Zhou Q, Munger ME, Veenstra RG, et al. Coexpression of Tim-3 and PD-1 identifies a CD8+ T-cell exhaustion phenotype in mice with disseminated acute myelogenous leukemia. *Blood*. 2011;117(17):4501-4510.
194. Zhang L, Chen X, Liu X, et al. CD40 ligation reverses T cell tolerance in acute myeloid leukemia. *J Clin Invest*. 2013;123(5):1999-2010.
195. Curran E, Chen X, Corrales L, et al. STING Pathway Activation Stimulates Potent Immunity against Acute Myeloid Leukemia. *Cell Rep*. 2016;15(11):2357-2366.
196. Stone ML, Chiappinelli KB, Li H, et al. Epigenetic therapy activates type I interferon signaling in murine ovarian cancer to reduce immunosuppression and tumor burden. *Proc Natl Acad Sci U S A*. 2017;114(51):E10981-E10990.
197. Gomez S, Tabernacki T, Kobyra J, Roberts P, Chiappinelli KB. Combining epigenetic and immune therapy to overcome cancer resistance. *Semin Cancer Biol*. 2020;65:99-113.
198. Roulois D, Loo Yau H, Singhania R, et al. DNA-Demethylating Agents Target Colorectal Cancer Cells by Inducing Viral Mimicry by Endogenous Transcripts. *Cell*. 2015;162(5):961-973.
199. Mopin A, Driss V, Brinster C. A Detailed Protocol for Characterizing the Murine C1498 Cell Line and its Associated Leukemia Mouse Model. *J Vis Exp*. 2016(116).
200. Zhang L, Gajewski TF, Kline J. PD-1/PD-L1 interactions inhibit antitumor immune responses in a murine acute myeloid leukemia model. *Blood*. 2009;114(8):1545-1552.
201. Musella M, Manic G, De Maria R, Vitale I, Sistigu A. Type-I-interferons in infection and cancer: Unanticipated dynamics with therapeutic implications. *Oncoimmunology*. 2017;6(5):e1314424.
202. Jorgovanovic D, Song M, Wang L, Zhang Y. Roles of IFN-gamma in tumor progression and regression: a review. *Biomark Res*. 2020;8:49.
203. Escobar G, Barbarossa L, Barbiera G, et al. Interferon gene therapy reprograms the leukemia microenvironment inducing protective immunity to multiple tumor antigens. *Nat Commun*. 2018;9(1):2896.
204. Ersvaer E, Hampson P, Hatfield K, et al. T cells remaining after intensive chemotherapy for acute myelogenous leukemia show a broad cytokine release profile including high levels of interferon-gamma that can be further increased by a novel protein kinase C agonist PEP005. *Cancer Immunol Immunother*. 2007;56(6):913-925.
205. Knaus HA, Berglund S, Hackl H, et al. Signatures of CD8+ T cell dysfunction in AML patients and their reversibility with response to chemotherapy. *JCI Insight*. 2018;3(21).
206. Kassem NM, Ayad AM, El Husseiny NM, El-Demerdash DM, Kassem HA, Mattar MM. Role of Granulocyte-Macrophage Colony-Stimulating Factor in Acute Myeloid Leukemia/Myelodysplastic Syndromes. *J Glob Oncol*. 2018;4:1-6.

207. Zhan Y, Lew AM, Chopin M. The Pleiotropic Effects of the GM-CSF Rheostat on Myeloid Cell Differentiation and Function: More Than a Numbers Game. *Front Immunol.* 2019;10:2679.
208. Beekman R, Touw IP. G-CSF and its receptor in myeloid malignancy. *Blood.* 2010;115(25):5131-5136.
209. Baker KJ, Houston A, Brint E. IL-1 Family Members in Cancer; Two Sides to Every Story. *Front Immunol.* 2019;10:1197.
210. Shu C, Li X, Li P. The mechanism of double-stranded DNA sensing through the cGAS-STING pathway. *Cytokine Growth Factor Rev.* 2014;25(6):641-648.
211. Basit A, Cho MG, Kim EY, Kwon D, Kang SJ, Lee JH. The cGAS/STING/TBK1/IRF3 innate immunity pathway maintains chromosomal stability through regulation of p21 levels. *Exp Mol Med.* 2020;52(4):643-657.
212. Fang R, Wang C, Jiang Q, et al. NEMO-IKKbeta Are Essential for IRF3 and NF-kappaB Activation in the cGAS-STING Pathway. *J Immunol.* 2017;199(9):3222-3233.
213. Ning S, Pagano JS, Barber GN. IRF7: activation, regulation, modification and function. *Genes Immun.* 2011;12(6):399-414.
214. Burnett A, Wetzler M, Lowenberg B. Therapeutic advances in acute myeloid leukemia. *J Clin Oncol.* 2011;29(5):487-494.
215. Versluis J, Cornelissen JJ, Craddock C, Sanz MA, Canaani J, Nagler A. Acute Myeloid Leukemia in Adults. In: Carreras E, Dufour C, Mohty M, Kroger N, eds. *The EBMT Handbook: Hematopoietic Stem Cell Transplantation and Cellular Therapies.* Cham (CH)2019:507-521.
216. Fathi AT, Karp JE. New agents in acute myeloid leukemia: beyond cytarabine and anthracyclines. *Curr Oncol Rep.* 2009;11(5):346-352.
217. Bao T, Smith BD, Karp JE. New agents in the treatment of acute myeloid leukemia: a snapshot of signal transduction modulation. *Clin Adv Hematol Oncol.* 2005;3(4):287-296, 302.
218. Karp JE, Smith MA. The molecular pathogenesis of treatment-induced (secondary) leukemias: foundations for treatment and prevention. *Semin Oncol.* 1997;24(1):103-113.
219. Patel K, Dickson J, Din S, Macleod K, Jodrell D, Ramsahoye B. Targeting of 5-aza-2'-deoxycytidine residues by chromatin-associated DNMT1 induces proteasomal degradation of the free enzyme. *Nucleic Acids Res.* 2010;38(13):4313-4324.
220. Jones PA, Taylor SM. Cellular differentiation, cytidine analogs and DNA methylation. *Cell.* 1980;20(1):85-93.
221. Steensma DP, Baer MR, Slack JL, et al. Multicenter study of decitabine administered daily for 5 days every 4 weeks to adults with myelodysplastic syndromes: the alternative dosing for outpatient treatment (ADOPT) trial. *J Clin Oncol.* 2009;27(23):3842-3848.
222. Cashen AF, Schiller GJ, O'Donnell MR, DiPersio JF. Multicenter, phase II study of decitabine for the first-line treatment of older patients with acute myeloid leukemia. *J Clin Oncol.* 2010;28(4):556-561.

223. Lubbert M, Ruter BH, Claus R, et al. A multicenter phase II trial of decitabine as first-line treatment for older patients with acute myeloid leukemia judged unfit for induction chemotherapy. *Haematologica*. 2012;97(3):393-401.
224. Kantarjian HM, Thomas XG, Dmoszynska A, et al. Multicenter, randomized, open-label, phase III trial of decitabine versus patient choice, with physician advice, of either supportive care or low-dose cytarabine for the treatment of older patients with newly diagnosed acute myeloid leukemia. *J Clin Oncol*. 2012;30(21):2670-2677.
225. Blum W, Garzon R, Klisovic RB, et al. Clinical response and miR-29b predictive significance in older AML patients treated with a 10-day schedule of decitabine. *Proc Natl Acad Sci U S A*. 2010;107(16):7473-7478.
226. Ritchie EK, Feldman EJ, Christos PJ, et al. Decitabine in patients with newly diagnosed and relapsed acute myeloid leukemia. *Leuk Lymphoma*. 2013;54(9):2003-2007.
227. Bhatnagar B, Duong VH, Gourdin TS, et al. Ten-day decitabine as initial therapy for newly diagnosed patients with acute myeloid leukemia unfit for intensive chemotherapy. *Leuk Lymphoma*. 2014;55(7):1533-1537.
228. Bouligny IM, Mehta V, Isom S, et al. Efficacy of 10-day decitabine in acute myeloid leukemia. *Leuk Res*. 2021;103:106524.
229. Stahl M, DeVeaux M, Montesinos P, et al. Hypomethylating agents in relapsed and refractory AML: outcomes and their predictors in a large international patient cohort. *Blood Adv*. 2018;2(8):923-932.
230. McLaughlin LJ, Stojanovic L, Kogan AA, et al. Pharmacologic induction of innate immune signaling directly drives homologous recombination deficiency. *Proc Natl Acad Sci U S A*. 2020;117(30):17785-17795.
231. de Bono J, Ramanathan RK, Mina L, et al. Phase I, Dose-Escalation, Two-Part Trial of the PARP Inhibitor Talazoparib in Patients with Advanced Germline BRCA1/2 Mutations and Selected Sporadic Cancers. *Cancer Discov*. 2017;7(6):620-629.
232. Litton JK, Rugo HS, Ettl J, et al. Talazoparib in Patients with Advanced Breast Cancer and a Germline BRCA Mutation. *N Engl J Med*. 2018;379(8):753-763.
233. Fritz C, Portwood SM, Przespolewski A, Wang ES. PARP goes the weasel! Emerging role of PARP inhibitors in acute leukemias. *Blood Rev*. 2021;45:100696.
234. Mufti G, Estey E, Popat R, et al. Results of a phase 1 study of BMN 673, a potent and specific PARP-1/2 inhibitor, in patients with advanced hematological malignancies. *Haematologica* 2014(99):33-34.
235. Gojo I, Beumer JH, Pratz KW, et al. A Phase 1 Study of the PARP Inhibitor Veliparib in Combination with Temozolomide in Acute Myeloid Leukemia. *Clin Cancer Res*. 2017;23(3):697-706.
236. Pratz KW, Rudek MA, Gojo I, et al. A Phase I Study of Topotecan, Carboplatin and the PARP Inhibitor Veliparib in Acute Leukemias, Aggressive Myeloproliferative Neoplasms, and Chronic Myelomonocytic Leukemia. *Clin Cancer Res*. 2017;23(4):899-907.

237. Cruz C, Castroviejo-Bermejo M, Gutierrez-Enriquez S, et al. RAD51 foci as a functional biomarker of homologous recombination repair and PARP inhibitor resistance in germline BRCA-mutated breast cancer. *Ann Oncol*. 2018;29(5):1203-1210.
238. Mah LJ, El-Osta A, Karagiannis TC. gammaH2AX: a sensitive molecular marker of DNA damage and repair. *Leukemia*. 2010;24(4):679-686.
239. Bonner WM, Redon CE, Dickey JS, et al. GammaH2AX and cancer. *Nat Rev Cancer*. 2008;8(12):957-967.
240. DiNardo CD, Garcia-Manero G, Pierce S, et al. Interactions and relevance of blast percentage and treatment strategy among younger and older patients with acute myeloid leukemia (AML) and myelodysplastic syndrome (MDS). *Am J Hematol*. 2016;91(2):227-232.
241. Le Naour J, Zitvogel L, Galluzzi L, Vacchelli E, Kroemer G. Trial watch: STING agonists in cancer therapy. *Oncoimmunology*. 2020;9(1):1777624.
242. Choubey D, Moudgil KD. Interferons in autoimmune and inflammatory diseases: regulation and roles. *J Interferon Cytokine Res*. 2011;31(12):857-865.
243. Pan H, Wang X, Huang W, et al. Interferon-Induced Protein 44 Correlated With Immune Infiltration Serves as a Potential Prognostic Indicator in Head and Neck Squamous Cell Carcinoma. *Front Oncol*. 2020;10:557157.
244. Swerdlow SH, International Agency for Research on Cancer., World Health Organization. *WHO classification of tumours of haematopoietic and lymphoid tissues*. 4th ed. Lyon, France: International Agency for Research on Cancer; 2008.
245. Cheson BD, Bennett JM, Kopecky KJ, et al. Revised recommendations of the International Working Group for Diagnosis, Standardization of Response Criteria, Treatment Outcomes, and Reporting Standards for Therapeutic Trials in Acute Myeloid Leukemia. *J Clin Oncol*. 2003;21(24):4642-4649.
246. Greve G, Schuler J, Gruning BA, et al. Decitabine Induces Gene Derepression on Monosomic Chromosomes: In Vitro and In Vivo Effects in Adverse-Risk Cytogenetics AML. *Cancer Res*. 2021;81(4):834-846.
247. Maifrede S, Le BV, Nieborowska-Skorska M, et al. TET2 and DNMT3A Mutations Exert Divergent Effects on DNA Repair and Sensitivity of Leukemia Cells to PARP Inhibitors. *Cancer Res*. 2021.
248. Lee EK, Konstantinopoulos PA. PARP inhibition and immune modulation: scientific rationale and perspectives for the treatment of gynecologic cancers. *Ther Adv Med Oncol*. 2020;12:1758835920944116.
249. Chabanon RM, Muirhead G, Krastev DB, et al. PARP inhibition enhances tumor cell-intrinsic immunity in ERCC1-deficient non-small cell lung cancer. *J Clin Invest*. 2019;129(3):1211-1228.
250. Chabanon RM, Soria JC, Lord CJ, Postel-Vinay S. Beyond DNA repair: the novel immunological potential of PARP inhibitors. *Mol Cell Oncol*. 2019;6(2):1585170.

251. Pantelidou C, Sonzogni O, De Oliveria Taveira M, et al. PARP Inhibitor Efficacy Depends on CD8(+) T-cell Recruitment via Intratumoral STING Pathway Activation in BRCA-Deficient Models of Triple-Negative Breast Cancer. *Cancer Discov.* 2019;9(6):722-737.
252. Liu Y, Bewersdorf JP, Stahl M, Zeidan AM. Immunotherapy in acute myeloid leukemia and myelodysplastic syndromes: The dawn of a new era? *Blood Rev.* 2019;34:67-83.
253. Wong KK, Hassan R, Yaacob NS. Hypomethylating Agents and Immunotherapy: Therapeutic Synergism in Acute Myeloid Leukemia and Myelodysplastic Syndromes. *Front Oncol.* 2021;11:624742.
254. Lambert J, Pautas C, Terre C, et al. Gemtuzumab ozogamicin for de novo acute myeloid leukemia: final efficacy and safety updates from the open-label, phase III ALFA-0701 trial. *Haematologica.* 2019;104(1):113-119.
255. Liao D, Wang M, Liao Y, Li J, Niu T. A Review of Efficacy and Safety of Checkpoint Inhibitor for the Treatment of Acute Myeloid Leukemia. *Front Pharmacol.* 2019;10:609.
256. Page DB, Bear H, Prabhakaran S, et al. Two may be better than one: PD-1/PD-L1 blockade combination approaches in metastatic breast cancer. *NPJ Breast Cancer.* 2019;5:34.
257. Toufekchan E, Toledo F. The Guardian of the Genome Revisited: p53 Downregulates Genes Required for Telomere Maintenance, DNA Repair, and Centromere Structure. *Cancers (Basel).* 2018;10(5).
258. Zhu G, Pan C, Bei JX, et al. Mutant p53 in Cancer Progression and Targeted Therapies. *Front Oncol.* 2020;10:595187.
259. Ceder S, Eriksson SE, Cheteh EH, et al. A thiol-bound drug reservoir enhances APR-246-induced mutant p53 tumor cell death. *EMBO Mol Med.* 2021;13(2):e10852.
260. Shaheen M, Allen C, Nickoloff JA, Hromas R. Synthetic lethality: exploiting the addiction of cancer to DNA repair. *Blood.* 2011;117(23):6074-6082.
261. Parrales A, Iwakuma T. Targeting Oncogenic Mutant p53 for Cancer Therapy. *Front Oncol.* 2015;5:288.